Summer 2015

THE SAUDI ARAMCO JOURNAL OF TECHNOLOGY
A quarterly publication of the Saudi Arabian Oil Company

Saudi Aramco Journal of Technology

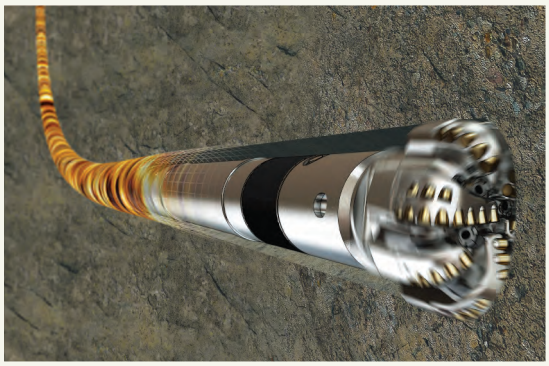

Horizontal drilling technology, a real marvel of engineering and scientific innovation, is used extensively to produce thin zones, fractured reservoirs, formations with bottom water, tight gas, heavy oil, and enabling to induce multiple hydraulic fractures in the reservoir. The cost of drilling multiple vertical holes has been significantly reduced. The maximum contact wells can only be achieved through horizontal drilling.

On the Cover

Intelligent well completion is used for both conventional and unconventional reservoirs incorporating downhole sensors and surface controlled downhole valves to evaluate, monitor and actively manage production in real time without well intervention. In the case of multilaterals and multiple zones, selective production can be an option to optimize uniform depletion.

MORE SAUDI ARAMCO JOURNAL OF TECHNOLOGY ARTICLES AVAILABLE ON THE INTERNET.

Additional articles that were submitted for publication in the *Saudi Aramco Journal of Technology* are being made available online. You can read them at this link on the Saudi Aramco Internet Website: www.saudiaramco.com/jot

The *Saudi Aramco Journal of Technology* is published quarterly by the Saudi Arabian Oil Company, Dhahran, Saudi Arabia, to provide the company's scientific and engineering communities a forum for the exchange of ideas through the presentation of technical information aimed at advancing knowledge in the hydrocarbon industry.

Complete issues of the Journal in PDF format are available on the Internet at: http://www.saudiaramco.com (click on "publications").

SUBSCRIPTIONS

Send individual subscription orders, address changes (see page 86) and related questions to:

Saudi Aramco Public Relations Department
JOT Distribution
Box 5000
Dhahran 31311, Saudi Arabia
Website: www.saudiaramco.com

EDITORIAL ADVISORS

Zuhair A. Al-Hussain
Vice President, Southern Area Oil Operations

Ibraheem Assa'adan
Vice President, Exploration

Abdullah M. Al-Ghamdi
General Manager, Northern Area Gas Operations

EDITORIAL ADVISORS (CONTINUED)

Sami A. Al-Khursani
Program Director, Technology

Ammar A. Nahwi
Manager, Research and Development Center

Waleed A. Mulhim
Manager, EXPEC ARC

CONTRIBUTIONS

Relevant articles are welcome. Submission guidelines are printed on the last page. Please address all manuscript and editorial correspondence to:

EDITOR

William E. Bradshaw
The *Saudi Aramco Journal of Technology*
C-86, Wing D, Building 9156
Dhahran 31311, Saudi Arabia
Tel: +966-013-876-0498
E-mail: william.bradshaw.1@aramco.com.sa

Unsolicited articles will be returned only when accompanied by a self-addressed envelope.

Amin H. Nasser
Acting President & CEO, Saudi Aramco

Nasser A. Al-Nafisee
Vice President, Corporate Affairs

Essam Z. Tawfiq
General Manager, Public Affairs

PRODUCTION COORDINATION

Richard E. Doughty

DESIGN

Pixel Creative Group, Houston, Texas, U.S.A.

ISSN 1319-2388.

© COPYRIGHT 2015
ARAMCO SERVICES COMPANY
ALL RIGHTS RESERVED

No articles, including art and illustrations, in the *Saudi Aramco Journal of Technology*, except those from copyrighted sources, may be reproduced or printed without the written permission of Saudi Aramco. Please submit requests for permission to reproduce items to the editor.

The *Saudi Aramco Journal of Technology* gratefully acknowledges the assistance, contribution and cooperation of numerous operating organizations throughout the company.

Summer 2015

THE SAUDI ARAMCO JOURNAL OF TECHNOLOGY
A quarterly publication of the Saudi Arabian Oil Company

Saudi Aramco Journal of Technology

Contents

Completion Optimization for an Unconventional Reservoir

Authors: Osman Hamid, Dr. Zillur Rahim, Munther M. Al-Shakhs, Ahmed H. Al-Mubarak, Kevin Fisher and Omar A. Bawazir

ABSTRACT

Successful production from unconventional reservoirs is made possible by horizontal drilling and reservoir stimulation through multistage hydraulic fracturing along the laterals. Although hydraulic fracturing techniques have been widely used for unconventional shale gas stimulation, a considerable percentage of perforations do not contribute to production. Reservoir characterization and the computation of completion parameters are essential for effective completion design to improve staging and perforation placement.

Challenges in the design of hydraulic fractures are the proper placement of fracturing ports or perforations and the location of isolation packers. The challenges are due to the large variability in fracture gradients, mechanical and reservoir properties, and petrophysical characteristics along the lateral. Industry experience shows that injection pressures required to fracture the formation (the fracture gradient) often vary significantly along a well and that there can be intervals where the formation cannot be fractured successfully by fluid injection[1] due to high in situ stress.

Geomechanical and petrophysical evaluations providing rock anisotropy and anisotropic stress properties along the wellbore play a fundamental role in completion and hydraulic fracture design. In this article, geomechanical and petrophysical properties from open hole logs and sonic anisotropy evaluations have been integrated to compute reservoir quality and completion quality. Intervals with similar properties are then grouped so as to better understand and optimize hydraulic fracture design and operations. This optimization procedure is then applied in a borehole within a potential shale gas reservoir that is targeting the hot shale facies formation in Saudi Arabia. This resulted in successful completion optimization and hydraulic fracture performance.

INTRODUCTION

Understanding the geomechanical and petrophysical properties of heterogeneous reservoir shale rocks is essential when evaluating reservoir quality and completion designs. Unconventional reservoirs exhibit log responses that differ from those of conventional reservoirs, and understanding this behavior shown in the logs is sometimes challenging. Moreover, basic logs alone are insufficient to adequately quantify unconventional rock parameters. Multiple techniques are required to detail the reservoir properties of shale plays.

In one of these advanced techniques, heterogeneous rock analysis (HRA), the measured and the interpreted open hole logs — gamma ray, neutron, density, effective porosity (PHIE), permeability and total organic contents (TOC) — are grouped in a manner that combines similar log responses to form facies or clusters. These new clusters or facies, represented in specific colors, are next re-sorted to give petrophysical meaning, such as showing the progression from the highest permeability cluster to the lowest permeability cluster. These re-sorted clusters are then integrated with anisotropic elastic properties to facilitate analysis and develop shale plays successfully. The theory of cluster analysis and the HRA methodology is reviewed in this article, and a case study from a well in Saudi Arabia is considered in the application of this technique.

CLUSTER ANALYSIS

Cluster analysis is simply defined as segmenting objects based on common characteristics. This concept is widely used in market segmentation to divide markets into groups with similar demands. The concept can be also used in defining different contexts. This article shows the implementation of this concept on well log readings. At the outset, a workflow explaining the fundamentals of basic cluster algorithms with examples is given, but more details are available in Mooi and Sarstedt (2011)[2].

The steps involved in any cluster analysis can be summarized as follows:

- Deciding on variables: It is a crucial starting step in the analysis to provide clear-cut differentiation between segments. For example, one should start with the variables, such as gamma ray, neutron, density and clay volume (VCL), to define and characterize the intervals.
- Deciding on a clustering procedure: The goal of the clustering procedure is to form objects or clusters. For example, this could mean minimizing the variance within a cluster or maximizing the distance between objects or clusters. There are many clustering

procedures, and each requires different decisions prior to analysis[3]. Hierarchical clustering methods are the most common and widely used approaches for forming objects or clusters. Most hierarchical techniques fall under a category called "agglomerative clustering" in which variables that are most similar are grouped or merged to form a new cluster. In subsequent steps, the distances between the newly formed clusters and all remaining variables are recalculated using a specific agglomerative clustering method. The number of clusters is thereby reduced by one in each iteration step. Figure 1 shows this process in its simplest forms.

Of the various types of agglomerative clustering methods, the most popular methods include the following:

- Single linkage: Depends on the shortest distance between a variable and a cluster or any two clusters.
- Complete linkage: Depends on the longest distance between a variable and a cluster or any two clusters.
- Average linkage: Depends on the average distance between all pairs of two cluster members.
- Ward method: Merges clusters by maximizing the overall variance within a cluster (most common).

Figure 2 illustrates the variations among these agglomerative procedures for members of two formed clusters. A common way to visualize the cluster analysis process is by drawing a dendrogram[4]. A dendrogram is a tree structure graph used to visualize the results of a hierarchical clustering calculation. Figure 3 shows an example of a single linkage method applied on seven points, together with dendrogram presentations. The next two steps in a cluster analysis are:

- Deciding on the number of clusters: There is no one way to select the number of clusters. It depends on the objectives of the analyst. It also requires a prior knowledge or theory on which one can formulate the choice. The ultimate goal is to ensure these results are interpretable and meaningful. In the example shown in Fig. 3, one could justify either a two cluster solution ([1, 2, 3, 4, 5, 6], [7]) or a five cluster solution ([4,5], [1,2], [3], [6], [7]).

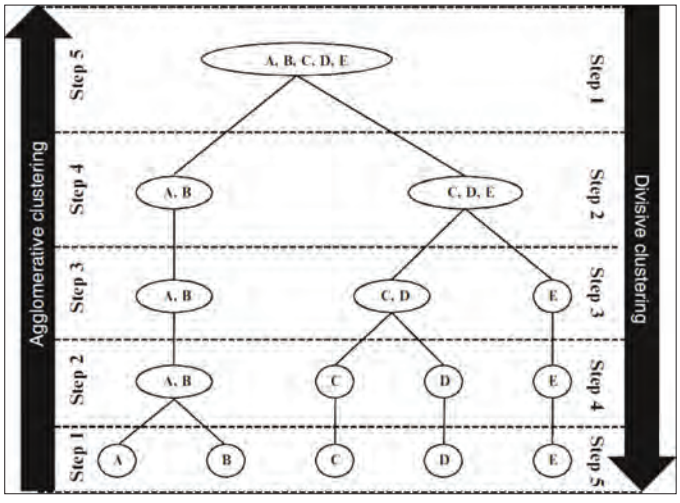

Fig. 1. Definition of agglomerative clustering[1].

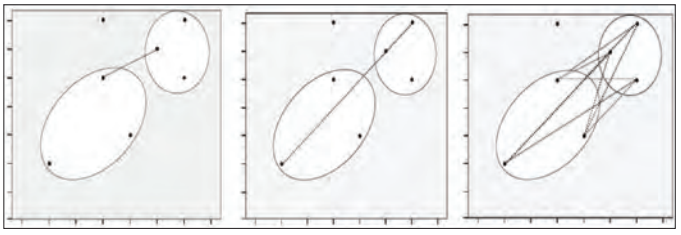

Fig. 2. Single linkage (left), complete linkage (middle), and average linkage (right) agglomerative clustering methods[1].

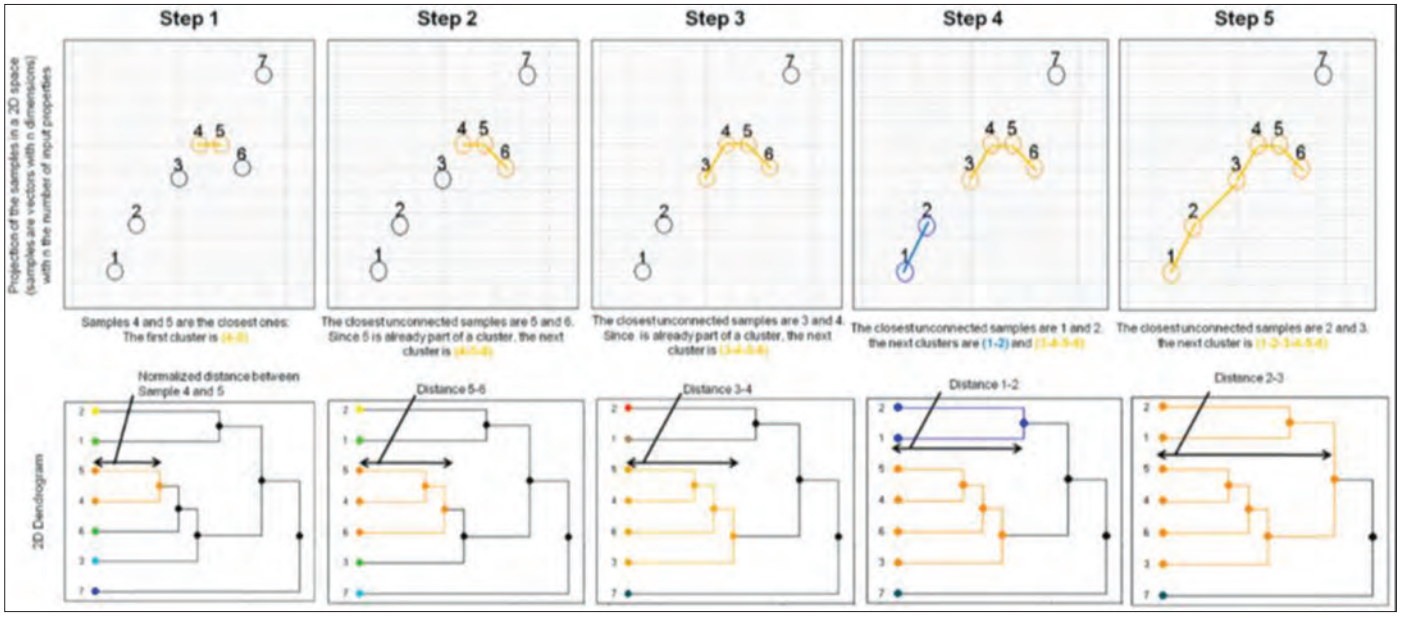

Fig. 3. Clustering with accompanying dendrograms on interpreting seven points as variables.

- Interpreting the cluster solutions: This step is of great importance because the analyst makes a decision on whether the formed clusters are conceptually distinguishable. The interpretation could involve assigning names or labels for each cluster and characterizing each cluster by means of observable variables, e.g., classifying the clusters as very good rocks, good rocks, fair rocks and bad rocks based on the permeability values for each cluster.

HISTOGRAM AND BOX PLOTS

As previously mentioned, interpreting the clusters is the final

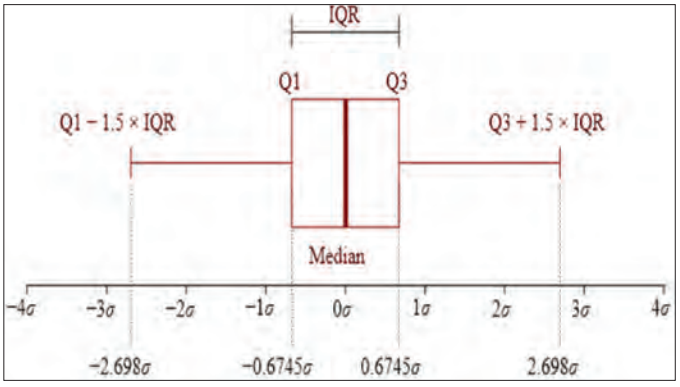

Fig. 4. The main parts of interpreting the box plot[4].

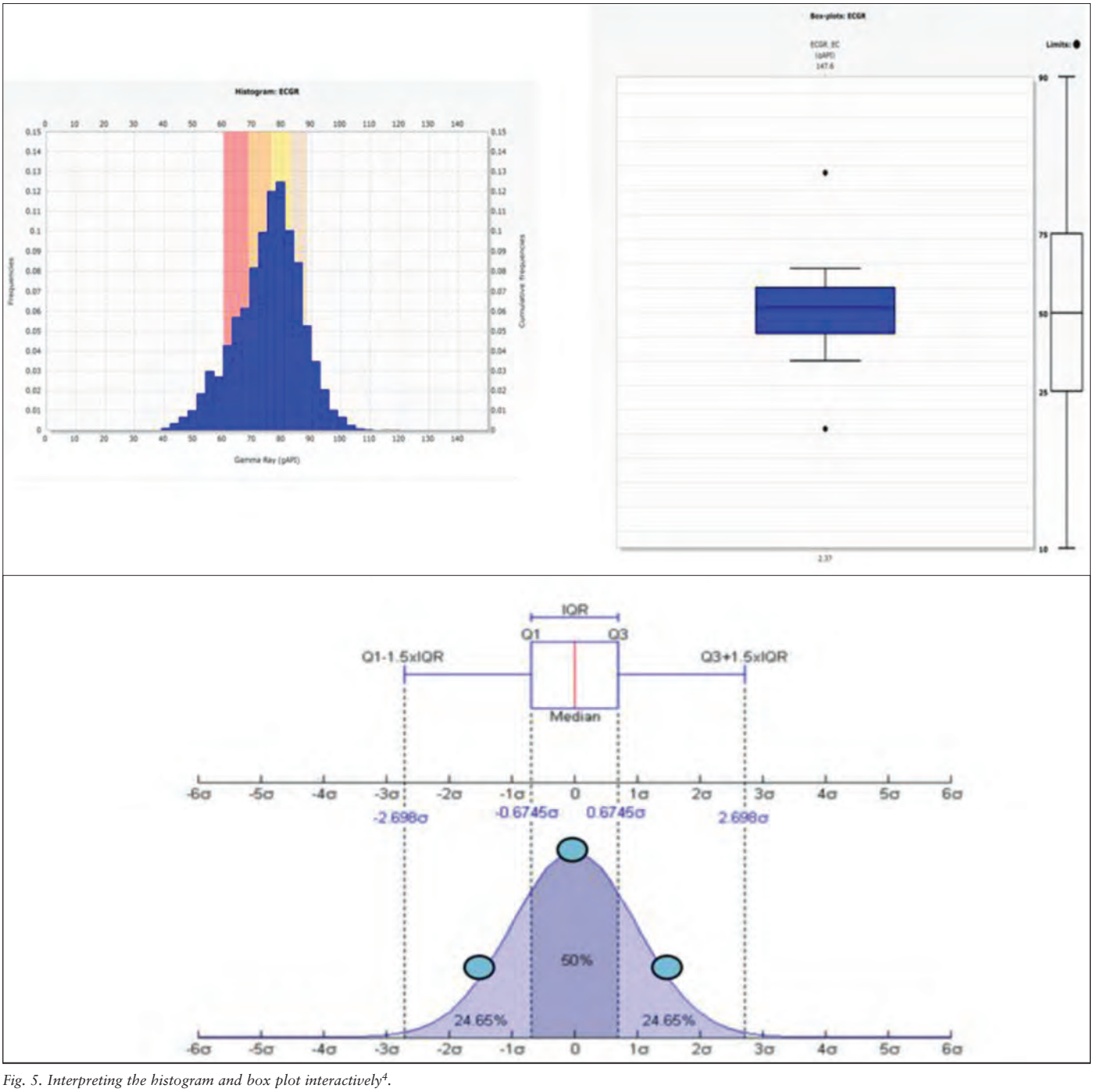

Fig. 5. Interpreting the histogram and box plot interactively[4].

— and a crucial step — in the analysis to show the value of their distributions. One way of interpreting the clusters is to look at the box plots or the histograms, Fig. 4[5]. The main parts of any box plot are:

- The first quartile (Q1) is the middle number between the smallest number and the median of the data set.
- The second quartile (Q2) is the median of the data.
- The third quartile (Q3) is the middle value between the median and the highest value of the data set.
- The interquartile range (IQR) is equal to the difference between the upper and lower quartiles, IQR = Q3 – Q1.
- Box plots may also have lines extending vertically from the boxes indicating variability outside the upper and lower quartiles.
- An outlier is an observation point that is distant from other observations. An outlier may be due to variability

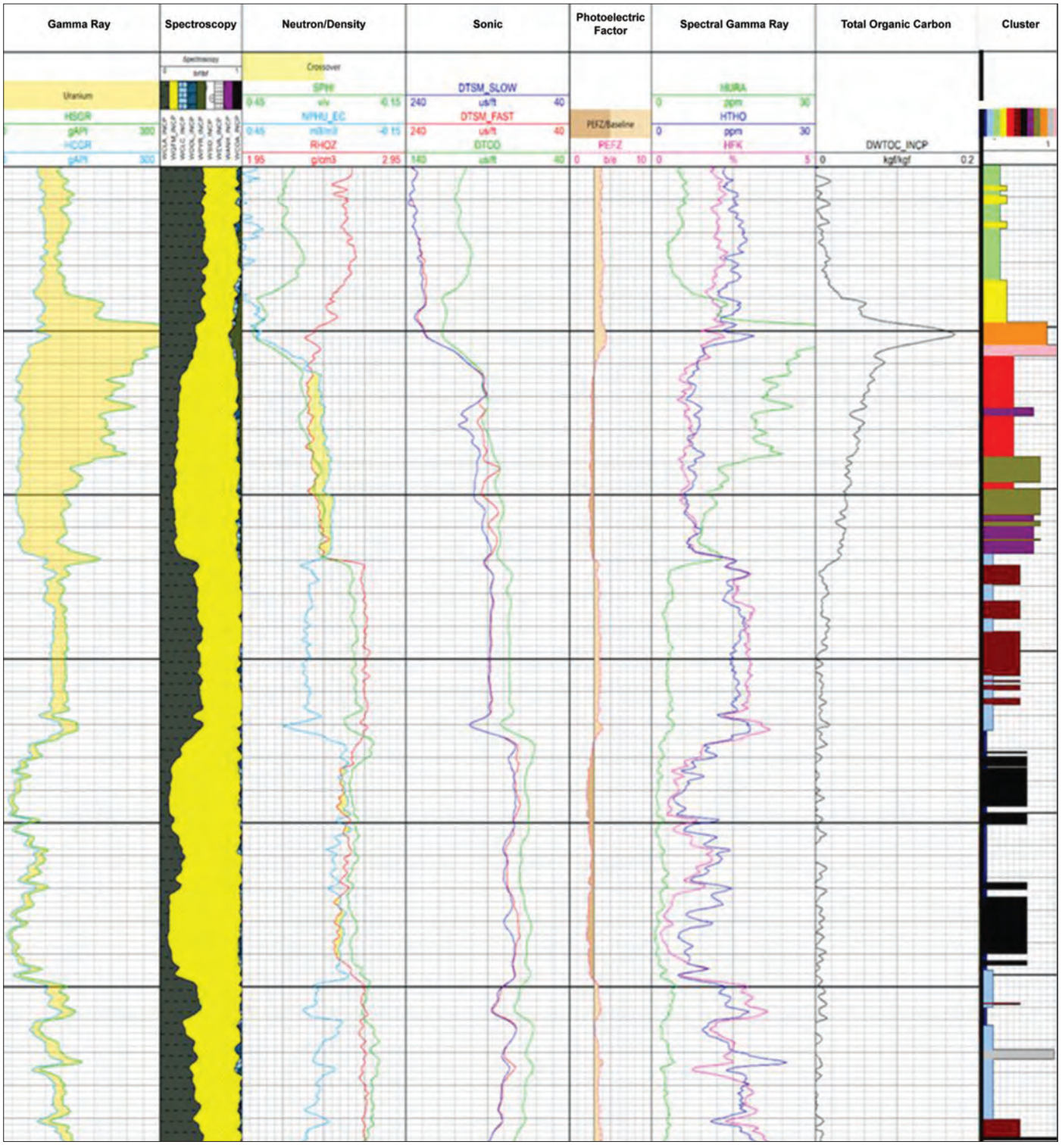

Fig. 6. Input logs.

in the measurement or experimental error. Outliers are plotted as individual points.

In well logs, the objective of these plots is to evaluate the uniqueness of each rock class. Uniqueness can be determined by one variable or multiple log inputs. For example, two rock classes are identified by having similar box plots for gamma ray and resistivity, but very different box plots for — and therefore different distributions of — bulk density and neutron porosity. These box plots can instead be visualized in histograms, Fig. 5[5].

CASE STUDY

Wireline logging data were acquired in a shale gas well to evaluate and characterize the hydrocarbon potentials within the heterogeneous rocks.

A cluster analysis was performed on this well with the goal to segment the intervals into various rock groups: sands, shales and organic rich intervals. The inputs in the cluster analysis were neutron porosity, bulk density, compressional and shear slowness, thorium and uranium concentration, calcium weight fraction, iron weight fraction, potassium weight fraction, silicon weight fraction, titanium weight fraction and TOC weight fraction.

From these 13 inputs, a sensitivity analysis was performed to determine the optimal number of classifications. Using the Ward method, 12 classifications were settled upon to represent the various rock groups in this section. Figure 6 shows the input logs with the cluster analysis results in Track 8.

Figure 7 shows the dendrograms of these 12 classifications in 2D and 3D images, respectively. The colors classified in this stage do not have meaning; they only show the similarity in log responses. Therefore, the next step was to re-sort these classifications to have petrophysical meaning and show the uniqueness of each classification.

After computing the formation evaluation in this well, it was observed that integrating three main properties simultaneously helped to organize and distinguish the rocks among these 12 classifications. These properties were VCL, PHIE and TOC.

Based on these three main properties, the classes were re-sorted in the following order: organic rich sand 1, organic rich sand 2, organic rich sand 3 (pay sand zones), clean sand, silty sand, high TOC shale, moderate TOC shale 1, moderate TOC shale 2, low TOC shale, very low TOC shale, nonorganic shale 1 and nonorganic shale 2.

Box plots were generated for VCL, PHIE and TOC for each classification, as shown in Figs. 8 through 10, respectively. The figures show these re-sorted 12 classifications.

The re-sorted cluster results, along with the petrophysical interpretation, are shown in Fig. 11. Each color code corresponds to the lithology description, Table 1.

Figure 11 shows the depth track, VCL (Track 1), TOC (Track 2), cluster after re-sorting (Track 3), formation evaluation

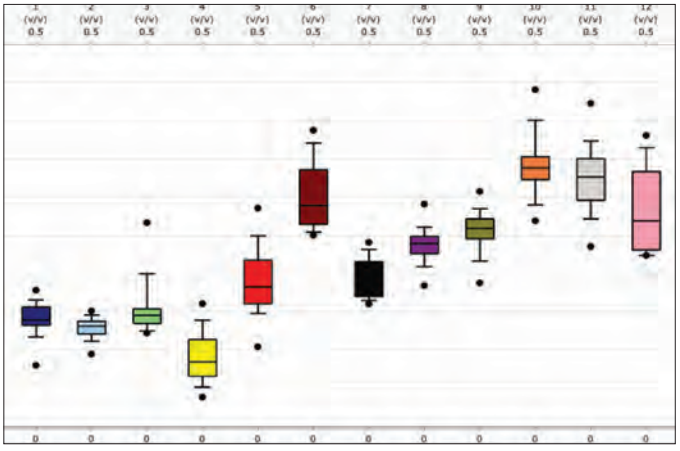

Fig. 8. VCL box plots for the 12 re-sorted classifications.

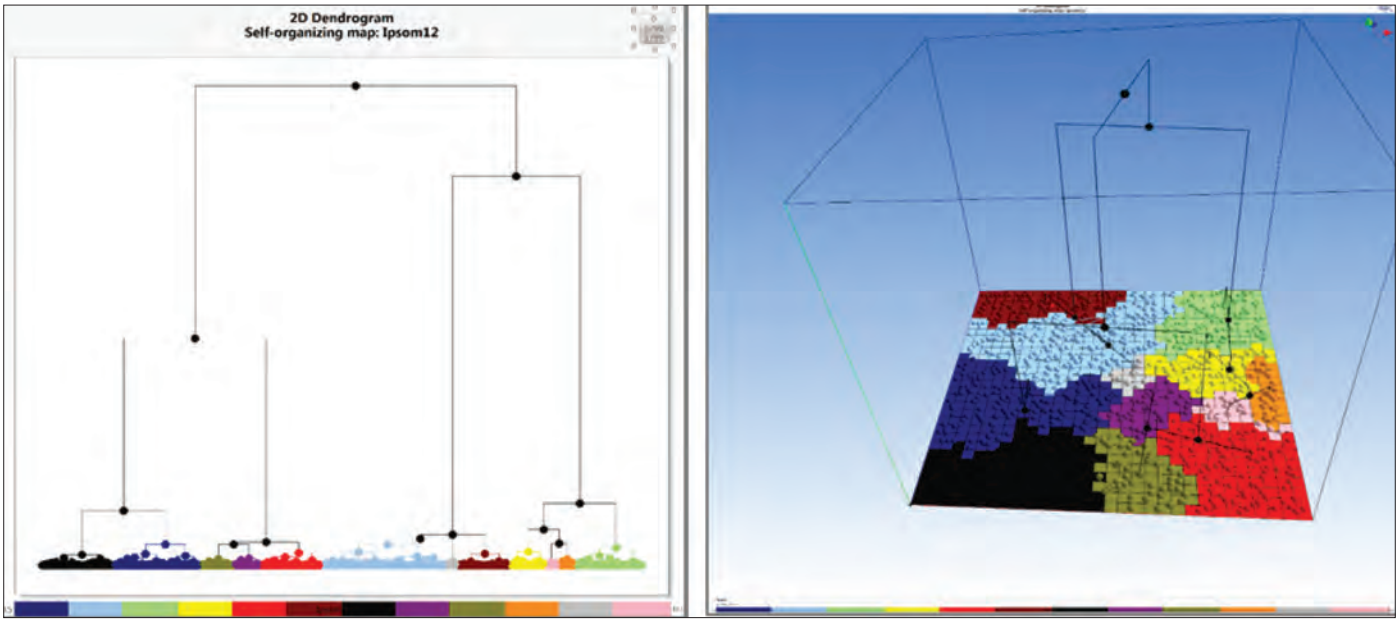

Fig. 7. 2D dendrogram (left) and 3D dendrogram (right) showing the 12 classifications.

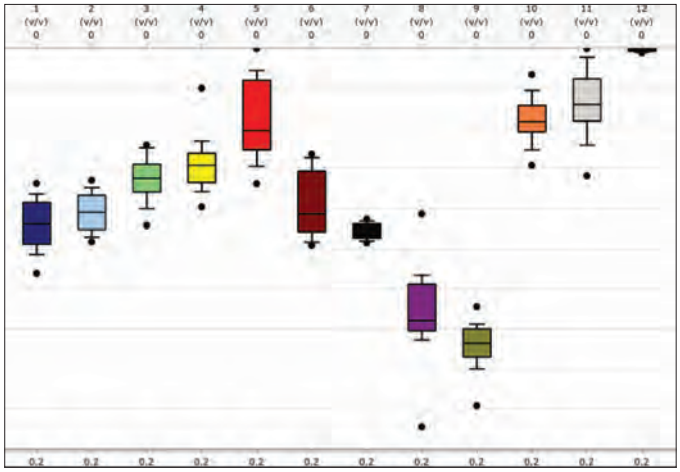

Fig. 9. PHIE box plots for the 12 re-sorted classifications.

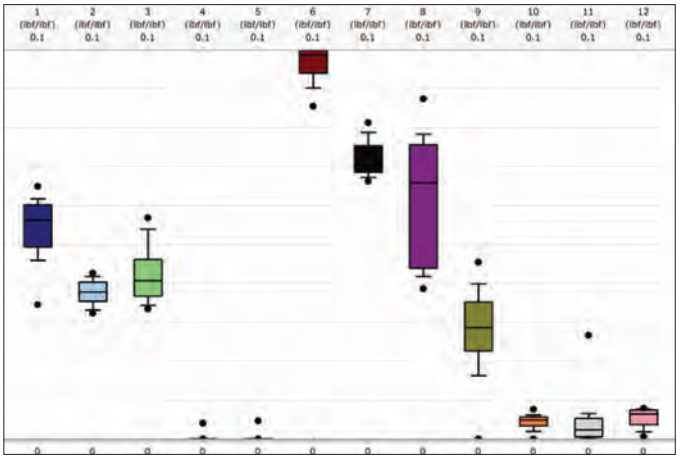

Fig. 10. TOC box plots for the 12 re-sorted classifications.

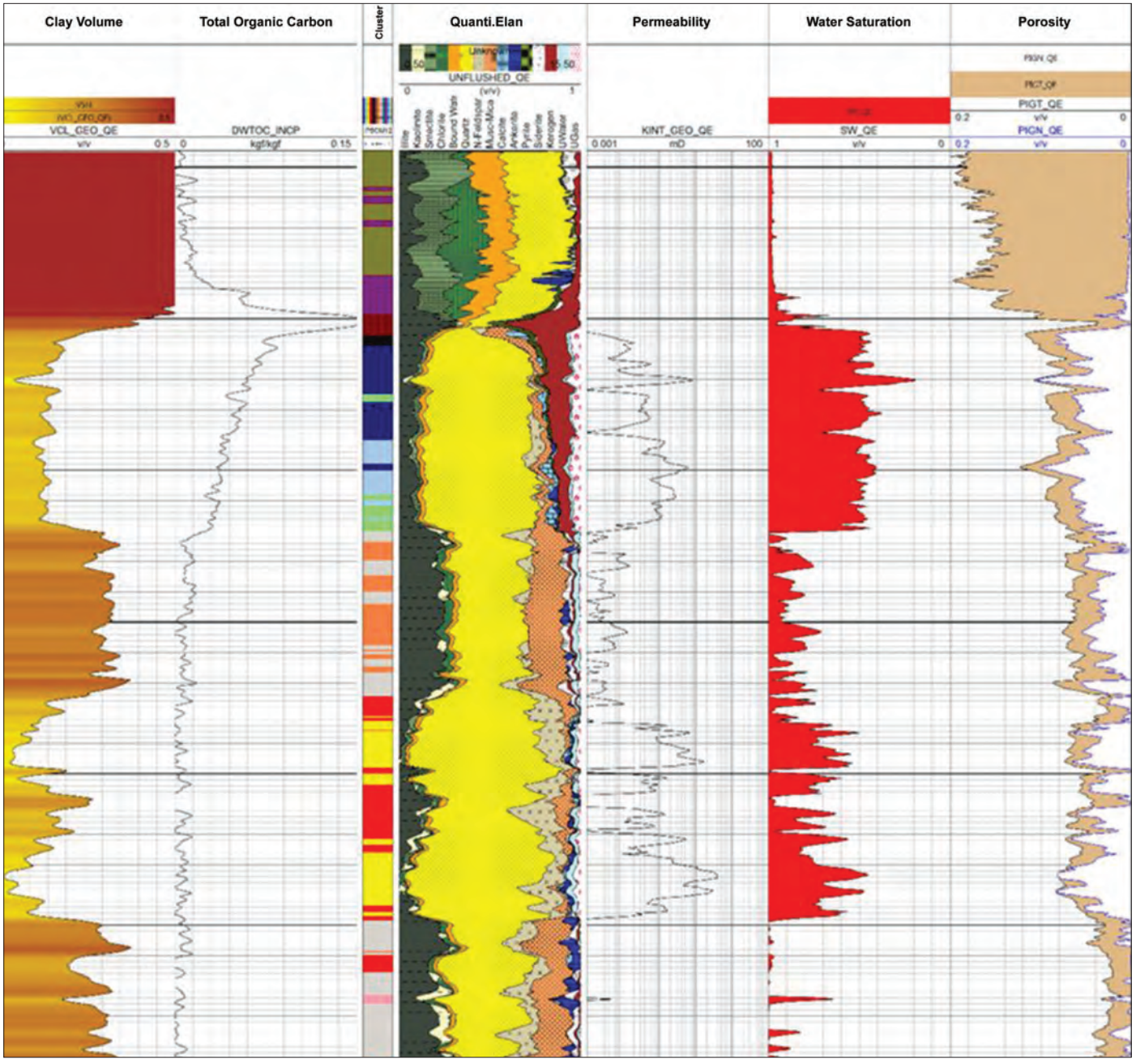

Fig. 11. Petrophysical analysis.

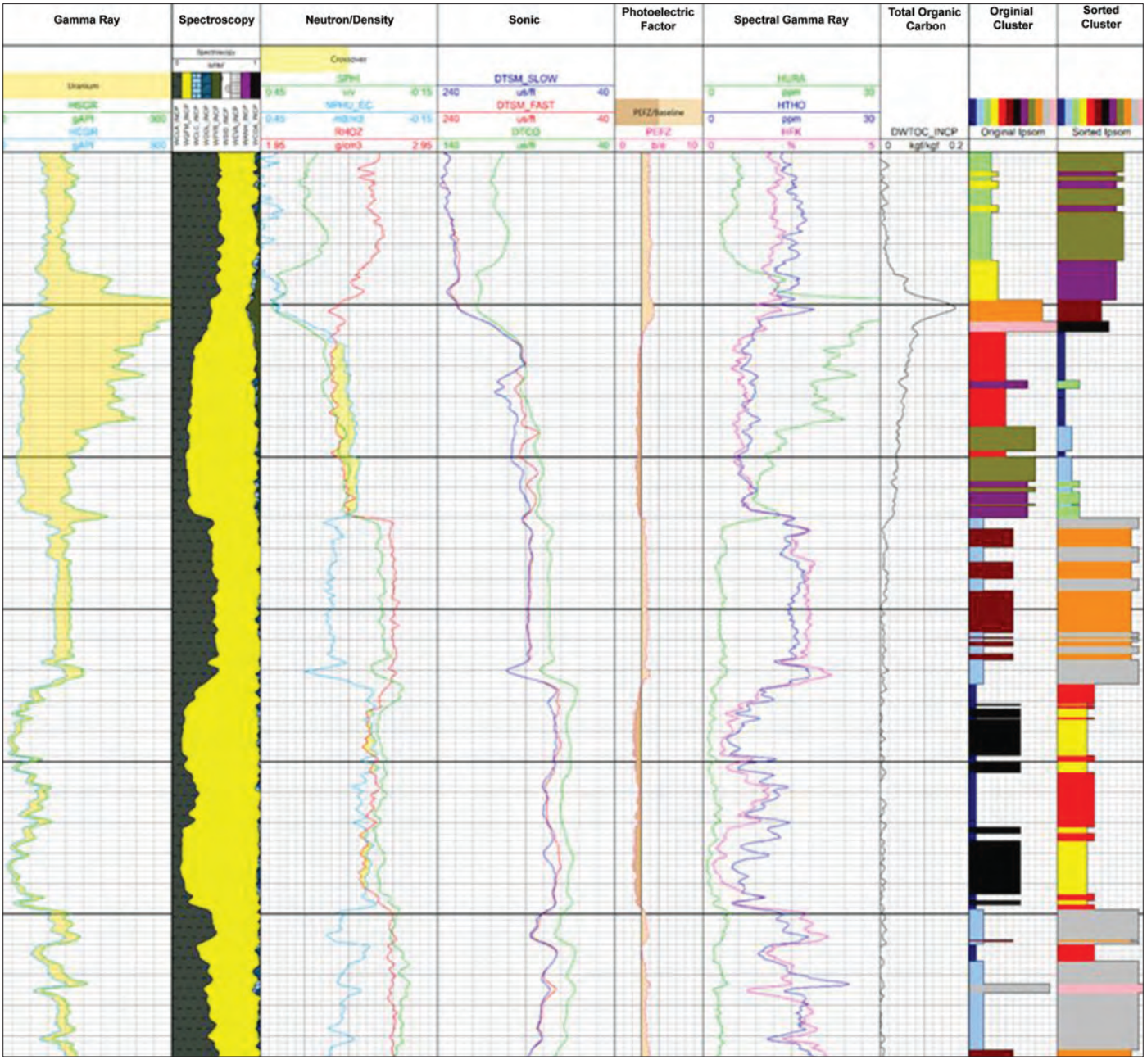

Fig. 12. Input logs, original rock groups with cluster analysis results before re-sorting and results after re-sorting.

(Track 4), permeability (Track 5), water saturation (Track 6) and porosity log (Track 7).

Figure 12 shows input logs with the cluster analysis results before re-sorting and after re-sorting — Tracks 8 and 9, respectively. The properties illustrated in Fig. 12 are gamma ray (Track 1), spectroscopy, or SpectroLith (Track 2), neutron density crossover (Track 3), sonic logs (Track 4), photoelectric factor (Track 5), gamma ray spectroscopy (Track 6) and TOC (Track 7). After highlighting the reservoir quality properties in this well, the re-sorted clusters were combined with the anisotropic elastic properties of the rocks in terms of Young quality, Fig. 13.

The result was a successful completion optimization and hydraulic fracture performance.

CONCLUSIONS AND RECOMMENDATIONS

An accurate petrophysical model combined with the geomechanical properties of shale plays is essential for completion and hydraulic fracture design. In this article, a novel technique has been presented that groups iso-property rocks of similar log responses, so that these new groups or facies can be simply recognized with maximum discrimination. This enables the quality of shale rocks to be quantified and identified, ensuring the effective placement of potential and prospective intervals. This technique has been implemented in a case study involving a shale gas well in Saudi Arabia extended across the hot shale facies of the Qusiaba formation.

After quantifying rock properties through the cluster analysis technique explained here, these formed clusters or facies

Color	IPSOM12	Description	VCL	PHIE	TOC
			v/v	v/v	%
	1	Organic Rich Sand 1	0.141	0.088	5.4
	2	Organic Rich Sand 2	0.129	0.082	3.8
	3	Organic Rich Sand 3	0.155	0.065	4.3
	4	Clean Sand	0.090	0.058	0.0
	5	Silty Sand	0.191	0.036	0.0
	6	High TOC Shale	0.302	0.077	9.8
	7	Moderate TOC Shale	0.194	0.091	7.2
	8	Moderate TOC Shale	0.237	0.131	6.1
	9	Low TOC Shale	0.255	0.148	2.8
	10	Very Low TOC Shale	0.342	0.036	0.4
	11	Non-Organic Shale	0.324	0.027	0.3
	12	Non-Organic Shale	0.286	0.001	0.5

Table 1. HRA classifications after re-sorting

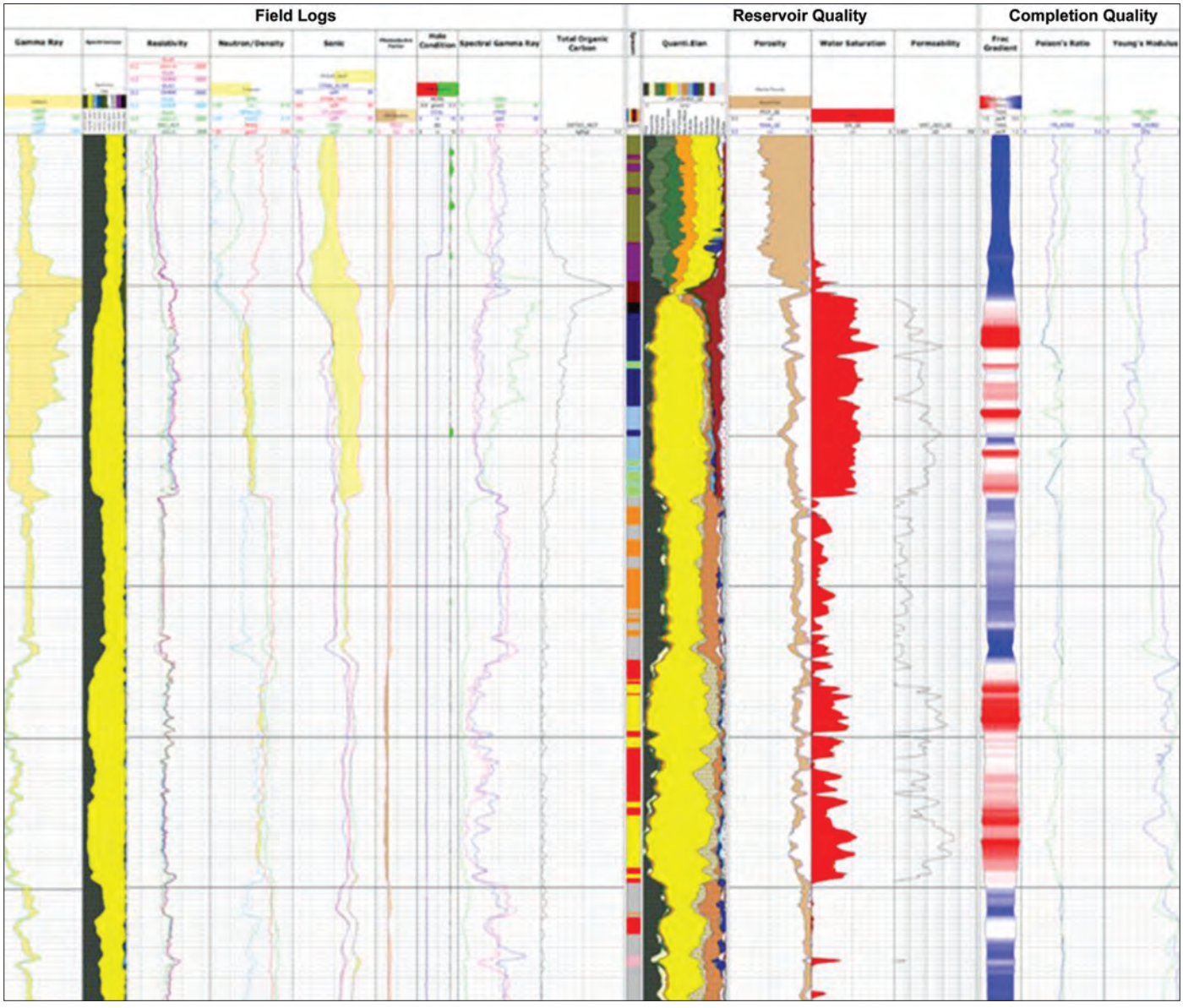

Fig. 13. Integrated solutions: Input logs, reservoir quality and completion quality.

should be propagated from the pilot to the lateral section to evaluate geosteering operations and the staging designs in the lateral sections.

ACKNOWLEDGMENTS

The authors would like to thank the management of Saudi Aramco for their support and permission to publish this article.

This article was presented at the SPE Middle East Oil and Gas Show and Conference, Manama, Bahrain, March 8-11, 2015.

REFERENCES

1. Daniels, J.L., Waters, G.A., Le Calvez, J.H., Bentley, D. and Lassek, J.T.: "Contacting More of the Barnett Shale through an Integration of Real-time Microseismic Monitoring, Petrophysics and Hydraulic Fracture Design," SPE paper 110562, presented at the SPE Annual Technical Conference and Exhibition, Anaheim, California, November 11-14, 2007.
2. Mooi, E. and Sarstedt, M.: *A Concise Guide to Market Research:* The Process, Data and Methods Using IBM SPSS Statistics, Springer, Berlin and Heidelberg, 2011, 308 p.
3. Wedel, M. and Kamakura, W.A.: *Market Segmentation: Conceptual and Methodological Foundations*, 2nd edition, Kluwer Academic, Boston, MA, 1998, 378 p.
4. Forina, M., Armanino, C. and Raggio, V.: "Clustering with Dendrograms on Interpretation Variables," *Analytica Chimica Acta*, Vol. 454, No. 1, March 4, 2002, pp. 13-19.
5. http://stn.spotfire.com/spotfire_client_help/hc/hc_clustering_methods_overview.

BIOGRAPHIES

Osman Hamid is a Petroleum Engineering Specialist with Saudi Aramco's Gas Reservoir Technical & Planning Unit in the Gas Reservoir Management Department. He has 20 years of well-rounded industry experience in various aspects of conventional and unconventional petroleum geomechanics engineering. Osman's work experience has been mainly in 1D, 3D and 4D geomechanics modeling and simulation, hydraulic fracture modeling, rock physics, pore pressure and fracture gradient prediction, wellbore stability modeling, in situ stress constrains and analysis for drilling events, sand prediction, reservoir geomechanics and temperature modeling.

He received his B.S. degree in Geology and Geophysics from the University of Khartoum, Khartoum, Sudan, and his M.S. degree in Geological Engineering and Petroleum Geomechanics from the University of Saskatchewan, Saskatoon, Saskatchewan, Canada.

Dr. Zillur Rahim is a Senior Petroleum Engineering Consultant with Saudi Aramco's Gas Reservoir Management Department (GRMD). He heads the team responsible for stimulation design, application and assessment for conventional and tight gas reservoirs. Rahim's expertise includes well stimulation, pressure transient test analysis, gas field development, planning, production enhancement and reservoir management. He initiated and championed several new technologies in well completions and hydraulic fracturing for Saudi Arabia's nonassociated gas reservoirs.

Prior to joining Saudi Aramco, Rahim worked as a Senior Reservoir Engineer with Holditch & Associates, Inc., and later with Schlumberger Reservoir Technologies in College Station, TX, where he consulted on reservoir engineering, well stimulation, reservoir simulation, production forecasting, well testing and tight gas qualification for national and international companies. Rahim is an instructor who teaches petroleum engineering industry courses, and he has trained engineers from the U.S. and overseas. He developed analytical and numerical models to history match and forecast production and pressure behavior in gas reservoirs. Rahim also developed 3D hydraulic fracture propagation and proppant transport simulators, and numerical models to compute acid reaction, penetration, proppant transport and placement, and fracture conductivity for matrix acid, acid fracturing and proppant fracturing treatments. He has authored more than 90 technical papers for local/international Society of Petroleum Engineers (SPE) conferences and numerous in-house technical documents. Rahim is a member of SPE and a technical editor for SPE's *Journal of Petroleum Science and Technology (JPSE)*. He is a registered Professional Engineer in the State of Texas, and a mentor for Saudi

Aramco's Technologist Development Program (TDP). Rahim teaches the "Advanced Reservoir Stimulation and Hydraulic Fracturing" course offered by the Upstream Professional Development Center (UPDC) of Saudi Aramco.

He is a member of GRMD's technical committee responsible for the assessment, approval and application of new technologies, and he heads the in-house service company engineering team on the application of best-in-class stimulation and completion practices for improved gas recovery.

Rahim has received numerous in-house professional awards. As an active member of the SPE, he has participated as co-chair, session chair, technical committee member, discussion leader and workshop coordinator in various SPE international events.

Rahim received his B.S. degree from the Institut Algérien du Pétrole, Boumerdes, Algeria, and his M.S. and Ph.D. degrees from Texas A&M University, College Station, TX, all in Petroleum Engineering.

Munther M. Al-Shakhs joined Saudi Aramco in 2009. Since then, he has worked in several different roles within various groups in the Exploration Department, including Well Site Geology, Geosteering Operations, Reservoir Characterization, Seismic Acquisition, Processing and Interpretation.

In 2012, he was selected to attend an 18-month program of intensive on-the-job training in unconventional gas with Schlumberger in North America. Upon Munther's return, he joined the Unconventional Resources Exploration and Development Department, working as part of an asset team for unconventional gas exploration in the Jafurah basin.

Munther received his B.S. degree in Geophysics from the University of Leeds, Leeds, U.K.

Ahmed H. Al-Mubarak joined Saudi Aramco in 2008 as a junior geologist specializing in development, horizontal well placement and planning, geosteering and well site geology operations. His experience has continued to grow to include core description, conceptual modeling, 2D and 3D seismic interpretation and prospect generation.

In 2012, Ahmed was selected to attend an 18-month program of intensive on-the-job training in the U.S., which targeted shale gas and unconventional exploration and development. After successfully completing his training, he is now working as a team leader with the Unconventional Resources Exploration and Development Department.

Ahmed received his B.S. degree in Geology with a concentration in Petroleum Geology from the University of Calgary, Calgary, Alberta, Canada.

Kevin Fisher is a Senior Petrophysicist for Schlumberger based in Houston, TX, with 25 years of experience in petrophysics and rock physics. He is currently working in the South Texas Technology Integration Group, focusing on unconventional resource plays, mainly in the Eagle Ford Shale. Kevin's additional areas of experience include the deepwater and shelf areas in the Gulf of Mexico, tight gas sands in South Texas, the Rocky Mountains, Alaska, the Permian Basin, unconventional gas and oil shales, coalbed methane and international areas (Australia, Brazil, Argentina, U.K., France, Nigeria, Angola, Turkey and Saudi Arabia).

He received his B.S. degree in Petroleum Engineering from the University of Tulsa, Tulsa, OK.

Omar A. Bawazir is a Senior Petrophysicist with Schlumberger Middle East. He has more than five years of experience in petrophysical activities associated with active field development, with the practical skills of interpreting real data for both conventional and unconventional resources. Omar's work experience involves integrating petrophysical analyses with mechanical elastic properties and differential stresses around boreholes utilizing acoustic data with the intent to optimize production.

He received his B.S. degree in Geophysics and an M.S. degree in Petroleum Geology, both from King Fahd University of Petroleum and Minerals (KFUPM), Dhahran, Saudi Arabia.

The Successful Application of MPD Technology in Drilling Horizontal Wells in High-Pressure Formation Heterogeneity to Mitigate Drilling Hazards: Case Study

Authors: Nelson O. Pinero, Abdulaziz S. Mutawa, Ayoub Hadj-Moussa, Mohamed Cherif Mazouz, Paco Viera and Ramon Zambrano

ABSTRACT

Highly pressurized intervals, coupled with high permeability, make the drilling of a 6⅛" horizontal hole section particularly challenging in water injector wells, as mud losses are frequently encountered along with differential sticking events. The objective of workover operations in the field is to sidetrack the power water injector (PWI) from the existing well motherbore, converting the well to a dual lateral, which will maintain the reservoir pressure and enhance oil recovery from the oil-bearing formation. The variance in formation pressure distribution makes drilling with high mud density systems a challenge and increases the risk of encountering losses and differential sticking.

To overcome the challenges mentioned, the application of managed pressure drilling (MPD) technology using the constant bottom-hole pressure (CBHP) method during the drilling of the 6⅛" hole section enables use of a mud system that is statically below the formation pressure, while keeping the equivalent circulating density (ECD) slightly over the formation pressure and constant at static and dynamic conditions. This is achieved by applying surface back pressure (SBP) using an automated MPD control choke manifold. As the drilling is continued in the lateral, a dynamic formation pressure evaluation can be performed to assess the changing formation pressure and to adjust the drilling parameters.

This article will summarize the results of using MPD, compare it to conventional drilling methods and highlight the lessons learned from the application of the MPD (CBHP variant) approach described to enhance drilling efficiency and to mitigate drilling hazards, such as losses and differential sticking. The analysis will further enhance the drilling practices of PWI wells.

INTRODUCTION

Saudi Aramco started a project to reenter and work over some power water injector (PWI) wells to maintain the reservoir pressure and increase oil recovery. The wells are drilled to an average measured depth (MD) of 14,000 ft, with an average of 6,500 ft of open hole section across the reservoir. This 6⅛" horizontal open hole section is particularly challenging in workover operations due to formation heterogeneity and the rapid change in formation pressure within the same lateral resulting from water injection activities around the area. Using conventional drilling techniques to work over these wells led to a significant increment in the nonproductive time (NPT) due to differential sticking and lost circulation. The campaign field in question has seen on average a 35% increase in reservoir pressure during the past three years due to water injection activity for production maintenance, which added to the complexity of the reentry operations. The PWI wells are drilled close to the field boundaries[1].

In an effort to apply the latest technology and new drilling methods to mitigate the challenges mentioned, Saudi Aramco started using managed pressure drilling (MPD) in late 2012 to work over wells in the campaign field. Previous experience in Saudi Arabia had proven the benefits of the MPD technology, which considerably reduced the NPT related to differential sticking, lost circulation and formation fluid influx. This was achieved by having a more accurate control of the annular pressure profile and by more precise monitoring of the well, which allowed for a much quicker response to pressure changes[2].

MPD is known as a drilling process optimization tool, whose main objectives are to mitigate the drilling hazards so as to enhance control of the well and reduce NPT. In other words, MPD helps operators to drill successfully to the planned target while saving costs and improving safety conditions[3].

MPD provides the ability to navigate through narrow drilling windows — in terms of formation pore/fracture pressures — and to avoid letting any fluid from the formation come into the wellbore. In case of an influx, a quick adjustment in the surface back pressure (SBP) can be made, which allows for a much faster response, thereby minimizing the consequences of the influx. Typically, the MPD provides the ability to circulate a kick while maintaining the drilling pump rate, which minimizes the time for kick circulation. These unique abilities proved essential in drilling wells in the campaign field, where high-pressure formation heterogeneity was encountered.

The MPD application and its results showcased here will illustrate how using MPD technology has enabled effective equivalent circulating density (ECD) management in challenging long horizontal laterals, eliminated differential sticking incidents, increased the rate of penetration (ROP), allowed for

better well construction design and reduced the overall cost of operations.

MPD APPLICATION SUMMARY

The first MPD application on the campaign field was in Well MPD-1 in November 2012. With the implementation of the MPD method, the proposed drilling performance objectives set during the planning phase of the well were achieved, as follows:

- The borehole pressure was successfully maintained above the pore pressure, avoiding influx, mud losses and hole instability. As a result, NPT due to stuck pipe and fishing events was mitigated.
- Enhanced formation evaluation while drilling was conducted by performing dynamic formation integrity tests (DFITs) and dynamic pore pressure tests (DPPTs) using the automatic MPD system.
- The drilling mud weight (MW) was reduced from up to 105 pounds per cubic foot (pcf) — as conventionally planned — to 80 pcf for the MPD wells, which reduced the formation damage across the reservoir and so yielded a better injectivity across the lateral.
- On average, the ROP was increased by 25% when comparing the drilling of MPD wells vs. their conventional counterparts.

By utilizing MPD, Well MPD-1 was successfully drilled as a 6⅛" horizontal lateral through the reservoir formation, achieving a total well depth of 13,618 ft MD, with a true vertical depth of 6,666 ft and a horizontal lateral footage of 7,003 ft, making it one of the longest horizontal laterals drilled using MPD in the world.

Table 1 summarizes the results from all the MPD wells drilled in the campaign field from 2012 to 2014. Figure 1 illustrates the ROP performance on the MPD wells.

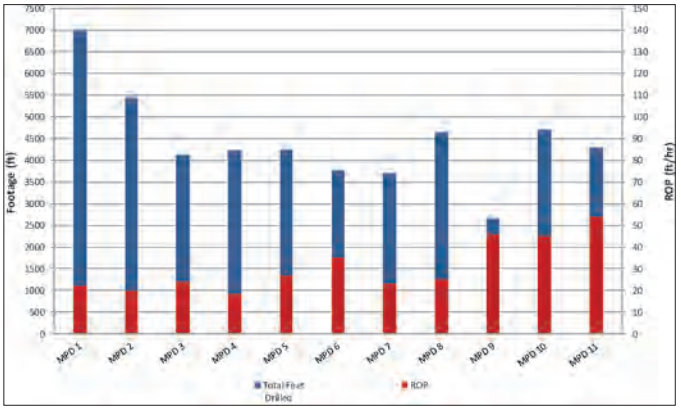

Fig. 1. Footage and ROP performance for MPD wells.

MPD ENGINEERING PLANNING

The approach taken to reach the MPD operation objectives was based on Saudi Aramco's Workover Program. The objectives were to apply the MPD technique to optimize the drilling process in a 6⅛" hole by using the lowest MW possible, and to apply the required pressure at the surface to achieve the targeted initial pore pressure value. Once the drilling operation started, the parameters were adjusted after performing a DPPT. The SBP could be adjusted according to the new pore pressure value, and if it was required, the MW could be changed to give more flexibility to cope with any rapid change in the pore pressure regime.

Hydraulic simulations were run with different MWs to determine the SBP needed to achieve the initial target ECD at the top of the window. Figure 2 shows an example of the ECD operating window that was prepared for each MPD application, then updated as required. The operating window plots show the effective ECD at the anchor point using a series of MWs vs. SBP; the operating limits were set in accordance with the surface equipment pressure rating, pore pressure and DFIT results, if available.

Year	Well Name	Hole Size	Total Ft Drilled	ROP (ft/hr)	Total Drilling Hours	MW (pcf)	ECD at Shoe (pcf)	ECD at Bottom (pcf)
2012	MPD-1	6⅛"	7,003	22	318	80	96	104
	MPD-2	6⅛"	5,438	20	272	80	98	101
2013	MPD-3	6⅛"	4,114	24	171	75	93	97
	MPD-4	6⅛"	4,222	18	235	80	94	98
	MPD-5	6⅛"	4,253	27	158	80	92	96
	MPD-6	6⅛"	3,759	35	107	80	90	96
	MPD-7	6⅛"	3,700	23	161	80	93	97
	MPD-8	6⅛"	4,643	25	129	80	93	97
	MPD-9	6⅛"	2,663	46	58	80	90-94	95
2014	MPD-10	6⅛"	4,712	45	106	85	104	106
	MPD-11	6⅛"	4,298	54	80	85	102	105

Table 1. MPD wells summary

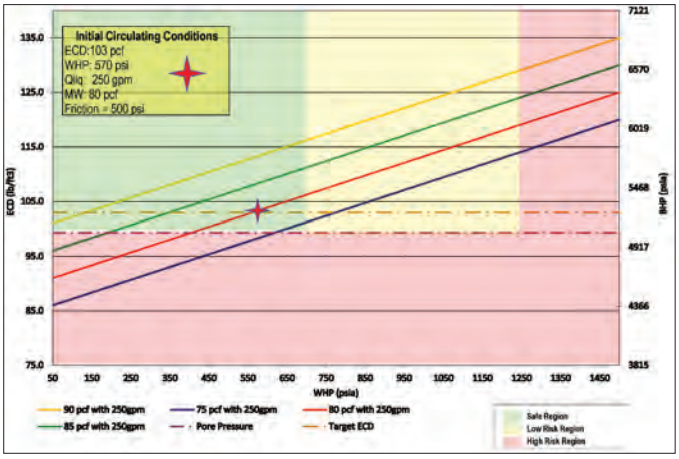

Fig. 2. MPD controllability window.

Safety and sound engineering planning are paramount in operations where MPD is applied. So, prior to the commencement of drilling, the following were prepared and communicated to all parties involved in the operations:

- The MPD drilling program — taking into consideration operational and health, safety and environment (HSE) contingencies.
- A set of detailed operational procedures.
- The well control matrix to set the drilling limits, kick tolerance and well shut-in point.
- Operating and drilling envelopes.
- A detailed set of decision trees.

PORE PRESSURE REGIME CHALLENGES

One of the most significant challenges in drilling the campaign field's wells was the presence of a nonhomogeneous pore pressure regime within the same formation, encountered as it was drilled horizontally. This was due mainly to the water injection activity in the field. This challenge was addressed by analyzing conventional MW management methods and comparing the results with the abilities of the MPD technique in regard to pore pressure determination and ECD management.

MW Management during Conventional Drilling

One of the methods used in conventional drilling to assist in improving MW management is the formation tester while drilling (FTWD) tool, Fig. 3, which is run to determine the pore pressure value, after which the MW is managed accordingly.

The tool utilizes a probe and packer concept similar to that used in conventional wireline formation tests. A packer and probe are extended into the formation, and a small sample chamber is used to pressure test the formation. To obtain a formation pressure value this way, operators have to stop drilling for a minimal period[4].

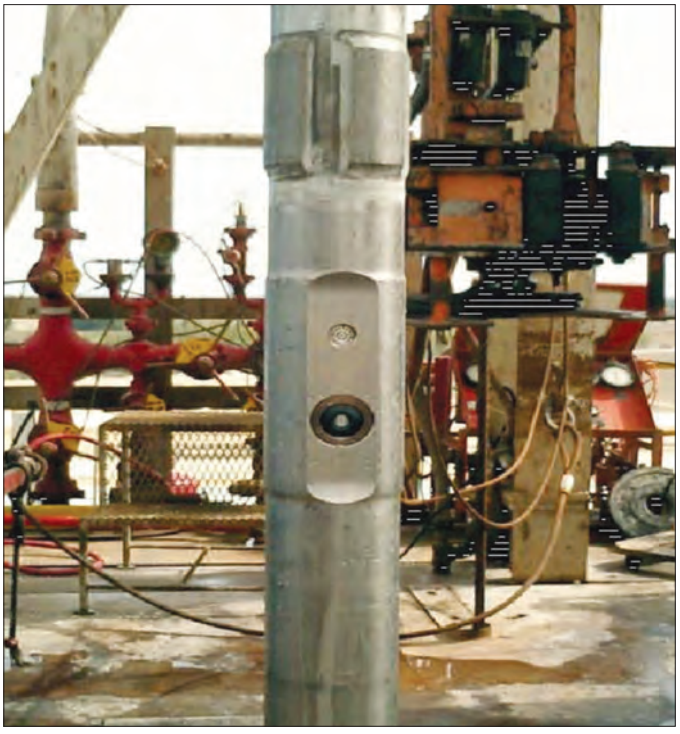

Fig. 3. The FTWD tool[4].

The FTWD tool was run in the 6⅛" hole section of Well CONV-1 in the campaign field to take pressure points in the drilling environment. Nine pressure test points were taken during the drilling operation. Figure 4 represents the formation pressure reading results. It can be observed that the pore pressure distribution within the same horizontal hole section is not constant; it starts from a higher value and decreases as drilling continues away from the original vertical motherbore. This phenomenon can be attributed to the water injection activity that was performed on the horizontal hole prior to the workover reentry.

Based on the results of each application of the FTWD tool, the MW can be adjusted to achieve the optimum overbalance condition on the drilling section. This method has the advantage of providing accurate pore pressure from the formation while drilling, since the FTWD is run as part of the measurement while drilling string.

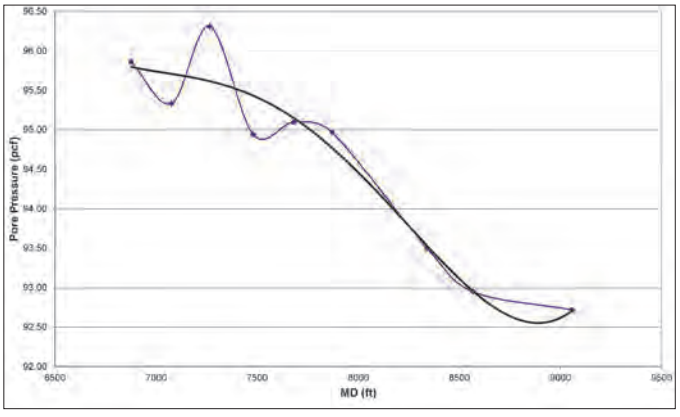

Fig. 4. Pore pressure distribution determined by using the FTWD tool.

The FTWD operation to record the formation pressure can take up to 1½ hours — according to actual drilling reports — during which time the drillstring has to be kept stationary with no circulation for 15 minutes to 45 minutes, depending on the formation and the hole condition. Keeping the drillstring static for the duration of the recording time poses a great risk for differential sticking in horizontal drilling applications.

After the tool provides the correct formation pressure, and if the decision is made to increase or decrease the MW, the well has to be completely displaced to the new MW, an operation that can take up to 3 hours — depending on the well geometry and the rig mud system capabilities.

This shows that the conventional FTWD method of MW management comes with high risk and is a time-consuming process.

Pore Pressure Determination Using a MPD System

One of the benefits of using the MPD technique is the ability to evaluate the formation pressure limit by performing a DPPT and DFIT. The DPPT is performed by gradually reducing the SBP in steps until a minor influx — less than 2 barrels — is observed and controlled. The ECD at which the influx is first registered represents the pore pressure value and is dynamically calculated by the MPD system. In the case where the MPD choke is completely open and no influx is observed, the pump rate will gradually be reduced in steps until a minor influx is observed and controlled, again resulting in the determination of the pore pressure value with high certainty. Figure 5 represents the DPPT performed in Well MPD-10.

Use of the ECD Management Feature of the MPD System

After identifying the MPD controllability window, circulating parameters to be used while drilling are defined. These parameters maintain the dynamic downhole pressure within an operational window that is bounded by the formation pressure (lower limit) and the fluid loss pressure (upper limit). Both limits are evaluated as drilling progresses by adjusting the surface pressure at the MPD choke.

The MPD choke adjustments produce instantaneous changes in the ECD to achieve the target bottom-hole pressure (BHP). Figure 6 shows the depth-based data of the BHP profile as changes were made during drilling.

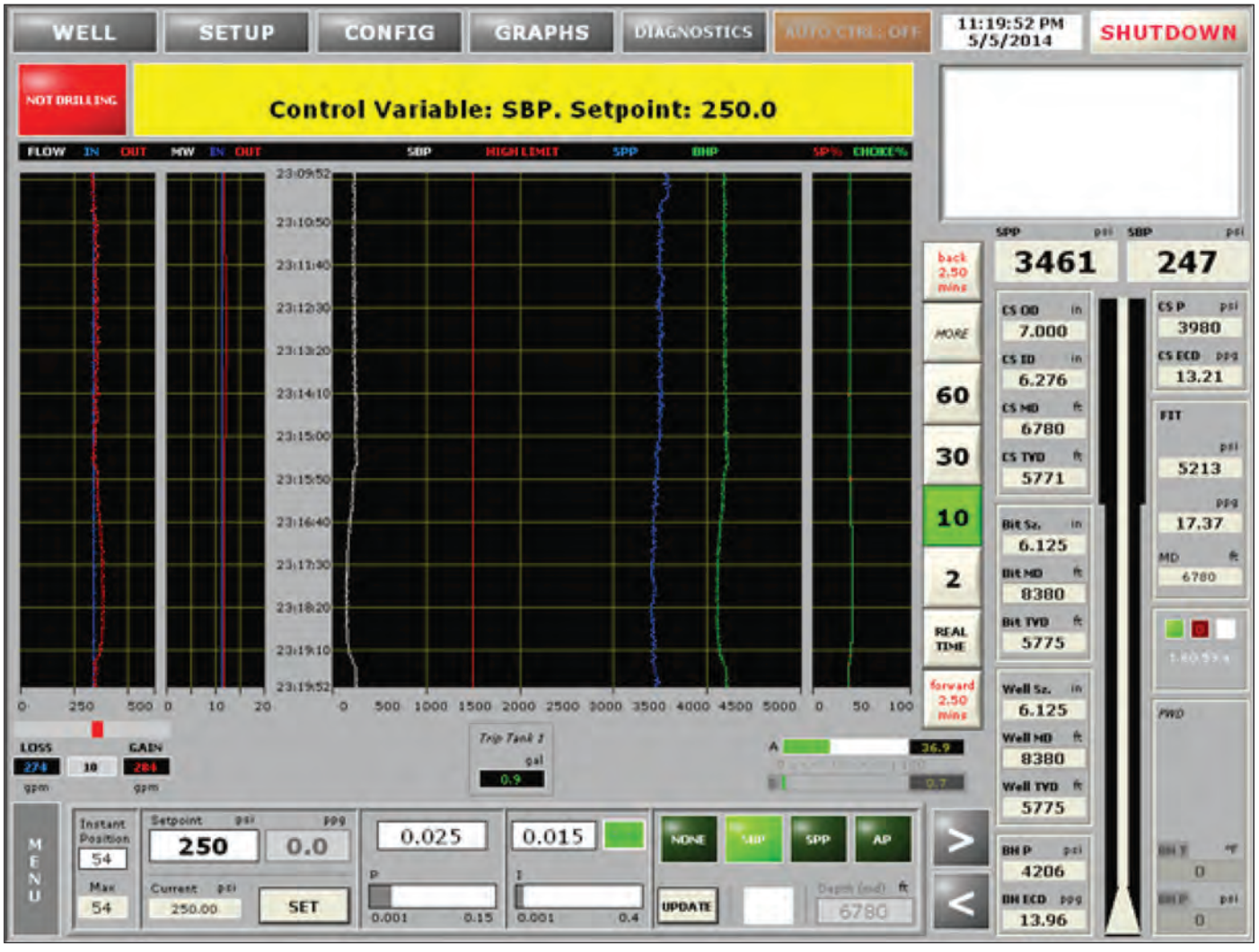

Fig. 5. DPPT for Well MPD-10.

As can be observed from Fig. 6, the pore pressure distribution determined by using the MPD DPPT is similar to the one registered by the FTWD tool in Well CONV-1, Fig. 4. This confirms the complexity of drilling reentry wells in the campaign field with one MW system. While with conventional drilling the whole mud system had to be changed over as the pressure regime required, using the MPD constant bottom-hole pressure (CBHP) technique required no change in MW since the system could achieve optimum ECD by simply adjusting the SBP.

DIFFERENTIAL STICKING

Stuck pipe incidents, and differential sticking in particular, are one of the major challenges to drilling reentry wells in the campaign field, raising the risk of a significant amount of lost time and associated costs. At Saudi Aramco, the recent increase in drilling activity, especially drilling in depleted/higher risk reservoirs, has led to an increased risk of stuck pipe, and so mitigating this challenge is a priority.

Efforts to minimize stuck pipe incidents are not new to Saudi Aramco. But the impact of those past efforts has not been consistent. The objective of the Saudi Aramco Stuck Pipe Task Force therefore was to concentrate on accelerating the reduction of Saudi Aramco's stuck pipe costs[5].

Conventional Strategies to Reduce Stuck Pipe Risk

Review of the Saudi Aramco Stuck Pipe Task Force findings and best practices of 2009 concluded that 69.5% of the total stuck pipe incidents were due to mechanical sticking, whereas 30.5% was attributed to differential sticking[6].

The following best practices were then implemented to mitigate stuck pipe incidents[6]:

- Raising the level of stuck pipe prevention awareness.
- Improving the response time for stuck pipe incidents to lower the event duration from an average of 60 hours to an average of less than 24 hours.
- Improving the planning for well direction, mud properties and hydraulics, and applying enhanced hole cleaning practices to reduce risks.
- Revising the bottom-hole assembly (BHA) design to enhance hole cleaning and optimize jar placement.

After the above practices were implemented, data analyzed from wells drilled between 2010 and 2011 showed a relatively modest positive impact[6]:

- There was a 12% drop in stuck pipe events reported in 2011 as compared to 2010.
- The average NPT related to each event was reduced by 13%.

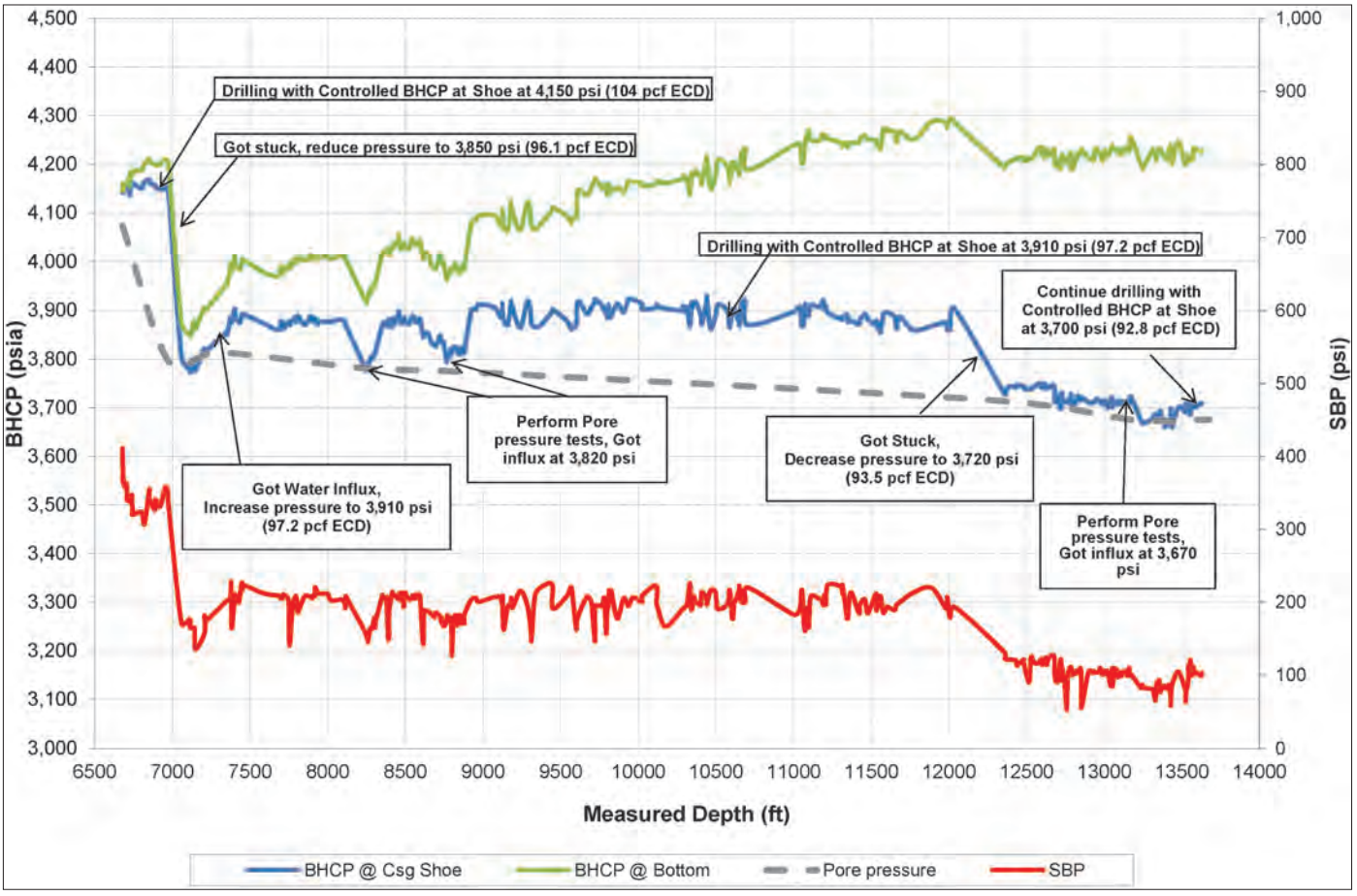

Fig. 6. Changes made in bottom-hole circulating pressure using the MPD system.

MPD Strategy to Reduce Stuck Pipe Risk

From the discussion of conventional strategies, it can be observed that even though a great deal of effort was made to reduce the risks of stuck pipe incidents, the incidents still were occurring and remained part of the inherent risks of drilling wells, especially in the campaign field.

Results showed, however, that the use of MPD as a stuck pipe prevention method can reduce, and in some cases eliminate, the occurrence of differential sticking by applying the following techniques made possible by the technology:

- Reduce the amount of overbalance applied against the formation as the well is drilled in near-balanced condition using the CBHP MPD technique.
- Exert and relieve pressure on the wellbore as required using the MPD system's programmable logic controller with its automatic control ability to increase or decrease the ECD instantly. This is done by manipulating the MPD choke manifold at the surface. The ability to manipulate the ECD as required can get the string unstuck within minutes.
- Reduce the amount of time the string is kept stationary by using the rotating control device (RCD) that allows both reciprocating and rotating movements of the string while holding pressure.
- Keep the pressure exerted on the wellbore constant while drilling, during connection, and when stripping in or out of hole by using the CBHP technique. Reducing the cycling of the pressure on the bottom reduces the risk of stuck pipe.
- The MPD system, in combination with the RCD, also provides the ability to strip out of hole under pressure, and in CBHP mode, to kill the well inside the casing shoe, where losses and gains are monitored to ensure the well is balanced.

While drilling the MPD reentry wells in the campaign field, operators encountered numerous instances where the string was differentially stuck — confirmed by the increase in torque and drag, inability to move or rotate the pipe, ability to circulate — due to the challenging pore pressure regime of the formation. In all such instances, shortly after confirmation of differential sticking, the MPD system was used to reduce the SBP gradually while monitoring returns, and at the moment where the well was in balance, the string became free — typically in less than 1 hour. The following describes one such sticking event involving Well MPD-1, Fig. 7.

As observed in Fig. 7, the sudden increase in the stand pipe pressure indicates the moment when the string became stuck for the first time in the section. At this moment, the hole depth was 6,981 ft MD. Prior to this event, the ECD being kept at the bottom was 104 pcf, having a SBP of 680 psi. Once the

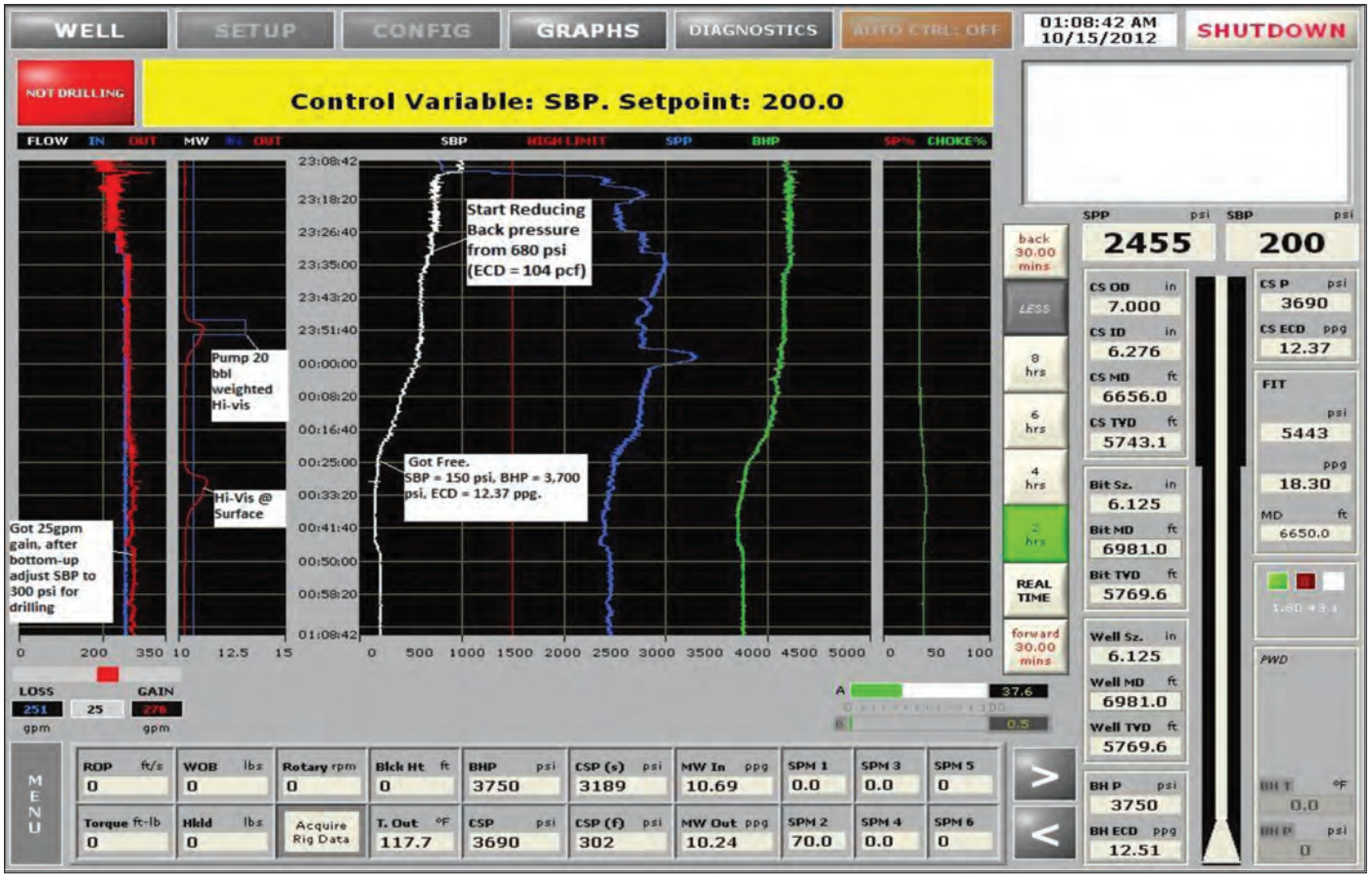

Fig. 7. Stuck pipe event (Well MPD-1).

pipe was confirmed to be differentially stuck, the SBP was brought down gradually, with operators closely monitoring the fluid returns. When an ECD of 92.5 pcf was reached, the pipe became free.

After drilling 11 wells as part of the MPD water injector project, the team observed that although 11 differential sticking events were encountered, using the MPD system's advantages enabled the drillstring to come free within 15 minutes to 60 minutes; drilling/stripping then continued after adjusting the surface pressure and drilling parameters. This practice resulted in no NPT due to stuck pipe in all MPD wells, in comparison to similar wells that were drilled conventionally in the campaign field, which showed an average of 151 hours of NPT per well, Table 2.

WELL CONSTRUCTION

Some of the reentry wells in the campaign field were designed to drill through two different formations. The pressure difference between two formations is an important factor in the design of a well. The uncertainties in these pressures, as well as the use of high-density mud, can create a condition of excessive overbalance, which is the main cause of differential sticking and lost circulation problems.

The conventional plan to drill through these two formations was first to mill a window through the 7" liner, next to drill a 6⅛" lateral hole section across the first formation and then to run an expandable liner to isolate that formation. The second formation would then be drilled as a 5½" hole section to total depth (TD) to avoid any problems related to the differential pressure between the two formations[7].

Using MPD as a drilling and well construction technique presented a solution to the challenge of different pressures as previously stated. The results of the well exceeded the original expectations for the benefits. Drilling two formations with two distinct pressure profiles in one hole section using CBHP MPD eliminated any differential sticking or lost circulation incidents as a result of precise ECD management. In addition, the cost of running the solid expandable liner across the first formation was saved, and the well was completed as a 6⅛" open hole instead of 5½" as originally planned.

Wells Drilled Conventionally		Wells Drilled with MPD	
Well	**NPT (hours)**	**Well**	**NPT (hours)**
Conv-1	615.5	MPD-1	4
Conv-2	126	MPD-2	0
Conv-3	74.5	MPD-3	0
Conv-4	0	MPD-4	0
Conv-5	0	MPD-5	0
Conv-6	150.5	MPD-6	0
Conv-7	88.5	MPD-7	0
Average	**151**	**Average**	**0.6**

Table 2. Stuck pipe NPT comparison (Conv. vs. MPD wells)

ROP IMPROVEMENT USING THE MPD SYSTEM

Several factors can affect the ROP, e.g., bit type, formation characteristics, rock properties, and most importantly, drilling fluid properties, mainly density. An increase in drilling fluid density causes an increase in the BHP beneath the bit, thereby causing an increase in the pressure differential between the drilling fluid pressure and the formation fluid pressure[8].

In MPD, the hydrostatic and dynamic pressures exerted by the drilling fluid are maintained in near-balanced conditions. The ROP is significantly increased while drilling with less positive differential pressure and improves even more when the differential pressure is negative — underbalanced condition[9].

Figure 8 illustrates the ROP trend for Well MPD-10 as an example in comparison with the average ROP trend registered when similar wells were conventionally drilled in the campaign field.

Table 3 summarizes the ROP performance of the MPD wells compared to similar conventional wells drilled in the

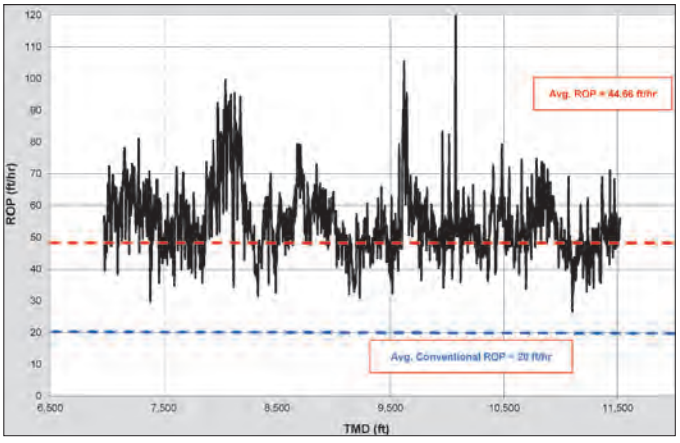

Fig. 8. ROP for Well MPD-10.

Wells Drilled Conventionally		Wells Drilled with MPD	
Well	**Average ROP (ft/hour)**	**Well**	**Average ROP (ft/hour)**
Conv-1	23	MPD-1	22
Conv-2	19	MPD-2	20
Conv-3	17	MPD-3	24
Conv-4	22	MPD-4	18
Conv-5	24	MPD-5	27
Conv-6	18	MPD-6	35
Conv-7	18	MPD-7	23
Average	**20**	**Average**	**25**

Table 3. ROP comparison (Conv. vs. MPD wells)

campaign field. All the wells mentioned in the comparison had the following characteristics:

- A 6⅛" horizontal hole section was drilled in the same formation as the PWIs.
- A similar BHA configuration was used.
- All of the wells required MWs of 95 pcf and above.

This data shows that utilizing MPD technology resulted in a 25% improvement in ROP.

MUD SYSTEM

Previous studies conducted by Saudi Aramco have shown that the use of conventional potassium chloride polymer, water-based drilling fluids or single salt brines weighted up with calcium carbonate can lead to several problems, including[10-12]:

- Differential sticking due to excessive overbalances exerted on the formation.
- Downhole fluid losses near the end of the horizontal section due to high ECD.
- Formation damage due to excessive solids invasion to the formation.

Prior to introducing the MPD technique to the campaign field, and to address the challenges previously mentioned, sodium/potassium formate or calcium bromide drilling fluids were used. These high-density — up to 142 pcf or 19 ppg — fluids can be mixed over a broad range of concentrations and/or temperatures without crystallization and solubility problems. These drilling mud systems were used to achieve a stable +96 pcf mud system, which is unattainable by using a calcium chloride ($CaCl_2$) mud system alone.

Introducing the MPD technique meant the use of a high-weight drilling fluid system was not required anymore. To achieve the target ECD required for the campaign field formation, the basic 80 pcf $CaCl_2$ and a more economical system could be used. Table 4 shows the different mud types used in conventional and MPD applications.

The use of a $CaCl_2$ mud system with the MPD technique reduced the mud cost 50% compared to the advanced drilling fluid system used conventionally to drill in the campaign field.

ECONOMIC COMPARISON

Comparing wells that were drilled with MPD technology with similar wells that were drilled conventionally reveals a significant overall cost saving with MPD.

- When the MPD system is used to determine the pore pressure value, the overall cost is reduced compared to using the FTWD tool while drilling conventionally. The DPPT time is 15 minutes to 20 minutes, compared to the FTWD time, which can take up to 1½ hours. In addition, if the MW must be changed, the adjustment of ECD using the MPD system takes minutes, compared to changing the entire mud system while drilling conventionally.
- For wells drilled with the MPD system in the campaign field, the average registered NPT due to differential pipe sticking was 0.6 hour per well, compared to an average of 151 hours per well in those drilled conventionally. This translates to a savings of more than 6.3 rig days per well.
- Drilling with MPD technology allows engineers, in some cases, to drill through multiple formations with different pore pressure regimes at one time, eliminating the need to case off the upper weaker zone. This was successfully demonstrated in Well MPD-9, where the lateral was drilled from the start to TD as a 6⅛" hole using MPD technology instead of covering the upper formation with a 7" × 5½" expandable liner, as originally planned. This yielded a significant savings in the running time and materials required for the expandable liner.

Wells Drilled Conventionally			Wells Drilled with MPD			
Well	**MW (pcf)**	**Mud Type**	**Well**	**MW (pcf)**	**Mud Type**	**ECD (pcf)**
Conv-1	105	Potassium Formate	MPD-1	80	$CaCl_2$	104
Conv-2	102	$CaBr_2$	MPD-2	80	$CaCl_2$	101
Conv-3	102	$CaBr_2$	MPD-3	75	$CaCl_2$	97
Conv-4	103	$CaBr_2$	MPD-4	80	$CaCl_2$	98
Conv-5	95	$CaCl_2/CaBr_2$	MPD-5	80	$CaCl_2$	96
Conv-6	104	$CaBr_2$	MPD-6	80	$CaCl_2$	96
			MPD-7	80	$CaCl_2$	97
			MPD-8	80	$CaCl_2$	97
			MPD-9	80	$CaCl_2$	95
			MPD-10	85	$CaCl_2$	106
			MPD-11	85	$CaCl_2$	105

Table 4. Drilling fluid systems for conventional and MPD applications

- As a result of using the MPD system, an improvement of 23% in rig time was observed, resulting in saving two rig days for every 4,000 ft drilled in the target formation. This is a direct result of increasing the ROP by 25% when compared to conventional drilling.
- When comparing MPD technology with conventional drilling in the campaign field in terms of mud costs, it was found that an average of 50% cost savings in drilling fluid was achieved.

CONCLUSIONS

When analyzing the data collected from all MPD and conventional applications in the campaign field, it is apparent that utilizing the MPD system presents a step change in the way to drill reentry horizontal water injector wells in the campaign field. This was proven without a doubt by an analysis of the drilling performance and the economics of the wells that were drilled using MPD as compared to similar wells drilled conventionally.

The successful MPD project in the campaign field is seen as the first stepping-stone in the adaptation of MPD in different applications across multiple fields in Saudi Arabia. The lessons learned (operations, engineering and quality HSE) from the campaign field application have been instrumental in the success of other ongoing projects involving MPD with Saudi Aramco.

ACKNOWLEDGMENTS

The authors would like to thank the management of Saudi Aramco and Weatherford International Ltd. for their support and permission to publish this article.

This article was presented at the SPE/IADC Managed Pressure Drilling and Underbalanced Operations Conference and Exhibition, Dubai, UAE, April 13-14, 2015.

REFERENCES

1. Kragjcek, R.H.T., Al-Dossary, A.S., Kotb, W.G. and El-Gamal, A.E.: "Successful Application of New Sliding Technology for Horizontal Drilling in Saudi Arabia," *Saudi Aramco Journal of Technology,* Fall 2011, pp. 28-33.
2. Al-Thuwaini, J., Emad, M., Iman, K., Torres, F., Russell, R. and Arnone, M.A.: "Managed Pressure Drilling, the Impact of Correctly Applying the Technology and the Results Obtained After Drilling an Exploratory Well in a Deep Gas Reservoir of Saudi Arabia," SPE paper 131960, presented at the SPE Deep Gas Conference and Exhibition, Manama, Bahrain, January 24-26, 2010.
3. Qutob, H.H., Vieira, P., Torres, F. and Arnone, M.A.: "Managed Pressure Drilling Applications Proves Successful in the Middle East and North Africa Region," SPE paper 148534, presented at the SPE/IADC Middle East Drilling Technology Conference and Exhibition, Muscat, Oman, October 24-26, 2011.
4. Seifert, D.J., Burinda, B.J., Kellett, S. and Al Dossari, S.: "Application for Formation Testing While Drilling in the Middle East," SPE paper 93392, presented at the SPE Middle East Oil and Gas Show and Conference, Bahrain, March 12-15, 2005.
5. Hopkins, C.J. and Leicksenring, R.A.: "Reducing the Risk of Stuck Pipe in The Netherlands," SPE paper 29422, presented at the SPE/IACD Drilling Conference, Amsterdam, The Netherlands, February 28 - March 2, 1995.
6. Muqeem, M.A., Weekse, A.E. and Al-Hajji, A.A.: "Stuck Pipe Best Practices — A Challenging Approach to Reducing Stuck Pipe Costs," SPE paper 160845, presented at the SPE Saudi Arabia Section Technical Symposium and Exhibition, al-Khobar, Saudi Arabia, April 8-11, 2012.
7. Pinero Zambrano, N.O., Al-Ageel, I.M., Muqeem, M.A., Al Mutawa, A.S., Mazouz, M.C., Hadj-Moussa, A., et al.: "Optimizing Well Design in Saudi Arabia: Successful Application of Managed Pressure Drilling Enables Drilling Across Multiple Pressure Zones and Running Liner Using Constant Bottom-hole Pressure Technique," SPE paper 170554, presented at the IADC/SPE Asia Pacific Drilling Technology Conference, Bangkok, Thailand, August 25-27, 2014.
8. Foster, J.K. and Steiner, A.: "The Use of MPD and an Unweighted Fluid System for Drilling ROP Improvement," SPE paper 108343, presented at the IADC/SPE Managed Pressure Drilling and Underbalanced Operations Conference and Exhibition, Galveston, Texas, March 28-29, 2007.
9. Garrido Cruz, R.A., Muqeem, M.A., Alghuryafi, A.M., Duran, R.C., Hadj-Moussa, A., Mazouz, C.M., et al.: "Combining Managed Pressure Drilling and Advanced Surface Gas Detection Systems Enables Early Formation Evaluation and Enhances the Drilling Efficiency in a Deep Gas Exploratory Well in Saudi Arabia," SPE paper 171495, presented at the SPE Asia Pacific Oil and Gas Conference and Exhibition, Adelaide, Australia, October 14-16, 2014.
10. Simpson, M.A., Al-Reda, S., Al-Khamees, S., Zhou, S., Treece, M. and Ansari, A.: "Overbalanced Drilling of Extended Horizontal Sections with Potassium Formate Brines," SPE paper 926407, presented at the SPE Middle East Oil and Gas Show and Conference, Bahrain, March 12-15, 2005.
11. Al-Harbi, A.A., Ersoz, H. and Abdrabalreda, S.: "Influence of Sodium/Potassium Formate-based Drilling Fluids on Nuclear Logs," SPE paper 94693, presented at the SPE Latin American and Caribbean Petroleum

Engineering Conference, Rio de Janeiro, Brazil, June 20-23, 2005.

12. Simpson, M.A., Al-Reda, S., Foreman, D., Guzman, J., Al-Fawzy, M. and Vice, P.: "Application and Recycling of Sodium and Potassium Formate Brine Drilling Fluids for Ghawar Field HPHT Gas Wells," OTC paper 19801, presented at the Offshore Technology Conference, Houston, Texas, May 4-7, 2009.

BIOGRAPHIES

Nelson O. Pinero began his career in 1996 when he went to work for Lagoven, a Venezuelan oil company, as a Foreman. In 1997, he began specializing as a Drilling Engineer and then began working as a Drilling & Workover Engineer. In 2003, Nelson started working as a Workover Foreman in Servicios Ojeda in the western part of Venezuela. Two years later, he went to work for BP Venezuela as a Workover Foreman. The following year, BP relocated him to Bogota, Colombia, to work as a Workover Engineer. Nelson joined Saudi Aramco's Workover Department as a Workover Engineer in 2007.

In 1995, he received his B.S. degree Mechanical Engineering from National Experimental Polytechnic University, Barquisimeto, Venezuela.

Abdulaziz S. Mutawa joined Saudi Aramco's Drilling and Workover Department in 2010, working on the operations side until 2013. He then joined the Workover Engineering Department as a Workover Engineer, where he worked on multiple critical projects, including managed pressure drilling utilization.

In 2010, Abdulaziz received his B.S. degree in Petroleum and Natural Gas Engineering from West Virginia University, Morgantown, WV.

Ayoub Hadj-Moussa is currently the Country Product Line Manager of Secure Drilling Services for Weatherford Saudi Arabia. With over 9 years of oil field experience, he specializes in controlled pressure drilling operations, such as underbalanced drilling (UBD) and managed pressure drilling (MPD). In 2005 Ayoub joined Weatherford, starting his oil field career as a Data Acquisition Engineer in Underbalanced Drilling Operations in Hassi-Messaoud, Algeria, gaining valuable hands-on experience. Since then, Ayoub has worked on a broad range of UBD and MPD operations in various countries in the MENA region.

In 2010 he relocated to Saudi Arabia to work on various projects, such as the Deep Gas Drilling Coil Tubing UBD project, High-Pressure Jilh Formation Depletion and the MPD project for Saudi Aramco's Drilling and Workover Department.

Ayoub has coauthored various Society of Petroleum Engineers (SPE) papers in the field of MPD.

In 2004, he received his B.S. degree in Systems Engineering from Carleton University, Ottawa, Ontario, Canada.

Mohamed Cherif Mazouz is currently working as the Technical Service Manager of Secure Drilling Services for Weatherford Saudi Arabia in Dammam, Saudi Arabia.

Prior to joining Weatherford, he worked as an instructor at the University of Boumerdes, Algeria, from 2003 to 2006. In 2007, Mohamed joined Weatherford-Algeria as an Underbalanced/Managed Pressure Drilling Engineer. In 2010, he joined Halliburton-Saudi Arabia as a Well Site Drilling Engineer and worked on the Coiled Tubing Underbalanced Drilling project for 2 years. Then, in 2012, Mohamed returned to Weatherford Saudi Arabia to start the Managed Pressure Drilling project for Saudi Aramco's Drilling and Workover Department.

He has coauthored various Society of Petroleum Engineers (SPE) papers in the field of managed pressure drilling and underbalanced drilling.

In 2002, Mohamed received his B.S. degree in Reservoir Engineering from the University of Boumerdes, Boumerdes, Algeria, and in 2006, he received his M.S. degree in Asset Management, from Robert Gordon University, Aberdeen, U.K.

Paco Vieira started his oil field career in 1995 as a Drilling Engineer for the Venezuelan national oil company PDVSA. In 2000, he began working on a team that was created to conduct the implementation of underbalanced and performance drilling technologies in PDVSA fields. Paco has worked in several research studies related to multiphase flow hydraulics. In 2004 he joined Weatherford International's Controlled Pressure Drilling and Testing Services for the Middle East and North Africa region. Paco currently works as the Regional Product Line Manager for the Secure Drilling Services product line.

He received his B.S. degree in Mechanical Engineering from the Universidad Metropolitana, Caracas, Venezuela, and his M.S. degree in Petroleum Engineering from the University of Tulsa, Tulsa, OK.

Ramon Zambrano is an Animal Science Engineer. He has over 15 years of experience in mud logging, underbalanced drilling (UBD) and managed pressure drilling (MPD) operations, both offshore and onshore. Ramon started his career with Datalog Technologies as a Field Technician, then worked on UBD operations in Venezuela as a Data Acquisition Technician, Rotating Control Device Technician and Compression Supervisor. While working with Secure Drilling Services, he concentrated on MPD operations in Latin America and North Africa.

After Weatherford acquired Secure Drilling Services, Ramon joined Weatherford and worked as a Well Site Supervisor, Project Manager and MPD Technical Manager. He is currently the Secure Drilling Services Operations Manager.

In 2001, Ramon received his B.S. degree in Animal Science from the National University of Táchira, Táchira, Venezuela.

Case History: New Horizons for Downhole Flow Measurements via Coiled Tubing Equipped with Real-Time Downhole Sensors at South Ghawar Field, Saudi Arabia

Authors: Shaker A. Al-BuHassan, Surajit Haldar, Hassan I. Tammar, Faisal I. Beheiri, Danish Ahmed, George Brown, Jeffrey T. MacGuidwin, Jacques Haus, Tullio Moscato, Nestor Molero and Fernando Baez

ABSTRACT

During the last five years, one of the most common matrix acidizing enhancement techniques for improving zonal coverage in open hole or cased hole wells has been to conduct a distributed temperature survey (DTS) using coiled tubing (CT) equipped with fiber optic and real-time downhole sensors during the preflush stage — before the main stimulation treatment. Measurements are then used to identify high and low intake zones so the pumping schedule can be modified to selectively place diverters and acidizing fluids with a high degree of control. Once the stimulation treatment has been completed, a final DTS analysis is performed to evaluate the zonal coverage and the effectiveness of the diversion.

Even though this technique has provided satisfactory results, alternative methods providing a faster and more accurate understanding of flow distribution between the zones and laterals are needed, especially in cases where there is limited temperature contrast between fluids and the reservoir. An innovative CT real-time flow (CTRF) tool has recently been developed to monitor flow direction and fluid velocity. This measurement is based on the direct measurement of the heat transfer from the sensors to the surrounding fluid using a calorimetric anemometry principle.

This article documents the first worldwide use of this technology in a Saudi Aramco injector well and provides perspectives and potential applications for this new measurement.

INTRODUCTON

Ghawar field is the world's largest, most prolific field, producing 30° to 31° API oil from the Arab-D carbonate reservoir. The field is more than 250 km (155 miles) long and as much as 30 km (18.5 miles) wide, and it has more than 300 m (1,000 ft) of structural closure. The Upper Jurassic Arab formation consists of four geographically widespread carbonate evaporite cycles or members. These members are labeled Arab-A, B, C and D. The Arab-D reservoir is limestone with some dolostone horizons. It stratigraphically comprises the Arab-D member of the formation and the upper part of the Jubaila formation, Fig. 1[1].

The reservoir has an average thickness of more than 60 m (200 ft), an average porosity of more than 15% and permeability that varies, but which can be up to several Darcy. The upper half of the reservoir is dominated by exceptionally high reservoir quality, while the lower half contains interbeds of high and relatively lower reservoir quality.

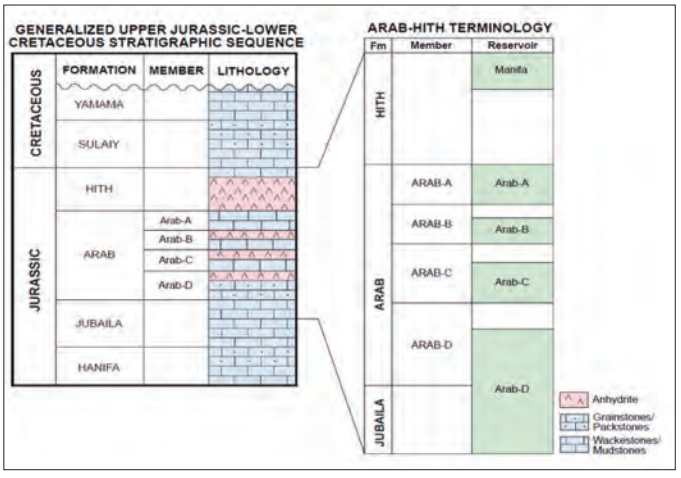

Fig. 1. Generalized stratigraphic and reservoir terminology of the Eastern Arabian Peninsula[1].

Acid stimulation treatments are regularly performed on Arab-D power water injection (PWI) wells in Ghawar field. Maintaining injectivity in PWI wells is considered of vital importance to maintain reservoir pressures above the bubble point, sustain production rates and maximize ultimate recovery. These acid stimulation treatments are performed to remove formation damage resulting from drilling or workover fluid invasion (near wellbore damage) and long-term fluid injection (deep damage). The objective of the stimulation work in the Arab-D PWI wells is to radially dissolve the near wellbore rock and use wormholing to attain acid penetration of the matrix throughout the entire porous interval, resulting in a significant amount of damage removal with very little rock dissolution[2].

The well used for the test was an open hole horizontal water injector in the Arab-D formation. The well was completed in 2000 and started injecting at 9,800 barrels per day (bpd). As the years passed, the well injection rate declined until it stabilized at 4,000 bpd, so the operator decided it required a matrix stimulation treatment. This article discusses the successful

matrix stimulation intervention where a new technology — the coiled tubing real-time flow (CTRF) tool — was used to measure bottom-hole parameters to help determine the invasion zone.

JOB OBJECTIVES AND CHALLENGES

The objectives of the job were:

1. Determination in real time of tight or damaged zones for proper placement of stimulation fluid[3].
2. Determination in real time of high permeability thief zones for proper placement of diverting fluid[3].
3. Use of bottom-hole temperatures to verify the working temperatures of stimulation fluids[3] and use of distributed temperature survey (DTS) temperature corrections in case of an offset.
4. Monitoring of real-time bottom-hole pressures during the stimulation to ensure the stimulation treatment is carried out below fracturing pressure[3].
5. Determination in real time of the pre- and post-stimulation injection profile.

Figure 2 shows the well deviation survey along with a well cross section.

CURRENT DTS METHODOLOGY

Coiled tubing (CT) with DTS for temperature measurement has been used widely for matrix stimulation treatment optimization and evaluation. The following two techniques are used for water injector wells to determine the well profile.

Injection and Warm-back Technique

When injection into a well is stopped, the well will warm up toward its geothermal gradient, though it will take some time to do so if there has been long-term injection. The warm-back rate is a function of injection permeability, and this can be modeled using an appropriate thermal model so the injection profile can be determined.

Hot Water Interface Velocity Measurement Technique

If the well has been injecting for an extended period of time, the reservoir will have completely cooled to the injection temperature and will stay cold long after injection has stopped. Therefore, when the well is shut-in, the water in the tubing and casing above the reservoir warms up quickly, usually in a few hours, because of heat conduction from the uninvaded formation. These conditions produce a volume of hot water in the tubing just above the reservoir[4]. Once injection is restarted, this hot slug of water can be tracked by the DTS fiber optic system, recording at a suitably high acquisition rate, as the slug moves down the reservoir interval. The velocity of the hot/cold water interface can be determined, and this then represents the flow profile into the reservoir. This technique can be used to complement the warm-back method, particularly in multilateral wells where fluid loss to the other laterals is a concern.

A DTS can provide quantitative analysis of the injection profile except in the following cases:

- There is cross flow, so the warm-back technique cannot be used.
- The injection rate cannot be kept constant, so the hot

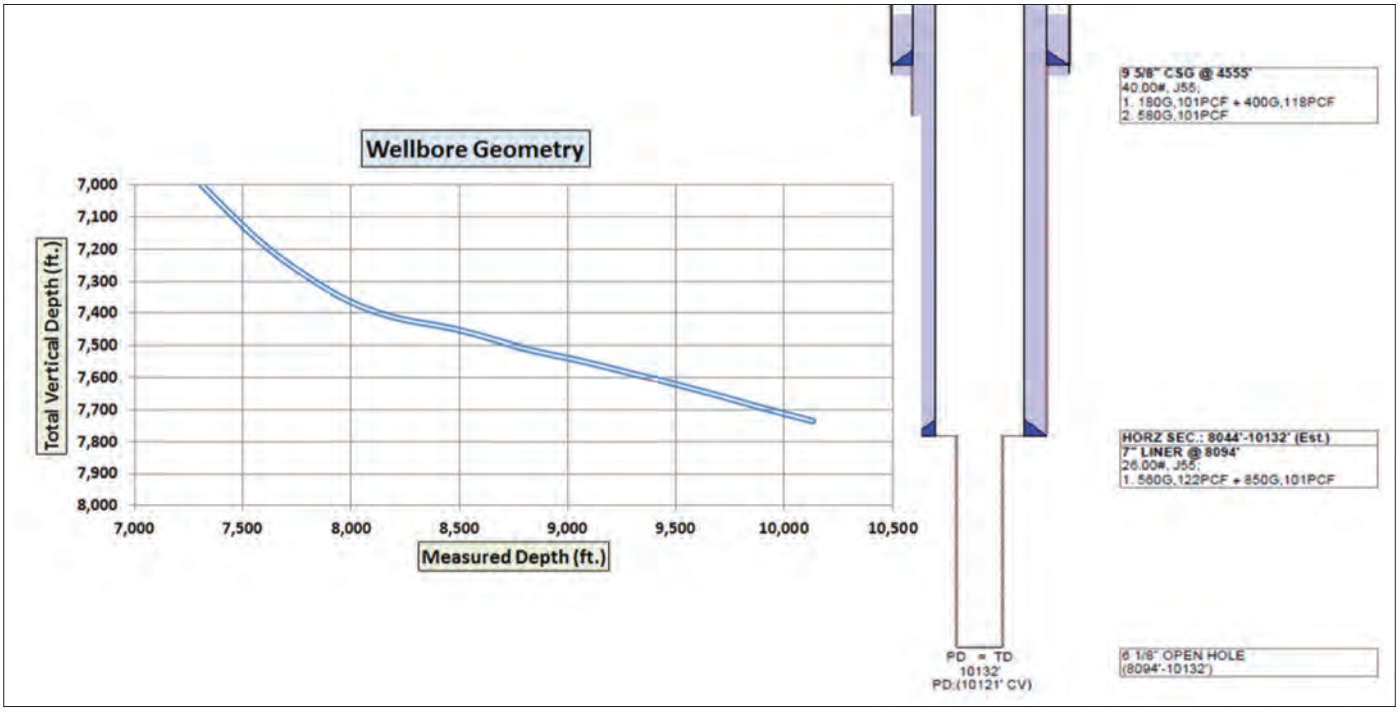

Fig. 2. Wellbore geometry and well cross section.

interface injection technique cannot be used.

- The CT has become differentially stuck during DTS acquisition.

CTRF TOOL

The CTRF tool technology, Fig. 3, combines the advantage of CT placement and real-time monitoring of the wellbore velocity during the matrix acidizing job. The tool sensors measure the mean fluid velocity in the gap between the tool and the outside tubing/casing/hole. The wellbore velocity is used to provide measurements of the real-time fluid distribution and direction of flow between the formation layers. The fluid injected through the CT passes inside the CTRF tool and exits at nozzles situated between the upper and the lower parts, Fig. 3a. Each part has a set of four sensors, referred to as A, B, C and D. They are situated away from the nozzles to avoid any jetting effects. Each sensor has three heating/sensing probes: up, middle and down, Fig. 3b. Every probe can be used either as a heater or as a temperature sensor; in the latter case, it is called an "ambient probe," Fig. 3c. When the probe in the middle is heated and the other two are ambient, the configuration allows the direction of the flow to be detected. Figure 4 shows the basic principle of detecting the direction through the CTRF tool.

When the middle probe is heated, the fluid temperature increases slightly in the thin layer adjacent to the sensor surface,

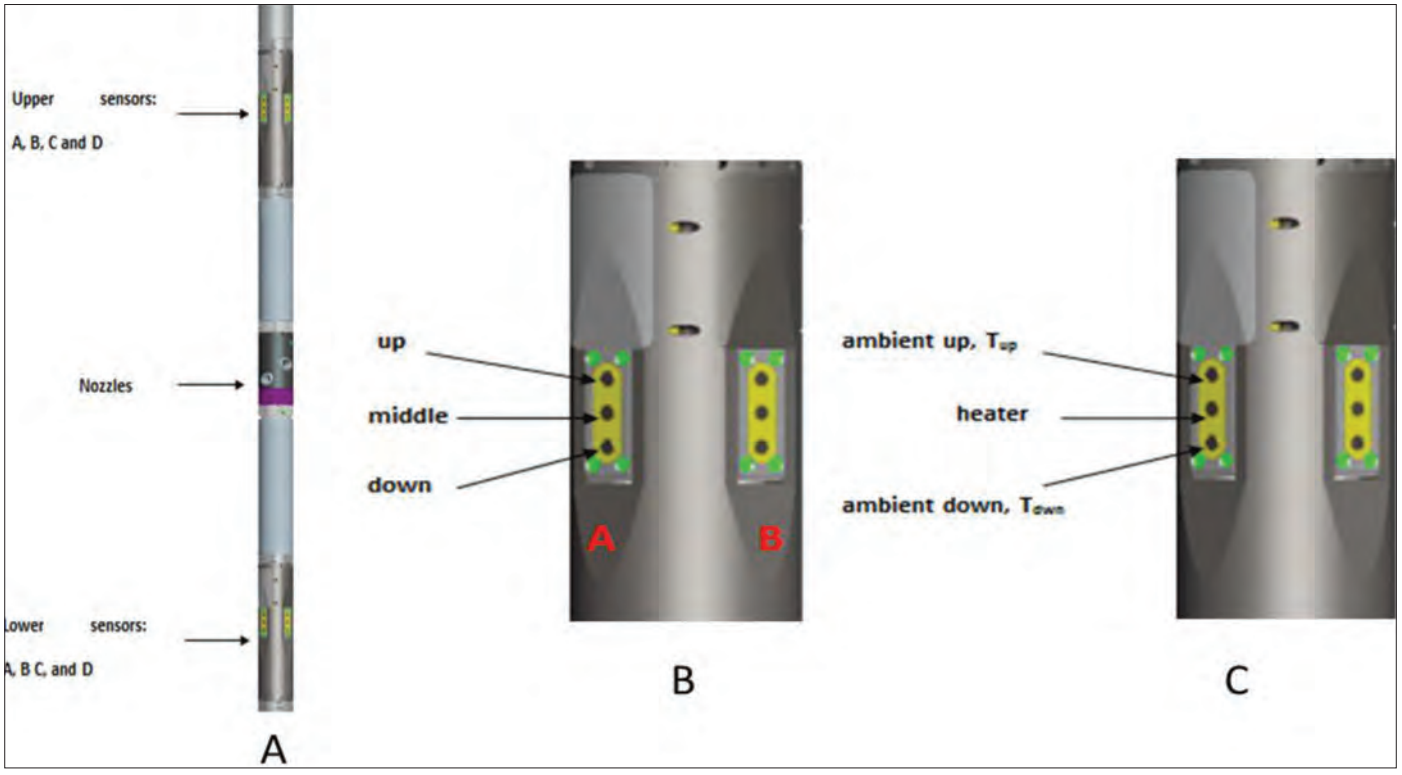

Fig. 3. CTRF tool.

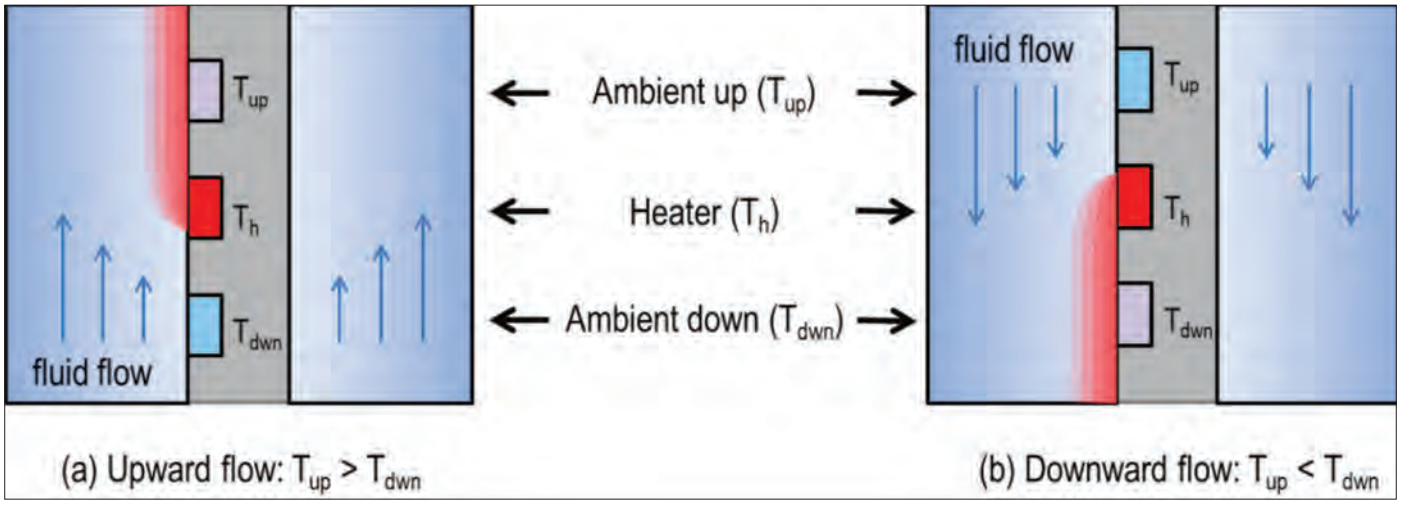

Fig. 4. Basic principle of fluid direction detection through the CTRF tool.

i.e., a thermal boundary layer is formed. This thermal boundary layer covers the downstream probe. The latter measures the temperature of the fluid inside the thermal boundary layer, which is higher than the temperature of the bulk fluid. The upstream probe is not affected by the presence of the thermal boundary layer, and therefore, measures the temperature of the bulk fluid. Direction detection is determined by calculating the temperature difference between the ambient probes, T_{up}-T_{dwn}. The positive values of this difference indicate an upward flow, or negative-downward flow. A minimal value between T_{up} and T_{dwn} gives the bulk fluid temperature.

The middle probe is heated in such a way that the temperature difference between the heater and the fluid, $\Delta T = Th - Tf$, remains constant. The amount of the dissipated power per one degree of the temperature excursion, $P/\Delta T$, depends on the fluid velocity. The exact functional relationship between the dissipated power and the fluid velocity can be obtained by performing a downhole calibration. During the job, the fluid velocity is obtained by measuring the dissipated power and inverting the calibration relationship. Above certain velocities, the system may not be able to provide sufficient power to keep the temperature excursion at the specified level. In this case, the probe is heated in a constant power regime. For certain fluids, a default calibration relationship may be available in a file containing the tabulated values of fluid velocity, *V*, as a function of the dissipated power and the fluid temperature. These values for the default calibration relationship have been obtained in a laboratory flow loop, so can be applicable to a group of fluids with similar thermophysical properties.

In practice, the best way to establish the calibration relationship is to perform a downhole calibration check. It consists of injecting the fluid at various rates and recording the dissipated power as a function of the mean fluid velocity in the annulus. The tool should be positioned in such a way that the totality of the injected fluid goes either up or down. To do so, three calibration methods can be used:

- Injecting the fluid at various pumping rates in the annular space between the tool and the tubing/casing.
- Injecting the fluid through the downhole CTRF, which measures rates at the tool nozzles (pumping in the CT) and ensures that all fluid goes either up or down.
- Moving the CT at various speeds.

CTRF tool measurements are recorded either during stations for precise local measurement or during the up or down passes of the CT to record log profiles. Figure 5 is an example of a 2-minute station recording, showing a stable fluid velocity measurement.

INTERVENTION WORKFLOW

An intervention workflow combining the DTS and CTRF tool measurements was defined as outlined here.

Step 1: CT real-time bottom-hole flow parameters tool calibration

1. With the well in the shut-in condition, run in hole (RIH) with the CT without pumping through the CT.
2. RIH/pull out of hole (POOH) with the CT at different speeds within the 7" tubing.
3. Pump water through the annulus, keeping the CT stationary, but increasing the pumping rates.
4. Pump water through the CT, keeping the CT stationary, but increasing the pumping rates.

Step 2: Pre-stimulation DTS and acid wash

1. RIH with the CT to total depth (TD) or maximum depth to record baseline temperatures. Record for a minimum of 2 hours or until temperature stabilization.
2. Pump a 20% hydrochloric (HCl) acid wash in the open hole section. Allow the acid to soak for 1 hour and flow back the well for cleanup.

Step 3: Pre-stimulation CTRF injection profile

1. RIH with the CT to TD and start the seawater injection down the CT annulus.
2. While bullheading, POOH with the CT while recording with the CTRF tool.
3. For bullheading with stations, stop for logging stations while recording with the CTRF tool.
4. RIH with the CT to TD or maximum depth while pumping via the CT at 2.0 barrels per minute (bpm), recording with the CTRF tool while RIH, then stop at maximum depth for 5 minutes.
5. POOH with the CT to the casing shoe, while pumping via the CT at 2.0 bpm, recording with the CTRF tool while POOH.

Step 4: Pre-stimulation preflush evaluation and DTS

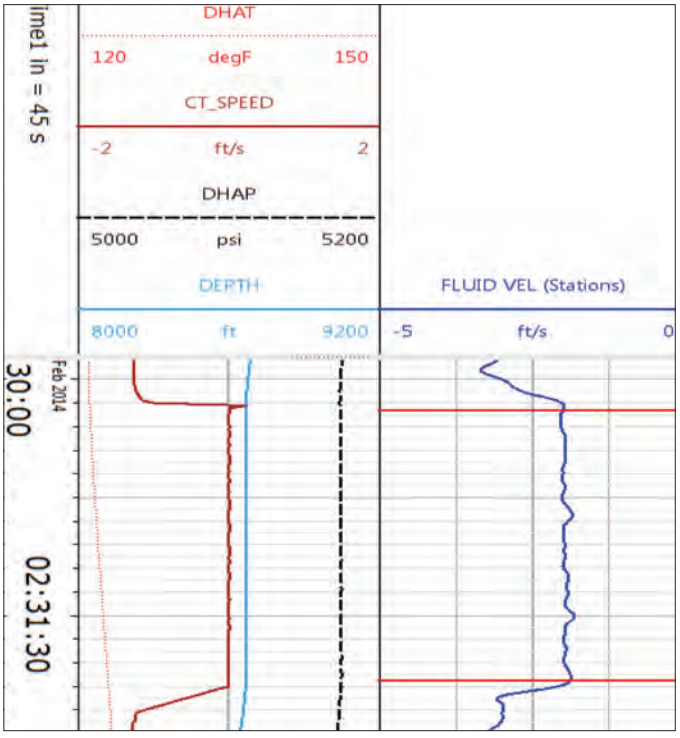

Fig. 5. Example of measurements recorded during the a CTRF station.

1. Begin pumping the preflush through the CT at increasing rates. Calibrate the CTRF tool while inside the casing shoe.
2. RIH with the CT to TD or maximum depth and continue spotting preflush across the open hole. Continue to record with the CTRF tool.
3. POOH with the CT to the casing shoe while pumping preflush through the CT. Continue to record with the CTRF tool.
4. Begin to displace the wellbore fluid with water by annular bullheading.
5. RIH with the CT to TD or maximum depth while recording with the CTRF tool.
6. While at TD or maximum depth, stop pumping through the annulus and begin recording the DTS warm-back for 1 to 2 hours.
7. After the warm-back is finished, begin the water injection through the annulus. POOH with the CT to the casing shoe while recording with the CTRF tool.

Step 5: Stimulation Treatment

1. Pump stimulation as per interpretation of the DTS and the CTRF tool results.

Step 6: Post-stimulation Treatment

1. Record the post-stimulation DTS.
2. Repeat step 1 and step 3.2 for the post-stimulation treatment evaluation.

JOB EXECUTION

The CT was RIH with pull tests performed at every 1,000 ft.

The CTRF tool calibration checks were performed using the three methods of calibration: (1) CT movement at different speeds; (2) annulus pumping at different rates; and (3) CT pumping at different rates.

The three methods provided similar results. In future interventions, calibration checks can be performed using the most appropriate method, depending on operational conditions. Figure 6 shows the CTRF calibration performed while the CT was in the cased hole section, i.e., with annulus pumping at different rates and with CT pumping at different rates. It can be seen that the CTRF responds to each rate change, and the measured velocity from the CTRF is the same as calculated on the surface for a given rate.

As soon as the CT reached the maximum depth of 9,731 ft, the DTS recording was performed to establish the baseline temperature profile of the well. Note that the well above the reservoir slowly warms up toward the real geothermal temperature. In the reservoir there is a zone that is very cold, and this only warms a little during the measurement period. This interval indicates where long-term injection has cooled the rock deep into the reservoir, so it would take a long time for this rock to warm back up to the true geothermal temperature, Fig. 7.

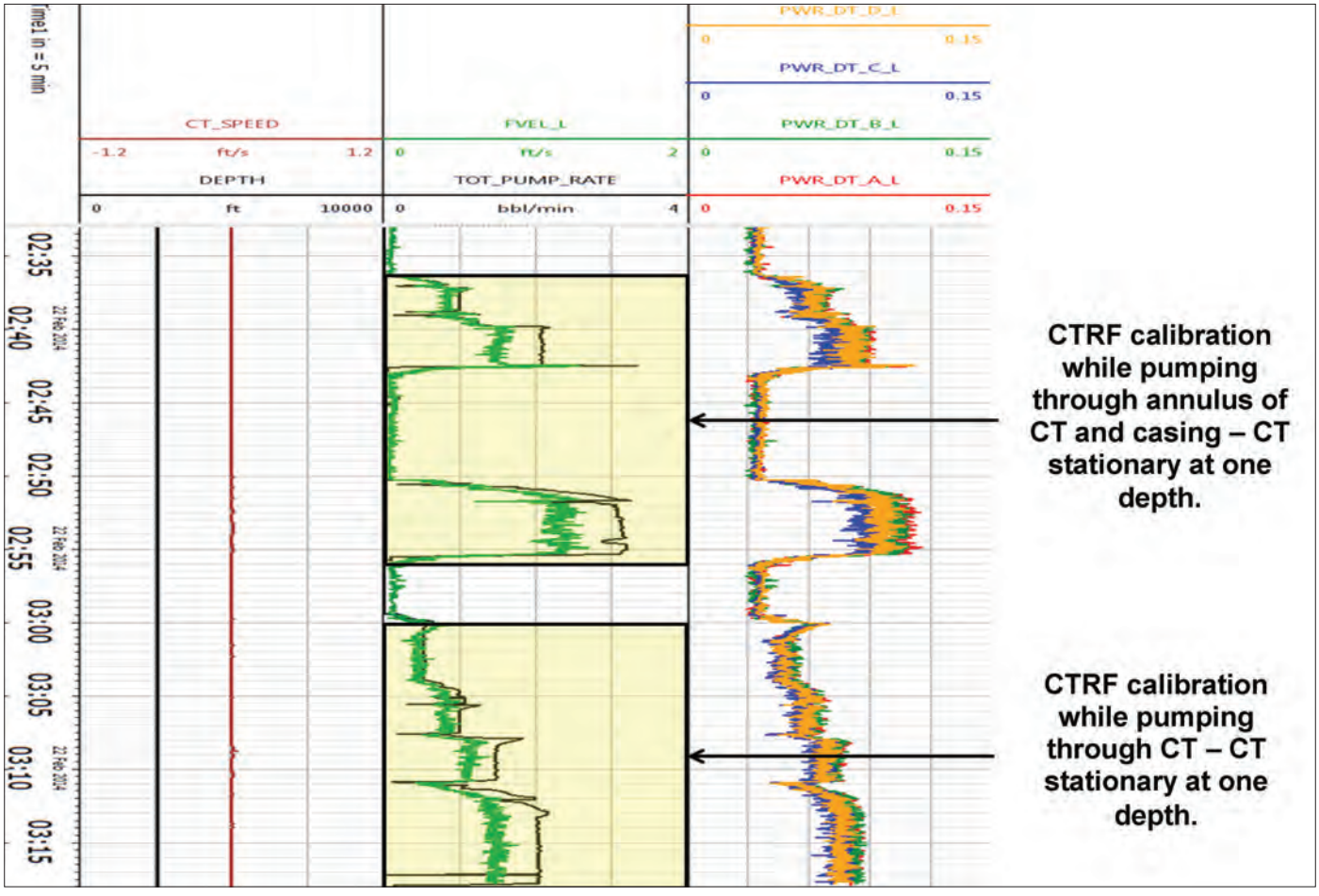

Fig. 6. CTRF tool log while pumping from annulus and while pumping though CT.

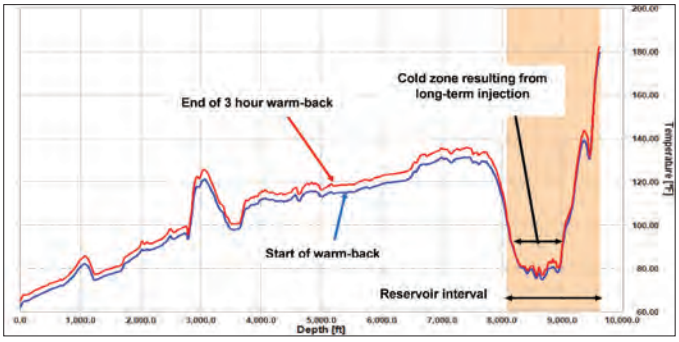

Fig. 7. Baseline DTS data.

Because the well had been on injection for some time, the warm-back analysis required the use of the long-term injection time, and the shut-in warm-back profile was calculated from the 7-day shut-in period to match the measured DTS data. In this well, out of the three red zones shown, the two thin zones from 8,560 ft to 8,600 ft and 8,680 ft to 8,720 ft show the highest inflow, Fig. 8.

Following the baseline temperature measurement, seawater was pumped through the annulus while monitoring the DTS temperatures. Figure 9 shows the plot with the results of the temperature traces recorded during injection. The initial annulus injection took place at 2.0 bpm, and the temperature traces moved from the green baseline to the blue trace (gray traces are the intermediate temperature events). The main injection interval is at 8,560 ft to 8,600 ft, although the data also shows qualitatively that there is a small amount of flow into the 8,680 ft to 8,720 ft zone.

Seawater was pumped through the annulus at a rate of 3.0 bpm. The CTRF tool data was recorded as the CT was POOH to the casing shoe. The station data (fluid velocity measure) was recorded at several depths, Fig. 10. The data is in line with the DTS data, showing a major intake zone down to 8,650 ft with no or limited flow below. The upward flow measured at 9,200 ft is a localized movement in time and depth, which is not representative of the general profile.

DTS data recorded during annulus injection was processed to track the thermal interface down the well and extract injection velocity profiles. The data was compared with the profile obtained from the CTRF tool velocity recording. As the injection rates were different for both measurements, the comparison is qualitative only. Results are shown in Fig. 11.

The CTRF tool identified the intake zone between 8,100 ft to 8,650 ft, which is similar to the results obtained from the DTS interpretation, with the main inflow zone on the lower end of the interval.

The matrix stimulation treatment was optimized based on the DTS and CTRF tool interpretation. The new schedule called for pumping a higher volume of diverters into the zones from the casing shoe to 8,650 ft and focusing the main acid concentration on the remaining open hole zones; this was followed by pumping diverter from 8,650 ft to the toe and pumping the main acid treatment from 8,650 ft to the casing shoe. The stimulation treatment consisted of HCl acid, a

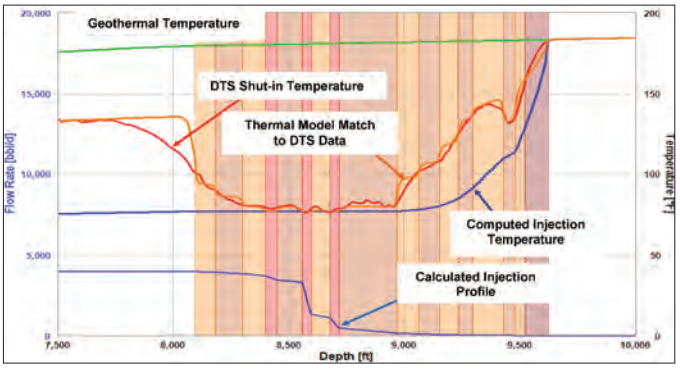

Fig. 8. Warm-back injection profile conducted using the baseline DTS.

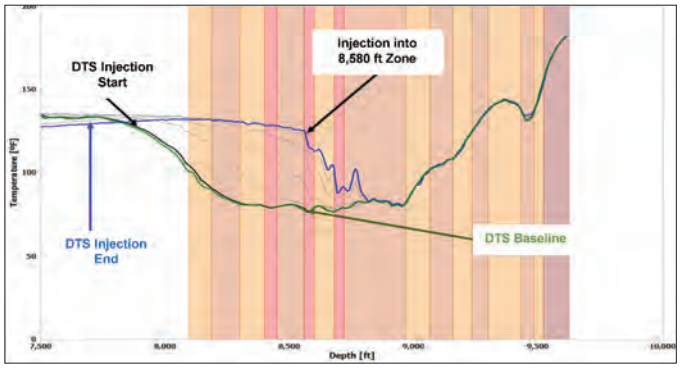

Fig. 9. Annulus injection with the CT at maximum depth and while recording with DTS sensors.

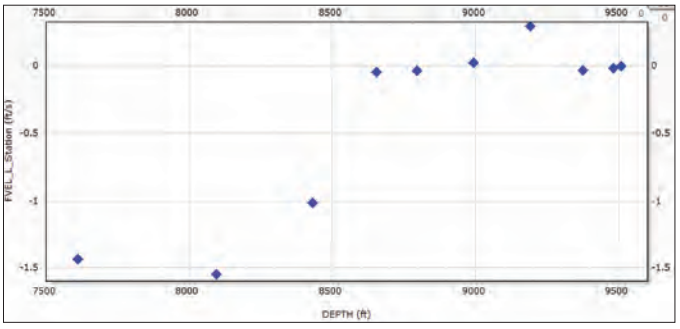

Fig. 10. CTRF fluid velocity measurement during pre-stimulation profiling (the blue diamonds indicate the station measurements).

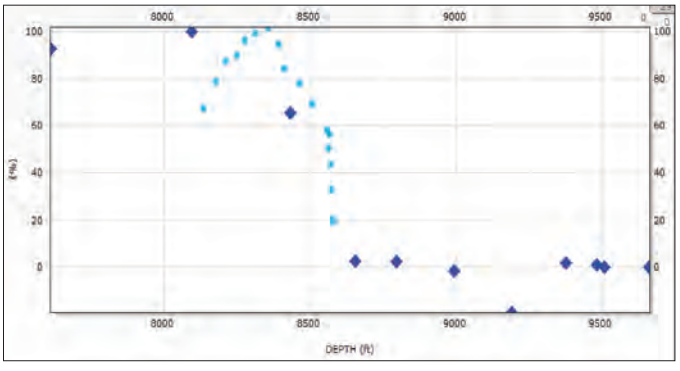

Fig. 11. Comparison of injection profile measured with CTRF tool (blue diamonds) and calculated from DTS annulus injection data (light blue circles).

viscoelastic diverter system and emulsified retarded acid. Once the stimulation treatment was pumped, a post-flush was pumped through the CT, and a DTS was conducted with annulus injection, Fig. 12.

The DTS analysis showed that the well was now injecting down to the 8,700 ft zone.

A post-stimulation continuous flow profile and measurements at additional stations were recorded by the CTRF tool, Fig. 13. This profile provides a detailed, quantitative measure of flow velocity during post-stimulation injection, showing the major intake zone from 8,660 ft to 8,720 ft.

DTS data recorded during the annulus injection was processed to track the thermal interface down the well and extract an injection velocity profile. The data was compared with the profile obtained from the CTRF tool velocity recording. As the injection rates were different for both measurements, the comparison is qualitative only. CTRF results are in line with DTS data, and the comparative data is displayed in Fig. 14.

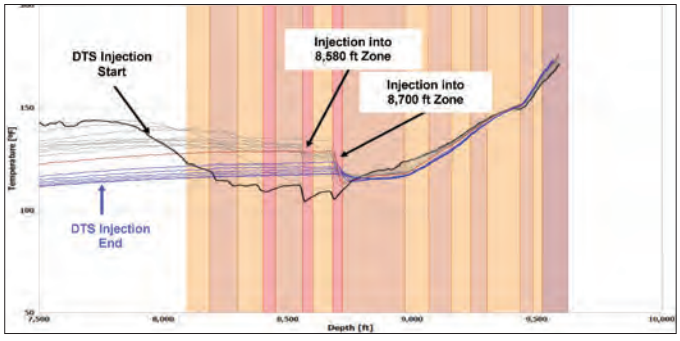

Fig. 12. Annulus injection while recording the DTS for post-job evaluation.

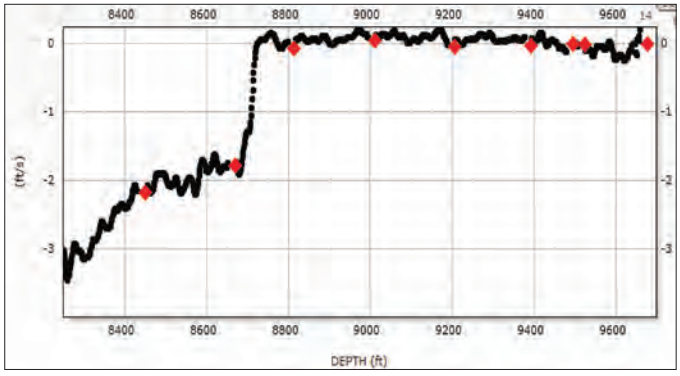

Fig. 13. CTRF fluid velocity measurement during post-stimulation profiling (the red diamonds indicate station measurements).

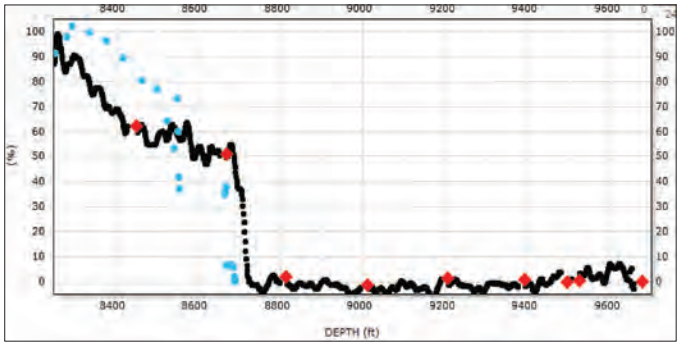

Fig. 14. Comparison of injection profile measured with CTRF tool (black line and red diamonds) and calculated from DTS annulus injection data (light blue circles).

CONCLUSIONS

This first CTRF tool field test allowed for the new flow measurements to be validated by comparing the results to the established DTS data. Indeed, pre- and post-stimulation velocity profiles from the CTRF tool and DTS were in agreement, and both measurements could be used to optimize the stimulation treatment.

Validation of the CTRF tool measurements opens the door to a new approach to downhole flow monitoring, allowing for real-time monitoring of the direction and velocity of the pumped fluid as it exits the CT using a sensor technology that makes the tool completely transparent to the operation — it is a flow-through tool with no fragile spinners, arms or protruding elements. The CTRF tool can be used as a stand-alone tool or with a DTS depending on the specific constraints of each intervention.

ACKNOWLEDGMENTS

The authors would like to thank the management of Saudi Aramco and Schlumberger for their support and permission to publish this article. Also, the authors would like to thank the Schlumberger CT Well Intervention Team for making this intervention a success.

This article was presented at the SPE Middle East Oil and Gas Show and Conference, Manama, Bahrain, March 8-11, 2015.

REFERENCES

1. Cantrell, D.L. and Hagerty, R.M.: "Microporosity in Arab Formation Carbonates, Saudi Arabia," *GeoArabia*, Vol. 4, No. 2, 1999, pp. 129-154.
2. Ginest, N.H., Phillips, J.E. and AI-Gamber, A.W.A.: "Field Evaluation of Acid Stimulation Diverter Materials and Placement Methods in Arab-D Injection Wells with Open Hole Completions," SPE paper 25412, presented at the SPE Middle East Oil Technical Conference and Exhibition, Bahrain, April 3-6, 1993.
3. Al-Gamber, S.D., Mehmood, S., Ahmed, D., Burov, A., Brown, G., Barkat, S., et al.: "Tangible Values for Running Distributed Temperature Survey as Part of Stimulating Multilateral Injection Well," SPE paper 167490, presented at the SPE Middle East Intelligent Energy Conference and Exhibition, Bahrain, October 28-30, 2013.
4. Schlumberger Ltd.: "The Essentials of Fiber Optic DTS Analysis," internal document, 2005.

BIOGRAPHIES

Shaker A. Al-BuHassan is a Petroleum Engineering Specialist working with the South Ghawar Engineering Division of the Southern Area Production Engineering Department. He has more than 20 years of oil production experience.

In 1992, Shaker received his B.S. degree in Petroleum Engineering from King Fahd University of Petroleum and Minerals (KFUPM), Dhahran, Saudi Arabia.

He is also a member of the Society of Petroleum Engineers (SPE).

Surajit Haldar joined Saudi Aramco 9 years ago and currently works as a Technical Support Unit Supervisor in Saudi Aramco's Southern Area Production Engineering Department. He has more than 25 years of experience in exploration and production in the oil and gas industry for national and international companies. His working experience includes 12 years in operations and production engineering, 6 years in research, development and consultancy, and over 7 years in supervisory and management level positions.

As a well-rounded and versatile professional, Surajit now provides engineering support and advice on new technologies for the largest onshore oil field in the world, working in the area of production monitoring and enhancement, well surveillance and well integrity management.

He has authored and published over 25 technical papers and articles in several industry journals and at Society of Petroleum Engineers/International Petroleum Technical Conferences.

Surajit received his B.S. degree in Chemical Engineering in 1989 from the Indian Institute of Technology, Kharagpur, India, and in 2006 he received his MBA from Yashwantrao Chavan Maharashtra Open University, Nashik, India.

Hassan I. Tammar began his career working for the Saudi Ministry of Petroleum and Minerals in 1988. In September 1991, he joined Saudi Aramco as a Drilling and Workover Engineer. In 1994, Hassan was transferred to 'Udhailiyah to work with the Southern Area Production Engineering Department as a Production Engineer. Since then, he has been supporting the oil production and water injection activities of South Ghawar field. Currently, Hassan works as a Senior Production Engineer with the Water Injection Unit of the South Ghawar Production Engineering Division.

In 1988, he received his B.S. degree in Petroleum Engineering from the University of Southern California, Los Angeles, California.

Faisal I. Beheiri is a Division Head at Saudi Aramco's Southern Area Production Engineering Department. During his career, he has gained diversified experience in production engineering of gas, oil and water wells. Faisal has also worked in various field and operational departments, including Well Completion Operations, Well Services, Project Coordination, Inspection, Plant Process Engineering, and HSE Advisory. He played a major role in developing a number of technical manuals and studies as well as coming up with new innovations.

Faisal has published several technical papers and articles, and has been a member of numerous upstream projects, multidisciplinary teams and taskforces. He has also led and chaired multiple committees, including the Behavior-based Safety Committee and Technical Prequalification Committee. Faisal has served the Society of Petroleum Engineers (SPE) community at many international events in the capacities of SPE Workshop Chairperson, Keynote Speaker and Sessions Chairman.

In 1999, Faisal received his B.S. degree with honors in Petroleum Engineering from the University of Montana Tech, Butte, MT, and in 2006, he received his M.S. degree in Oil and Gas Engineering from the University of Western Australia, Crawley, Western Australia.

Danish Ahmed is a Senior Intervention Production Engineer currently working with Schlumberger Well Intervention – Coiled Tubing Services supporting the ACTive Services Platform. His experience involves working as a Field Engineer with Well Production Services, based in 'Udhailiyah, Saudi Arabia, supporting proppant/acid fracturing and matrix acidizing jobs, followed by working as a Production Technologist with Petro Technical Services (formerly called Data and Consulting Services) in Dhahran, Saudi Arabia. Danish began working for Saudi Schlumberger in 2007.

In 2007, he received his M.S. degree in Petroleum Engineering from Heriot-Watt University, Institute of Petroleum Engineering, Edinburgh, Scotland.

George Brown is an Advisor with Schlumberger. He started with Schlumberger Wireline in 1973, working in both the Middle East (Saudi Arabia, Dubai and Turkey) and the North Sea (Aberdeen and Norway) in a variety of operational and management positions.

Then he spent 15 years with BP Exploration, where he was Head of the Petrophysics group at the Sunbury Research Center and later a Senior Formation Evaluation Consultant working with BP's "Intelligent Wells" team.

George joined Sensa in March 1999 as Manager of Interpretation Development; Sensa was bought by Schlumberger in 2001.

He has published over 40 technical papers, been awarded several patents and was a Society of Petroleum Engineers Distinguished Lecturer during 2004/2005.

George received his B.S. degree (with first class honors) in Mechanical Engineering from Coventry University, Coventry, U.K.

Jeffrey T. MacGuidwin is the Engineer-in-Charge of the CoilTOOLS sub-segment within Schlumberger Well Intervention, Saudi Arabia.

He has more than 4 years of oil field experience. Jeffrey is also a member of the Society of Petroleum Engineers.

In 2009, he received his B.S.E. degree in Industrial and Operations Engineering from University of Michigan, Ann Arbor, MI.

Jacques Haus is the Interpretation Champion for ACTive Answer Products, Schlumberger. He has more than 15 years of experience working in tool and interpretation product development for production and production logging applications.

He is a member of the Society of Petroleum Engineers.

In 1990, Jacques received his B.S. degree in Mechanical Engineering, and in 1991, he received his M.S. degree in Oceanography, both from Université de Liège, Liège, Wallonia, Belgium. In 1996, Jacques received an M.S. degree in Computer Science from Georgia Institute of Technology, Atlanta, GA.

Tullio Moscato is the Project Manager, and an inventor of new coiled tubing and wireline downhole measurement tools, at Schlumberger SRFE (Paris). He has more than 15 years of downhole tool engineering and measurement experience.

He is a member of the Society of Petroleum Engineers.

Tullio received his M.S. degree in Mechanical Engineering from the Politecnico di Milano University, Milan, Italy, and Ecole Nationale Superieure des Techniques Avancees, Palaiseau, France.

Nestor Molero is a Sales & Technology Manager for Schlumberger Well Intervention in Mexico and Central America. He is a Technical Engineer with more than 15 years of experience in the design, execution and evaluation of coiled tubing (CT) workover interventions in onshore and offshore environments.

From March 2013 until September 2014, Nestor was Technical Manager for Schlumberger Well Intervention in Saudi Arabia, leading the Schlumberger CT Technical Team and supporting Saudi Aramco on the technical aspects of CT interventions in oil, gas and power water injector wells conducted for matrix stimulation, descaling, perforating, clean outs, milling, fishing, zonal isolation, etc. Prior to this assignment, he held technical and sales positions in Egypt and Mexico, where he was responsible for the introduction of new technologies for CT and matrix stimulation. Nestor started his career in Venezuela in 1999 as a Field Engineer for Schlumberger Well Services, completing his field assignment in Colombia and Ecuador.

He has authored several Society of Petroleum Engineers papers and articles that have appeared in various industry magazines.

Nestor received his B.S. degree in Mechanical Engineering from Universidad del Zulia, Maracaibo, Venezuela.

Fernando Baez joined Schlumberger in 2000. He is currently the ACTive Domain Champion for the company's fiber optic enabled coiled tubing (CT) service in Saudi Arabia, Kuwait and Bahrain. Before this, Fernando was part of the CT software team in various capacities that included field operations in Colombia; technical instruction in Kellyville, OK; coordination of fast track training of specialists in Mexico; and Field Service Manager in the north of Mexico. Prior to joining Schlumberger, Fernando worked for Ecopetrol, a national oil company in Colombia.

Fernando has coauthored several patents and papers related to his specialized field.

In 1999, he received his M.S. degree in Mechanical Engineering from the Universidad de los Andes, Bogota, Colombia.

Well Testing Analysis of Horizontal Open Hole Multistage Fracturing Wells in Tight Gas Condensate Reservoirs in Saudi Arabia to Characterize Production Performance and Fracture Behavior: Case Studies

Authors: Mahdi S. Al Dawood, Ahmad Azly Abdul Aziz, Dr. Zillur Rahim, Ahmed M. Al-Omair and Dr. N.M. Anisur Rahman

ABSTRACT

A horizontal open hole multistage fracturing (MSF) completion is the preferred completion method to develop a tight and heterogeneous carbonate reservoir. Production data analyses and pressure transient tests are systematically and routinely conducted on such wells to determine the well productivity indices (PIs) and evaluate key reservoir and fracture parameters. Open hole MSF completions have been implemented since 2009 and have shown remarkable results compared to other completions and stimulation strategies, such as vertical wells with single-stage fracturing or MSF, and open hole multilateral wells with maximum reservoir contact.

This article presents the modeling and interpretation of the production and actual pressure transient responses of horizontal open hole MSF wells that were drilled in both the minimum horizontal stress (σ_{min}) direction and the maximum horizontal stress (σ_{max}) direction to assess the production and fracture behavior. Creating transverse fractures has led to better productivity compared to longitudinal fractures in terms of production performance, which is corroborated in the article through pressure transient analyses (PTA) and results from field data. The article evaluates the impact of fracture parameters, such as fracture half-length, conductivity, orientation and the number of fractures, on production and pressure behavior. Well testing and production analysis are very powerful techniques to assess and compare different types of flow regimes for horizontal open hole MSF wells drilled in different azimuth directions.

This article discusses and explains the different derivative shapes captured during well tests and compares these to the simulated and theoretical models. Also, the transmissibility values obtained from the mini falloff (MFO) test during the fracture injectivity operations are compared with the flow capacity values calculated from the PTA. Challenges to measuring pressure transient responses, such as high wellbore storage, are addressed, and proper planning and use of best practices in the PTA to obtain accurate results are discussed and presented.

INTRODUCTION

The main challenges that limit the productivity of gas wells in carbonate retrograde gas condensate reservoirs are tightness and heterogeneity. Drilling horizontal wells and stimulating them with multiple hydraulic fractures have been extremely successful in developing these tight reservoirs. It was found, however, that fracture geometry is affected by stress variations and drilling directions. Wells drilled toward the minimum horizontal stress (σ_{min}) direction that are subsequently stimulated generate fractures perpendicular to the wellbore axis, thereby allowing multiple independent fracture placement and minimizing communication risk between the stages. Drilling toward the maximum horizontal stress (σ_{max}) direction creates longitudinal fractures along the wellbore axis. These fractures can lead to pressure communications between stages as fractures from one interval overlap the neighboring fractures. Another challenge of open hole MSF completion is that it requires geometric trajectory without geosteering to avoid deployment problems due to doglegs. This approach may result in less net reservoir contact. These detailed challenges were addressed in a previous study[1].

The reservoir evaluated in this study has an average permeability of 0.2 millidarcy (mD) and contains a substantial gas volume in place. It was determined that drilling horizontal wells in the σ_{min} direction to create transverse fractures during stimulation treatment with open hole multistage fracturing (MSF) completion was the best strategy in this field as it overcame interstage fracture communication and attained high reservoir contact and gas rates. Initially, the wells had been drilled in the σ_{max} direction to avoid drilling difficulties and ensure borehole stability. Drilling parallel to the σ_{min} direction presents challenges in controlling borehole breakouts, but these difficulties were resolved with the application of real-time geomechanics, where reservoir pressure and the safe drilling mud weight envelope are computed based on the data collected and analyzed using a logging-while-drilling approach.

Prior to putting such wells on production, the completion performance is assessed. The initial assessment is limited to the data available from the initial post-fracture rate and the estimated transmissibility obtained during the mini falloff (MFO) test. To better evaluate the performance of the horizontal well and each individual fracture, production logging must be run. This option is not always realistic due to the high cost and operational risks associated with well intervention. Therefore, the pressure transient analysis (PTA) is used and has become vital

to understanding the reservoir and fracture behaviors and estimating their properties. Additionally, the results from the PTA are used in calibrating the inflow and outflow well performance, using the wellbore hydraulic models, to design production strategy and predict well performance with more accuracy.

In this study, we reviewed seven horizontal wells with open hole MSF completions whose production and pressure data had been analyzed; two of these wells were drilled toward the σ_{min} direction, while the remaining wells were drilled toward the σ_{max} direction. This article details several case histories using actual PTA. It also addresses the challenges that affect the interpretation of the derivative plot in terms of flow regimes identification, reservoir properties and fracture geometry.

In general, the PTA results and the performance data of the horizontal open hole MSF wells indicated promising improvement in well productivity, particularly in tight and heterogeneous layers. This finding is consistent with the overall assessment of horizontal open hole MSF wells in other fields in Saudi Arabia[1].

Interpretation of PTA in a horizontal well with hydraulic fracturing is very challenging, especially in tight and heterogeneous gas reservoirs. Adding to that complexity is the possibility of multiphase flow when the flowing bottom-hole pressure drops below the dew point pressure. Different flow regimes exist in a multiple fracture system, Fig. 1, as covered in the literature[2]. The two main regimes for wells with multiple fractures shown in Fig. 1 are the compound linear flow and the compound pseudo-radial flow, but that interpretation can still be inconclusive as it is very difficult to detect flows around the fracture. We noticed that the wells drilled in the σ_{min} direction showed some sort of dual radial flow regime, as is discussed later.

The bilinear flow occurs at a very early time, when the flow is orthogonal to the fracture, and subsequently along the fracture length into the wellbore. It is indicated by a quarter-slope on the log-log plot. This flow regime is short and usually masked by the wellbore storage effect. The early time linear flow also occurs when the flow is orthogonal to the fracture, with no pressure losses in the fracture, and is characterized by a straight line of half-slope on the log-log plot in the pressure derivative response[3]. This flow regime is important in computing fracture parameters and thereby in evaluating stimulation effectiveness. Results in the very early time period are usually affected by wellbore storage as the downhole gauges are normally not at the sand face, but instead are set about 800 ft above the horizontal section and with surface shut-in tools to avoid any operational risks.

A brief reservoir description and a discussion of the PTA analysis, productivity comparison with other completion assemblies and MFO test results are provided in the following sections.

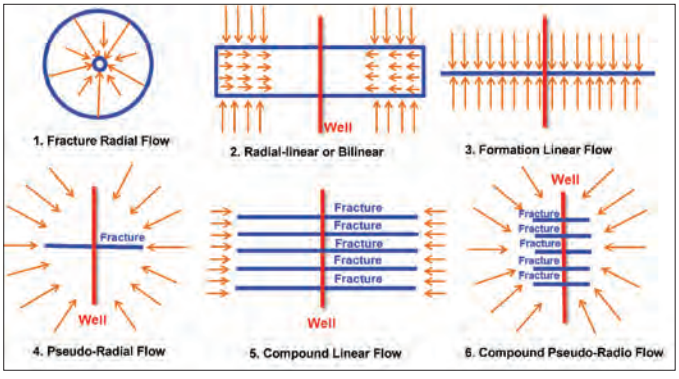

Fig. 1. Potential flow regimes for fractured horizontal wells[2].

RESERVOIR DESCRIPTION

The carbonate reservoir depositional environment is from the early Triassic period, mainly consisting of dolomites, limestones and anhydrites. The reservoir is subdivided in seven stratigraphic layers, B1 to B7, by porosity, Fig. 2. Porosity development is mainly found in the B1 layer, which is the main producing layer. In certain wells, discontinuous porosity development is seen in the B2 layer. Even in the B1 layer, the reservoir is heterogeneous with significant porosity variations occurring within the layer. This poses a major challenge in developing this reservoir[4]. Typical logs of this carbonate reservoir across the field indicated a wide range of porosity variations, Fig. 2. Average porosity and net pay in the productive reservoir layer varies from 6% to 10% and 10 ft to 50 ft, respectively. Figure 3 shows a typical lithological distribution for this reservoir, where B1 is mostly dominated by limestones,

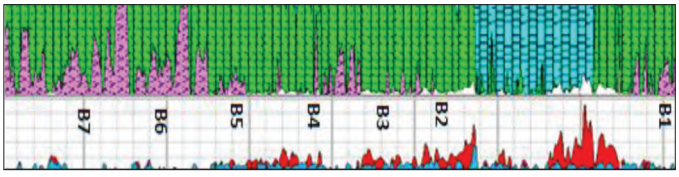

Fig. 2. Typical reservoir layers by porosity.

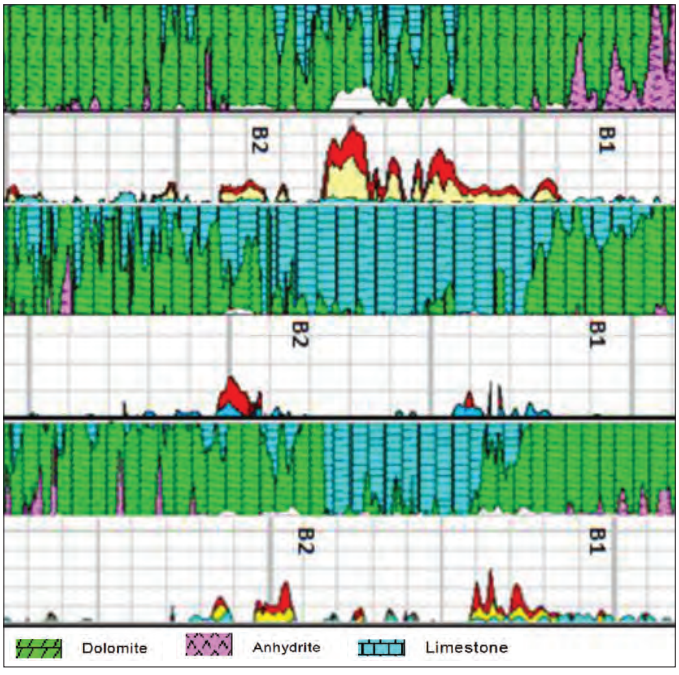

Fig. 3. Typical logs showing lithology for B-1 and B-2 layers across the field.

favorable to acid reaction. The placement of the lateral (stress direction) will dictate the angle between the induced fractures and the wellbore — transverse or longitudinal — Fig. 4.

PTA ANALYSIS

Transverse Fractures

This section provides examples of two wells, Well-A and Well-B, drilled in the direction of σ_{min}. We will be focusing on Well-B as a case study.

Well-B

This well was initially drilled as a vertical pilot hole across multiple reservoirs. Subsequently, it was sidetracked as a geometric single lateral well across the carbonate reservoir in the σ_{min} direction and completed with the five-stage balanced open hole MSF completion system. The lateral encountered about 1,300 ft net reservoir contact with 10% average porosity. Three stages were successfully fractured, while two stages had poor injectivity so the formation could not be broken down. A deliverability test was conducted after two months of production to evaluate key reservoir and fracture parameters. Figure 5 shows the pressure derivative response from the PTA with a reasonable analytical match to a fractured horizontal well placed in a homogeneous reservoir with an infinite boundary. A clear stimulation signature can be seen through the linear flow at early times, using a half-slope line fit on the log-log plot.

Sensitivity analyses were subsequently performed, varying four important parameters to evaluate their impact on the derivative plot, Fig. 6. The analyses show that increasing the number of fractures results in less pressure drop in the wellbore at early times. Almost the same results were obtained while increasing the fracture half-length, but the pressure drop extended through the entire test. The analyses also indicate that increasing the horizontal well length will eventually result in delaying the radial flow regime, with less downward shift of the derivative plot. It can be noticed that in a horizontal fracture well model, the well length obtained is less compared to the one obtained when matched using a horizontal well model. This is due to less rate contribution and dominance from the horizontal section. The sensitivity analyses shall be used to optimize open hole MSF completion designs, as well as planning future PTAs.

Table 1 shows the main PTA results for Well-B.

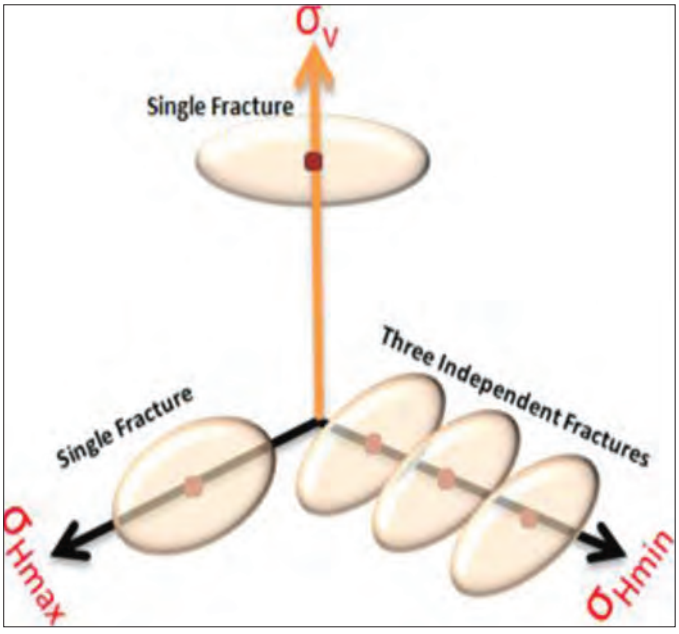

Fig. 4. Fracture geometry relative to stress direction.

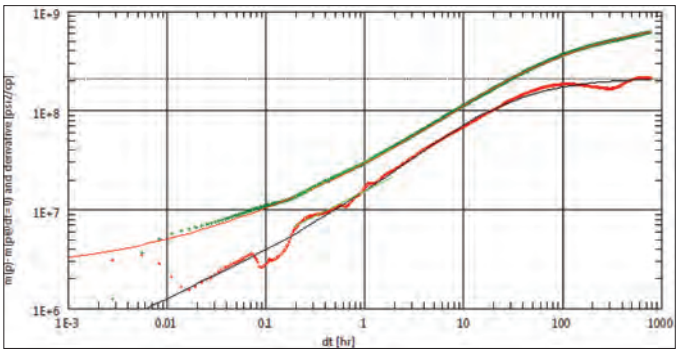

Fig. 5. Well-B pressure derivative response with the match.

LONGITUDINAL FRACTURES

This section will discuss the PTA of the wells drilled in the σ_{max} direction, Well-C through Well-G. In this article, we will be focusing on Well-F. Table 2 is a summary of data for the stress direction and number of fractured stages compared to the planned stages for Well-A to Well-G.

Well-F

This well was sidetracked as a geometric single lateral, 50° to σ_{min} direction, and completed with four-stage balance open hole MSF across the carbonate reservoir. The sidetrack encountered 1,385 ft net reservoir contact with 5% average porosity. The first stage was acid fractured, but the second,

Well-B	
Parameters	**Value (Analytical)**
Fracture Half-Length (ft)	259
Drilled Horizontal Section (ft)	3,750
Total Net Reservoir Contact (log), (ft)	1,600
Number of Fractures	3
Total Skin	-6.4
Flow Capacity, kh (mD.ft)	22.5
PI (Mscfd/psi)	5.2
Radius of Investigation (ft)	1,220

Table 1. Well-B main PTA results

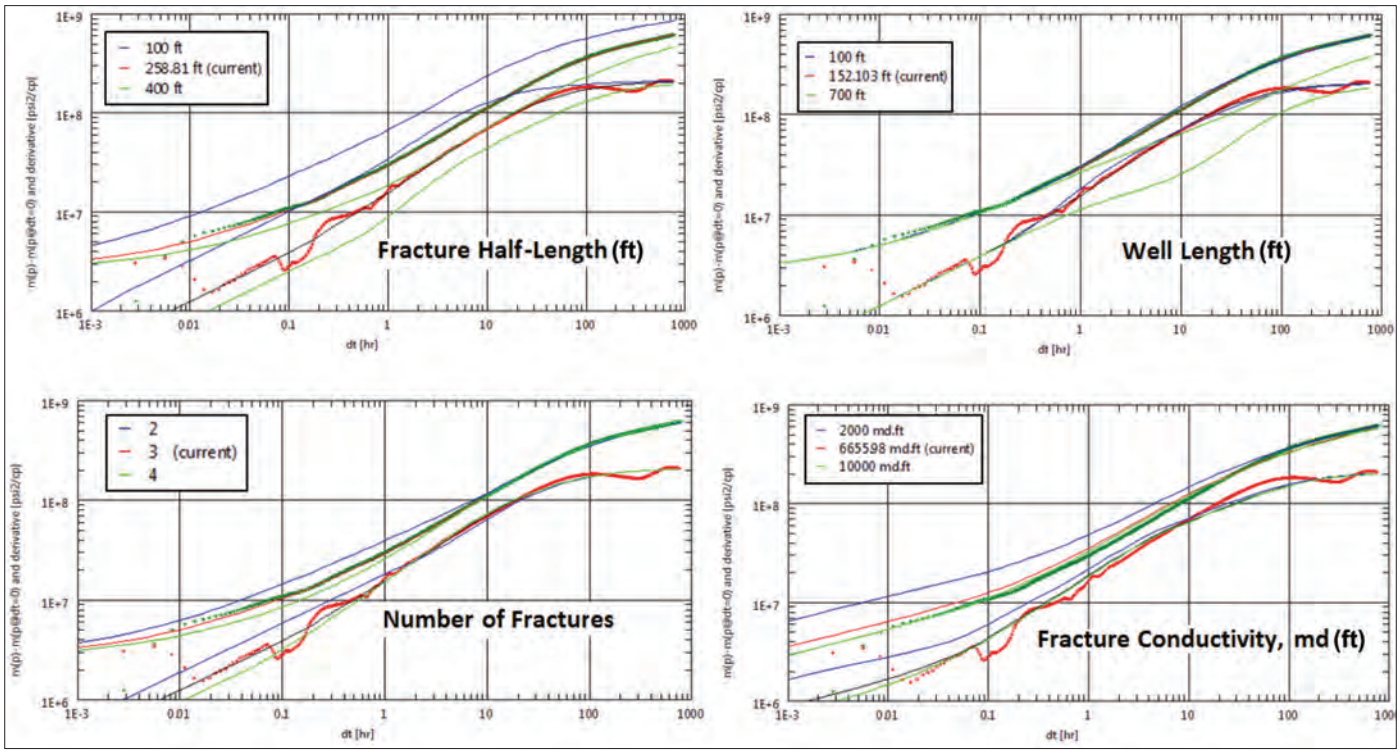

Fig. 6. Sensitivity analyses for fracture half-length, well length, number of fractures, and fracture conductivity.

	Well-A	Well-B	Well-C	Well-D	Well-E	Well-F	Well-G
Stress Direction	Minimum Horizontal Stress	Minimum Horizontal Stress	Maximum Horizontal Stress	Maximum Horizontal Stress	Maximum Horizontal Stress	Maximum Horizontal Stress	Maximum Horizontal Stress
Stages Fracked	2 out of 4	3 out of 5	1 out of 3	1 out of 2	0 out of 3	1 out of 4	2 out of 3

Table 2. MSF summary data

third and fourth stages were matrix acidized due to communication occurring between the stages. A deliverability test was conducted after four months of production to evaluate key reservoir and fracture parameters.

Figure 7 shows the log-log plot of the response from the pressure buildup test, which has been reasonably matched by using a horizontal well in a homogeneous reservoir with an infinite boundary. The early time region is masked by wellbore storage effects. The radial flow regime was reached after about 300 hours, and key reservoir parameters were calculated using this test period, Table 3. Due to reservoir heterogeneity, the total net reservoir contact is 60% of the total drilled length. Furthermore, the effective well length obtained from matching the derivative plot is almost half the total net reservoir contact. The total skin value of -4.43 indicates effective stimulation,

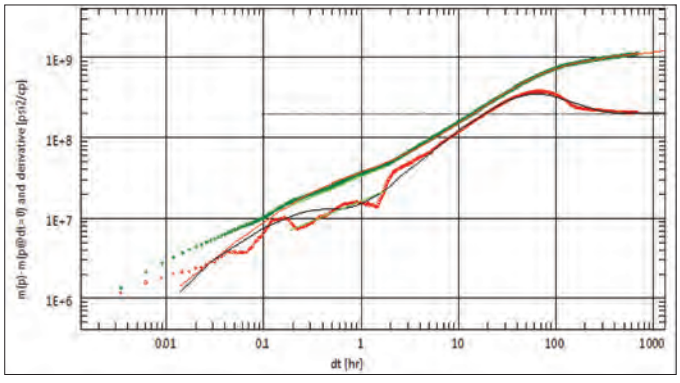

Fig. 7. Well-F pressure derivative response with the match.

Well-F	
Parameters	**Value**
Fracture Half-Length (ft)	195
Drilled Horizontal Section (ft)	3,650
Total Net Reservoir Contact (log) (ft)	1,385
Number of Fractures	1
Total Skin	-4.43
Flow Capacity, kh (mD.ft)	7.44
PI (Mscfd/psi)	0.8
Radius of Investigation (ft)	793

Table 3. Well-F main PTA results

even though there is a slight skin damage of 1.35 due to flow restriction from the fracture to the wellbore. The calculated flow capacity value is very close to the one obtained from the injectivity test. A linear flow is identified at early time, using the half-slope line as indicated.

FURTHER PTA OBSERVATIONS

Figure 8 shows a normalized log-log pressure plot for the wells drilled in the σ_{min} direction. Both wells show a short fracture radial flow at very early times, followed by a linear flow and finally by a pseudo-radial flow[5, 6]. Well-B confirms that more fractures result in longer linear flow. The late time on both derivative plots shows two radial flow regimes that could be attributed to either reservoir heterogeneity or the boundary effect. Another explanation could be that the two radial flows are separated by some sort of transitional flow (close to linear) in both wells[7]. Also, the larger the spacing between fractures, the longer the transitional period will be. These conclusions will be confirmed with more well data in the future. The shape of the derivatives matches what has been modeled and simulated for a horizontal well intercepted by an infinite conductivity longitudinal fracture[7, 8], Fig. 9.

Figure 10 compiles the normalized log-log responses for all wells drilled in the σ_{max} direction to identify distinct reservoir and fracture features. Well-C, Well-E and Well-F show a clear linear flow at early times. Well-D and Well-G do not exhibit hydraulic fracture behavior; they are reasonably matched using

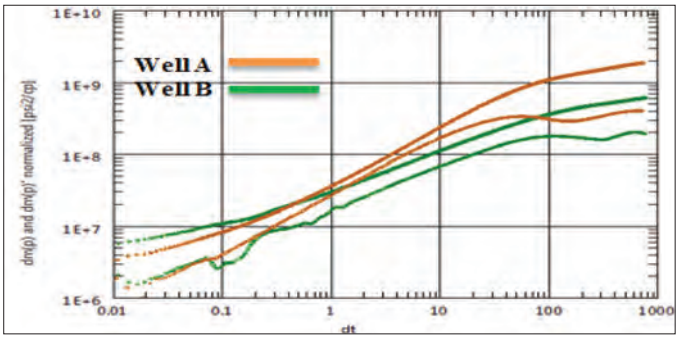

Fig. 8. Log-log pressure plot for the wells drilled in the σ_{min} direction.

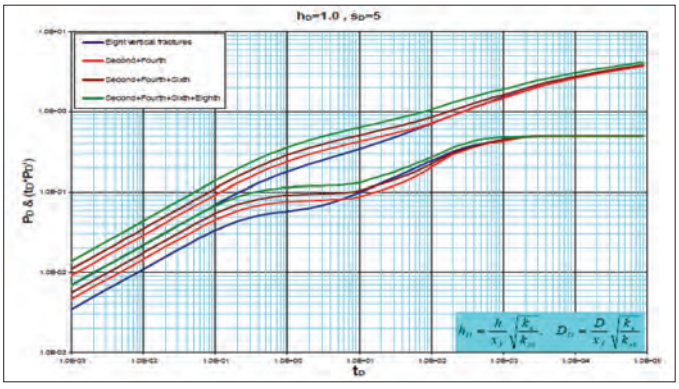

Fig. 9. Hydraulic fracture system with large spacing[8].

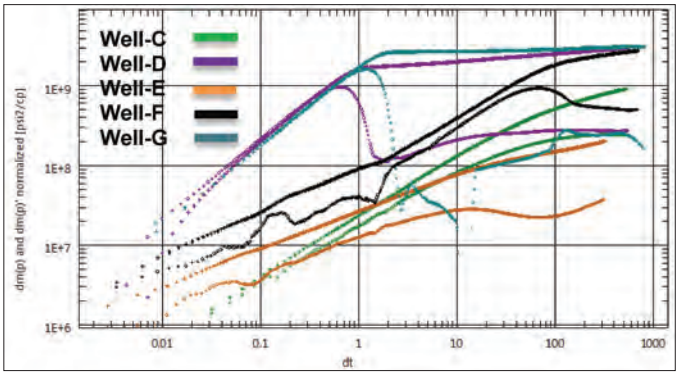

Fig. 10. Log-log pressure plot for the wells drilled in the σ_{max} direction.

only the horizontal well model. The behavior of the other wells closely resembles horizontal wells with longitudinal fractures, Fig. 11. This observation is consistent with the fact that these wells were fractured in the σ_{max} direction, but the fracture signature was masked by the wellbore storage. The shape of the derivatives matches what has been modeled and simulated for horizontal wells intercepted by an infinite conductivity longitudinal fracture[8], Fig. 11. Based on the production performance, Well-D and Well-G are low producers compared to the rest of the wells, Fig. 12. The same figure shows that the productivity is maximized when the well is drilled in the σ_{min} direction.

PRODUCTIVITY COMPARISON WITH OTHER COMPLETIONS

The productivity of the open hole MSF wells was compared against the productivity of other completion methods using the productivity index (PI) and *kh* data derived from the PTAs. The comparison wells were completed as a vertical cased hole completion — with single acid fracturing — and as a horizontal open hole (with acid matrix), Fig. 13. The results show that open hole MSF wells can provide higher PI for this reservoir, with *kh* in the range of 5 mD-ft to 30 mD-ft. Well-G and Well-D again are low performers compared to wells with other

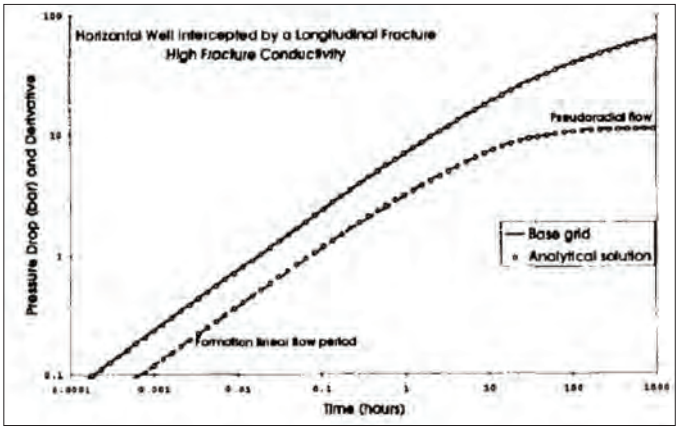

Fig. 11. Analytical and simulated pressure behavior of a horizontal well intercepted by a highly conductive longitudinal fracture[8].

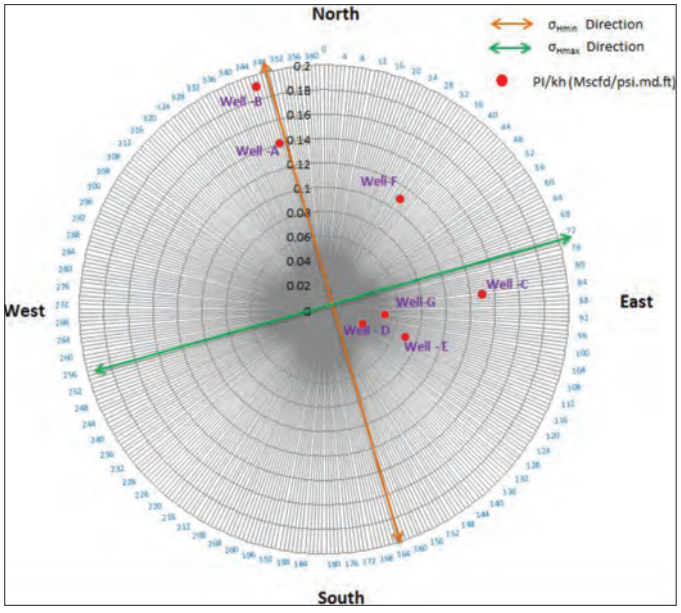

Fig. 12. Radar map that shows the PI/flow capacity vs. azimuth.

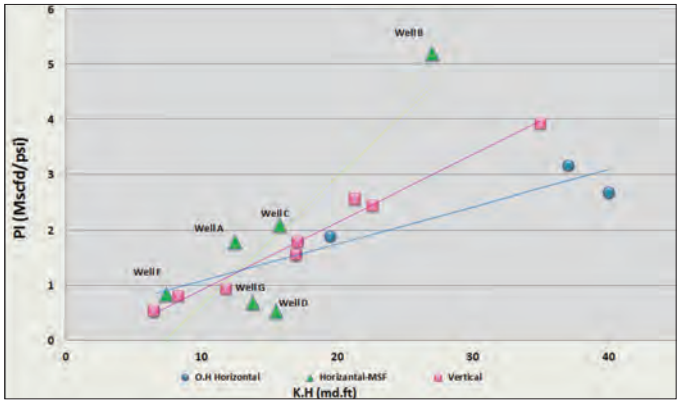

Fig. 13. PI vs. kh for open hole horizontal, open hole MSF and vertical wells.

completions, due to the low stimulation effectiveness as previously discussed.

MFO INJECTION TESTS

MFO injection tests are conducted in the injection period when treated water is pumped into the formation to create a small fracture as the pressure is being recorded by a downhole gauge, Fig. 14[9].

The MFO tests are used to determine the transmissibility values, along with the reservoir pressures, by identifying the

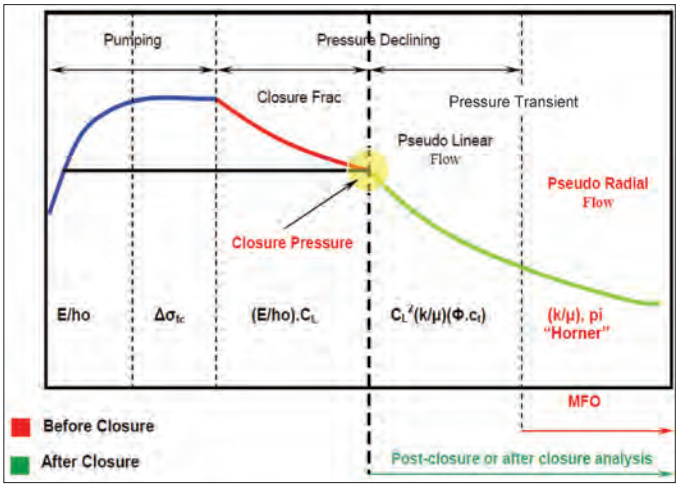

Fig. 14. Illustration of flow periods illustration during a MFO test[9].

pseudo-radial flow regime and the other fracture parameters from linear flow after shut-in. The data is also used later to calibrate the main fracture design. This method was developed by Kenneth Nolte in 1997. The reliability of this kind of test is dependent on a good estimation of reservoir parameters, such as reservoir pressure and permeability, which are test designing purposes[9]. The radial flow region sometimes cannot be interpreted from pressure transient response. The objective here is to compare the *kh* values obtained from the MFO test with the ones obtained from the PTA test.

Table 4 shows the calculated transmissibility values from the MFO test with the *kh* values for all the wells. We noticed that many wells did not show reasonable values because the tests were perturbed due to communication between the stages. The transmissibility values computed from the first stage therefore will likely be the most accurate one since that stage occurs under virgin reservoir conditions. Based on the findings presented in Fig. 15, only Well-F and Well-G showed

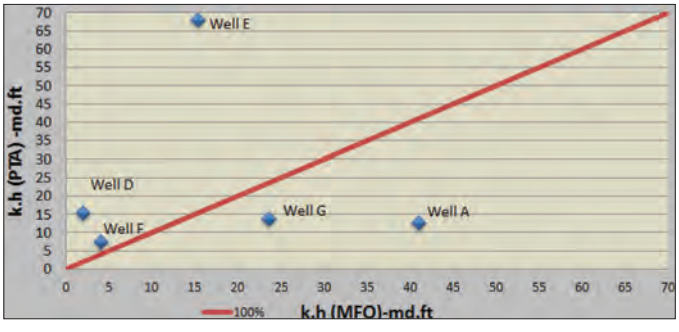

Fig. 15. Comparison of kh values obtained from MFO tests and PTA.

Stage 1	Well-A	Well-D	Well-E	Well-F	Well-G
Transmissibility, kh/μ, (mD.ft/cP)	1,368	68	509	138	785
Calculated kh (mD.ft)	41	2	15.3	4.1	23.6
kh (PTA) (mD.ft)	12.5	15.5	68	7.4	13.8

Table 4. Valid transmissibility values obtained from the MFO test

reasonable matches from the tests. Therefore, it can be concluded that *kh* derived from the MFO test can be misleading, and the best estimate for *kh* is using PTA.

The validity of the test cannot be generalized for open hole MSF wells because they require more time to reach radial flow compared to vertical wells. Therefore, it has been considered with more precautions.

CONCLUSIONS AND RECOMMENDATIONS

1. Drilling in the σ_{min} direction helps to increase reservoir contact, create more independent transverse fractures and increase well performance.
2. Based on PTA results showing the normalized PI, wells drilled in the σ_{min} direction are better performers compared to wells drilled in the σ_{max} direction.
3. For wells drilled in the σ_{min} direction, the flow regimes seen are linear or bilinear, radial, transitional and final pseudo-radial.
4. For wells drilled in the σ_{max} direction, the only flow regimes seen are linear and pseudo-radial. Also, the linear flow lasts for a long period since the fractures are created along the wellbore.
5. Not all MSF wells exhibit the same flow regimes as the regime is more dependent on the number of fractures, spacing between the fractures, fracture conductivity and orientation of the fracture.
6. Some wells — drilled in the σ_{max} direction — did not show a clear fracture signature because the direction was not favorable for creating multiple independent fractures.
7. Based on the sensitivity analyses, a smaller pressure drop in the wellbore is attained with an increase in the number of fractures, well length, and fracture half-length and fracture conductivity.
8. The effective well length obtained from PTA is generally less than the actual net reservoir contact obtained from the open hole log.
9. Drilling open hole MSF horizontal wells in a *kh* range of 5 mD-ft to 30 mD-ft in the σ_{min} direction can provide better performance, compared to open hole horizontal wells and cased vertical wells.
10. Wellbore storage can mask the early time features. Therefore, installing a downhole shut-in tool gauge close to the reservoir is recommended for better evaluation, especially for the early flow regimes.
11. The kh values obtained from the MFO test can be misleading when compared with the kh values obtained from the PTA due to reservoir heterogeneity.

ACKNOWLEDGMENTS

The authors would like to thank the management of Saudi Aramco for their support and permission to publish this article.

This article was presented at the SPE Middle East Oil and Gas Show and Conference, Manama, Bahrain, March 8-11, 2015.

NOMENCLATURE

μ Viscosity
X_f Fracture half-length
F_c Fracture conductivity

REFERENCES

1. Al-Dawood, M., Abdulaziz, A., Al-Omair, A. and Rahim, Z.: "Performance Evaluation and Challenges Using Open Hole Multistage Fracturing Completion to Develop Tight Gas Reservoirs in Saudi Arabia," SPE paper 172219, presented at the Saudi Arabia Section Technical Symposium and Exhibition, al-Khobar, Saudi Arabia, April 21-24, 2014.
2. Al-Kobaisi, M., Ozkan, E., Kazemi, H. and Ramirez, B.: "Pressure Transient Analysis of Horizontal Wells with Transverse, Finite Conductivity Fractures," PETSOC paper 2006-162, presented at the Canadian International Petroleum Conference, Calgary, Alberta, Canada, June 13-15, 2006.
3. Cinco-Ley, H. and Samaniego-V., F.: "Transient Pressure Analysis for Fractured Wells," *Journal of Petroleum Technology*, Vol. 33, No. 9, September 1981, pp. 1749-1766.
4. Al-Anazi, H.A., Abdulbaqi, D.M., Habbtar, A.H. and Al-Kanaan, A.A.: "Successful Implementation of Horizontal Multistage Fracturing Enhanced Gas Production in Heterogeneous and Tight Gas Condensate Reservoir: Case Studies," SPE paper 161664, presented at the Abu Dhabi International Petroleum Exhibition and Conference, Abu Dhabi, UAE, November 11-14, 2012.
5. Hegre, T.M. and Larsen, L.: "Productivity of Multi-fractured Horizontal Wells," SPE paper 28845, presented at the European Petroleum Conference, London, U.K., October 25-27, 1994.
6. Larsen, L. and Hegre, T.M.: "Pressure Transient Analysis of Multifractured Horizontal Wells," SPE paper 28389, presented at the SPE Annual Technical Conference and Exhibition, New Orleans, Louisiana, September 25-28, 1994.
7. Al Rebeawi, S.J. and Tiab, D.: "Transient Pressure Analysis of a Horizontal Well with Multiple Inclined Hydraulic Fractures Using Type-Curve Matching," SPE paper 149902, presented at the International Symposium and Exhibition on Formation Damage Control, Lafayette, Louisiana, February 15-17, 2012.
8. Hegre, T.M.: "Hydraulically Fractured Horizontal Well

Simulation," SPE paper 35506, presented at the European 3D Reservoir Modeling Conference, Stavanger, Norway, April 16-17, 1996.

9. Ceccarelli, R.L., Ciuca, A. and Tambini, M.: "New Methodology of Mini Falloff Test to Optimize Hydraulic Fracturing in Unconventional Reservoirs," SPE paper 122326, presented at the European Formation Damage Conference, Scheveningen, The Netherlands, May 27-29, 2009.

BIOGRAPHIES

Mahdi S. Al Dawood is a Reservoir Engineer in Saudi Aramco's Gas Reservoir Management Department. He joined the company in June 2011 and has been working in well planning, pressure transient analysis, reservoir stimulation, reservoir surveillance and well modeling.

Mahdi is a member of the Society of Petroleum Engineers (SPE) and is a Certified Petroleum Engineer.

He received his B.S. degree in Petroleum and Natural Gas Engineering from West Virginia University, Morgantown, WV.

Ahmad Azly Abdul Aziz is currently the Lead Engineer for the 'Uthmaniyah gas fields in Saudi Aramco's Gas Reservoir Management Department. He has 20 years of diversified experience in reservoir management in oil and gas fields. Ahmad's expertise includes general reservoir engineering, well testing, and planning and development of oil and gas reservoirs. Prior to joining Saudi Aramco, he held senior positions in reservoir engineering in Qatar Petroleum and Petronas Carigali Vietnam.

In 1989, Ahmad received his B.S. degree in Petroleum and Natural Gas Engineering from Pennsylvania State University, University Park, PA.

Dr. Zillur Rahim is a Senior Petroleum Engineering Consultant with Saudi Aramco's Gas Reservoir Management Department (GRMD). He heads the team responsible for stimulation design, application and assessment for conventional and tight gas reservoirs. Rahim's expertise includes well stimulation, pressure transient test analysis, gas field development, planning, production enhancement and reservoir management. He initiated and championed several new technologies in well completions and hydraulic fracturing for Saudi Arabia's nonassociated gas reservoirs.

Prior to joining Saudi Aramco, Rahim worked as a Senior Reservoir Engineer with Holditch & Associates, Inc., and later with Schlumberger Reservoir Technologies in College Station, TX, where he consulted on reservoir engineering, well stimulation, reservoir simulation, production forecasting, well testing and tight gas qualification for national and international companies. Rahim is an instructor who teaches petroleum engineering industry courses, and he has trained engineers from the U.S. and overseas. He developed analytical and numerical models to history match and forecast production and pressure behavior in gas reservoirs. Rahim also developed 3D hydraulic fracture propagation and proppant transport simulators, and numerical models to compute acid reaction, penetration, proppant transport and placement, and fracture conductivity for matrix acid, acid fracturing and proppant fracturing treatments. He has authored more than 90 technical papers for local/international Society of Petroleum Engineers (SPE) conferences and numerous in-house technical documents. Rahim is a member of SPE and a technical editor for SPE's *Journal of Petroleum Science and Technology (JPSE)*. He is a registered Professional Engineer in the State of Texas, and a mentor for Saudi Aramco's Technologist Development Program (TDP). Rahim teaches the "Advanced Reservoir Stimulation and Hydraulic Fracturing" course offered by the Upstream Professional Development Center (UPDC) of Saudi Aramco.

He is a member of GRMD's technical committee responsible for the assessment, approval and application of new technologies, and he heads the in-house service company engineering team on the application of best-in-class stimulation and completion practices for improved gas recovery.

Rahim has received numerous in-house professional awards. As an active member of the SPE, he has participated as co-chair, session chair, technical committee member, discussion leader and workshop coordinator in various SPE international events.

Rahim received his B.S. degree from the Institut Algérien du Pétrole, Boumerdes, Algeria, and his M.S. and Ph.D. degrees from Texas A&M University, College Station, TX, all in Petroleum Engineering.

Ahmed M. Al-Omair is a Reservoir Engineer and Supervisor for Saudi Aramco's Gas Reservoir Management Department, overseeing Shedgum and 'Uthmaniyah fields. His expertise includes reservoir development, well testing and production forecasting.

Ahmed received his B.S. degree from the University of Louisiana, Lafayette, LA, and his M.S. degree from the University of New South Wales, Sydney, Australia, both in Petroleum Engineering.

Dr. N.M. Anisur Rahman is a Petroleum Engineering Consultant with the Well Testing Division at Saudi Aramco, where he designs and interprets transient tests on oil production and water injection wells.

Before joining Saudi Aramco, he worked for the Bangladesh University of Engineering and Technology, the University of Alberta, Fekete Associate Inc. and Schlumberger. Anisur Rahman developed analytical solutions for a number of pressure transient models, including methods for short well tests.

He received both his B.S. and M.S. degrees in Mechanical Engineering from the Bangladesh University of Engineering and Technology, Dhaka, Bangladesh, and his Ph.D. degree in Petroleum Engineering from the University of Alberta, Edmonton, Alberta, Canada.

Anisur Rahman is registered as a Professional Engineer in the Province of Alberta, Canada.

Treated Sewage Effluent Injection — Microbial and Formation Damage Assessment for a Low Permeability Carbonate Reservoir

Authors: Peter I. Osode, Dr. Tony Y. Rizk, Marwa A. Al-Obied, Ahmed S. Alutaibi and Dr. Mohammed H. Al-Khaldi

ABSTRACT

Large-scale seawater injection in two high permeability carbonate reservoirs within the Khurais field commenced with the onset of oil production in early 2008. Following the recent proposal for an incremental development plan that includes an underlying low permeability (2 millidarcies (mD)) reservoir with high calcium content (37,000 mg/L) formation water, it became necessary to examine alternative options to the seawater injection to avoid calcium sulfate scaling and microbial fouling. Secondary treated sewage effluent (TSE) from nearby urban treatment plants is abundant and presents an attractive option for injection in the high-risk, divalent ion formation brine (FB) environment.

An initial feasibility study focused on geochemical and microbial compatibility to assess the benefits expected from substituting TSE for costly desulfated water was conducted. A formation damage risk evaluation was also considered critical for the planned low permeability reservoir development since the significantly high initial capital expenditure associated with a new injection water processing facility would further erode the economic value of the project. Laboratory coreflood experiments and conventional bottle tests were therefore conducted, in addition to software simulation to appraise the TSE interaction with the formation fluid, and the inorganic scale deposition tendency at in situ conditions. The microbial study looked at the potential impact on the reservoir for both microbial contamination and the nutritional load of TSE.

The study confirmed that the sampled TSE had a relatively low level of contaminants, such as oxygen demanding substances (ODS), heavy metals and dissolved solids, and presented minimal formation damage risk compared to both seawater and field produced water. But it also revealed various total organic carbon (TOC) content, which may enhance troublesome microbial activities and impact the various systems' operational stages.

This article discusses the laboratory experiments and simulation conducted to assess the impact of injected TSE on microbial growth and in situ scale deposition, and the associated formation damage risk. It also provides insight into the quality threshold required for effluent injection in a reservoir of high divalent salt connate water.

INTRODUCTION

The target oil reservoir, Lower Fadhili (LFDL), is relatively heterogeneous with a permeability variation of 0.1 millidarcy (mD) to 10 mD and a porosity range of 5% to 20%. The formation mineralogical composition obtained from X-ray diffraction (XRD) analysis indicated 70% to 80% calcite and 10% to 20% ankerite, with less than 10% clay material. The network of wastewater treatment plants is located approximately 145 km southwest of the field. The undeveloped reservoir is approximately 5,000 ft subsea with an initial pore pressure of ~2,800 psi and a static temperature of ~155 °F. The formation brine (FB) is very saline — total dissolved solids (TDS) are ~205,000 mg/L — with a calcium content of ~37,000 mg/L and undetermined amounts of total organic carbon (TOC). The Arabian Gulf seawater is relatively rich in sulfate, > 4,000 mg/L, compared to the low sulfate ion content in treated sewage effluent (TSE), indicating a considerably lower risk of calcium sulfate scale deposition should TSE replace seawater injection, Table 1. Available information on the use of TSE for secondary recovery injection is scarce[1]. Depending on the physical, chemical and biological processing specifications for its treatment, it is not unexpected for TSE to carry elevated concentrations of residual suspended matter with high numbers of aerobic and anaerobic bacteria, Fig. 1. Major risks associated with use of the effluent for injection have since been identified as follows:

- Solids/sediments-related formation plugging.
- Presence of sulfate reducing bacteria (SRB) and other troublesome microorganisms leading to fouling and microbially induced corrosion (MIC).
- Chemical component incompatibility related problems as a result of precipitates, e.g., phosphates associated with the presence of detergent soaps[2] and process treatment byproducts in the TSE.
- Health, safety and environmental (HSE) related problems due to the presence of heavy metals/hazardous components in the TSE, such as cadmium, chromium, lead, aluminum and mercury, associated with the effluent's residue from manufacturing industries.

Wastewater pollutants[3] can be classified into four main categories, as given here:

Chemical and Physical Properties	Formation Water (Lower Fadhili Reservoirs)	Produced Water (Offset Reservoirs)	Treated Arabian Gulf Seawater (Quarrayah Seawater Plant)	TSE (Public Wastewater Treatment Plant)
Ionic Composition				
Calcium, Ca^{2+} (mg/L)	37,000	4,900	630	14
Magnesium, Mg^{2+} (mg/L)	6,700	1,100	2,100	44
Sodium, Na^{+} (mg/L)	34,000	20,100	17,200	274
Potassium, K^{+} (mg/L)	1,000	500	NA	31
Barium, Ba^{2+} (mg/L)	< 1	-	-	< 1
Strontium, Sr^{2+} (mg/L)	1.4	-	0.1	< 1
Total Iron, Fe^{2+} (mg/L)	NA	-	-	< 1
Chloride, Cl^{-} (mg/L)	122,500	38,500	31,200	349
Bicarbonate, HCO_3^{-} (mg/L)	330	430	190	224
Sulfate, SO_4^{2-} (mg/L)	480	470	4,100	446
Phosphate, PO_4^{3-} (mg/L)	NA	NA	NA	< 10
Heavy Metals				
Aluminum	NA	NA	< 10	< 10
Arsenic			< 10	< 10
Cadmium	0.01	NA	< 1	< 1
Chromium	-	+/-1.0	< 1	< 1
Lead			< 10	< 10
Zinc			NA	NA
Mercury			NA	NA
Physical Properties				
TDS (mg/L)	205,000	63,500	55,000	1,351
Specific Gravity	1.15	1.05	1.05	1.001
pH	4.8	6.5	7.0 - 7.2	7.4
Particle Size Distribution	NA	NA	300 - 1,000	NA
Total Suspended Solids (mg/L)	NA	NA	3 - 4	NA

Table 1. Water composition analysis

- Oxygen demanding substances (ODS): These pollutants place demand on the wastewater's natural supply of dissolved oxygen.
- Pathogens: Infectious microorganisms from city sewage or certain kinds of industrial food wastes present a considerble risk of waterborne diseases in the absence of disinfection/chlorination treatment.
- Nutrients: Sewage/industrial wastewater is rich in carbon, nitrogen and phosphorus used by oil field bacteria.
- Inorganic and synthetic organic chemicals: These vary from household cleaning/washing chemicals and detergents to manufacturing/heavy industry waste (cement, paint, synthetic organic chemicals, heavy metals, etc.), some of which may be toxic and harmful at relatively low concentrations.

Adequate wastewater treatments, such as settling, filtration and chlorination, can result in usable premium quality water for waterflooding in a specific reservoir. International regulatory bodies for wastewater systems have set recommended minimum quality[4] specifications for discharging effluents such as TSE. While these may vary depending on the local environment, a minimum standard based on critical HSE-related parameters is presented in Table 2. Since complete removal of pollutants may not be necessary, our investigation focused on determining if the existing TSE quality would effectively limit formation damage and induce better injectivity in the carbonate reservoir as compared to the alternative seawater.

The authors are not aware of previous Saudi Aramco experience regarding the use of sewage effluent for water injection operations; however, topside applications of secondary effluent from a Riyadh sewage treatment plant for a cooling water system at a Riyadh refinery[5] have established that TSE increases the risk of biological fouling, calcium phosphate ($Ca_3(PO_4)_2$) scaling and foaming. Biocides, scale and corrosion inhibitors, anti-foams and blowdown control were consequently used to control the problems encountered at the refinery.

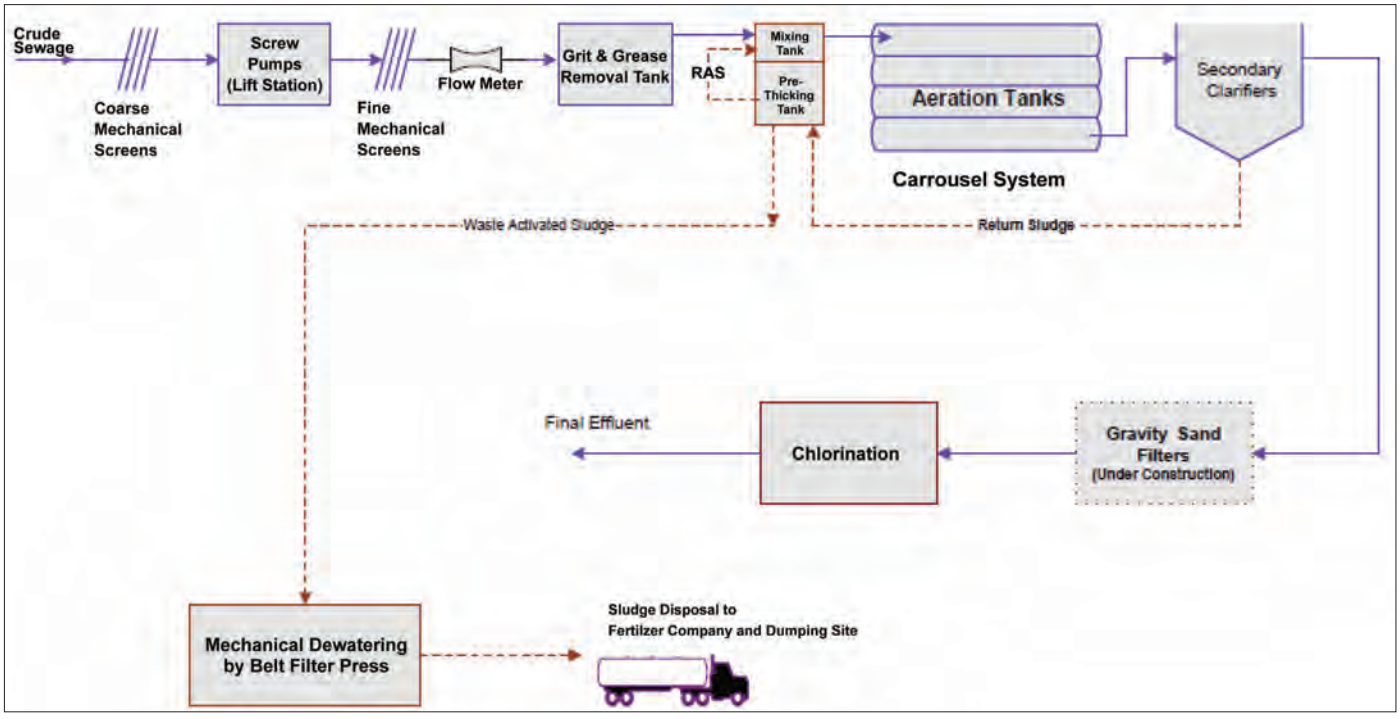

Fig. 1. Schematic of sewage treatment plant.

HSE-Related Parameter	Threshold Value	Remarks
Biochemical Oxygen Demand (BOD) (mg/L)	20	*TOC[10]
Total Suspended Solids (mg/L)	25	
Fecal Coliforms (counts per 100 ml)	400	After disinfection
Residual Chlorine (mg/L, min/max)	0.50/1.0	Minimum after 30 minutes contact time
pH (unitless)	6.0 - 9.0	
Phenols (micrograms/L)	20	
Oils and Greases (mg/L)	15	
Total Phosphorus (mg/L)	1.0	
*BOD ≈ 23.7 + 1.68 × TOC		

Table 2. International EPA recommended wastewater HSE-related threshold limits

WATER COMPOSITION ANALYSIS AND SCALE DEPOSITION RISK

Geochemical analysis was conducted to determine the amount of major pollutants, including ODS, nutritional load and inorganic compounds such as heavy metals in the TSE. The ion concentrations indicated that TSE is relatively "sweet" compared to seawater and formation water — with lower concentrations of calcium, sodium, chloride, sulfate and TDS. The amount of heavy metals, i.e., arsenic, cadmium, chromium, copper, lead, mercury and zinc, with densities above 4 g/cc was determined to be below the critical threshold for hazardous materials.

The reservoir brine is dominated by Na-Ca-Cl ions (~96%) with a high calcium content, unlike the offset reservoirs (Arab-D and Hanifa). The critical chemical ions concentration ratios (Mg/Ca, Na/Ca and SO_4/HCO_3) of the different waters (TSE, FB and seawater), as well as the calcium sulfate scale deposition risk at downhole physical conditions, are summarized in Table 3. Since the Mg/Ca ratio of the seawater (0.33%) is much higher than that of the FB (0.18%), seawater injection is expected to trigger an ion exchange to balance the chemical disequilibrium. This will result in magnesium ions from the mixed brine phase being retained onto the rock, while calcium ions are stripped from the carbonate rock matrix in the brine phase[6]. TSE injection, however, presents minimal scale deposition risk due to low sulfate (< 450 mg/L) and phosphate (< 10 mg/L) ions content. The scale prediction using fluid mixed with FB was facilitated with the ScaleSoftPitzer (version 4.0) computer application, which is an Excel™ based simulation program that can be used to calculate inorganic scale tendency parameters — scaling index (SI) and mass deposition (MD).

Test Conditions	FB	Seawater	TSE
Mg/Ca Cation Ratio	0.18	0.33	3.14
Na/Ca Cation Ratio	0.92	27.3	19.57
SO_4/HCO_3 Cation Ratio	1.45	21.6	1.99
*Calcium Sulfate Scale Risk - SI/MD (mg/L)	NA	0.58/2940	None
*Mixed fluid with FB at in situ conditions			

Table 3. Critical chemical ions concentration ratio and calcium sulfate scale risk

ROCK MINERALOGY AND CLAY SWELLING/ DISPERSION RISK

The mineralogical composition of the formation, obtained from XRD analysis of the reservoir rock, indicated 70% to 80% calcite and 10% to 20% ankerite with less than 10% clay material. Further analysis of the clay content indicated that the rock is composed of illite and a layer of mixed illite/smectite clays (6% to 7%) in addition to kaolinite (3% to 4%). The reservoir rock mineralogy, pore structure and formation fluid in combination with the injection TSE biochemical composition were used to infer the potential formation damage effects due to the interaction between the injection fluid and the reservoir.

A risk of smectite clay swelling due to osmotic pressure differentials, which can bridge the pore throats and lead to a gradual reduction in permeability[7], is present given the salinity contrast between the relatively fresh TSE (350 mg/L Cl-) and the high salinity FB (122,500 mg/L Cl-). Additionally, kaolinite clay deflocculation and dispersion could have a similar effect on permeability in this case, due to the narrow pore throats of the low permeability reservoir. The critical flow rate, corresponding to the interstitial velocity beyond which clay mobilization is expected, can be determined through a critical rate test in the laboratory[8]. This data then can be used with appropriate simulation models to determine the maximum TSE injection rate and the sensitivity of variable reservoir properties to the expected long-term injection. The currently planned water injection rate per well is 10,000 barrels per day, which translates to an equivalent flow velocity of ~0.03 ft/minute at the 8½" wellbore sandface. Given the LFDL reservoir depth and permeability, the critical velocity is expected to be higher than that of shallower reservoirs at similar water injection rates.

RESERVOIR FLUIDS AND MICROBIAL-INDUCED RISKS

Bacteria colonization of oil field systems is a major cause of concern and can lead to a number of operational complications. SRB, a group of the best known heterotrophic microorganisms, is the prime cause of reservoir souring, process equipment fouling and MIC in processing installations. Bacteria fouling is also responsible for lowering the quality and quantity of recovered oil and for a number of operational complications. For microbes to develop into an operational problem, a number of prerequisites have to be met:

- Availability of an electron donor.
- Availability of nutrients, including those required in minute concentrations.
- Availability of an electron acceptor.
- Water activity of $a_w > 0.92$.
- Tolerable operating conditions.
- Absence of inhibitory compounds.

The chemical compositions of the relevant compounds in TSE and the formation water were previously shown in Table 1. The nutritional composition of different TSE samples considered for injection into the reservoir for secondary recovery is shown in Table 4. Formation water contains sulfate (480 mg/L); no known volatile fatty acid and no hydrogen sulfide (H_2S) were reported. Laboratory tests further indicated that formation water is free of known inhibitory compounds and therefore presents a suitable environment for prokaryotic growth when supplemented with a source of utilizable organic carbon. The commingling of untreated TSE with formation water is therefore expected to stimulate microbial growth in

Nutritional Parameter	TSE/WWTP-1	TSE/WWTP-2	TSE/WWTP-3	Formation Water
TOC (mg/L)	40.3	32.155	57.3	Undetermined
Sulfate (mg/L)	476	422	413	480
Phhosphate (mg/L)	5.5	6.6	10.4	NA
Ammonia (mg/L)	~5.0	~5.0	~5.0	NA
*WWTP field samples collected May-June 2014				

Table 4. Average nutritional composition of three TSE samples and formation water

the reservoir and production system. Consequently, a study to remove the organic carbon from the TSE prior to injection is underway to curtail the growth of microorganisms.

LABORATORY EXPERIMENTS

The three effluent samples were collected and duly preserved at 39 °F (4 °C) during their transportation from the wastewater plant to the laboratory. Microbial analysis using the serial dilution most probable number (MPN) method was then conducted to enumerate values for SRB and general aerobic bacteria (GAB) in the TSE. The growth broths used for the serial dilution enumeration were prepared using sterile wastewater treatment plant (WWTP-2) effluent. The resulting data is critical to evaluate the suitability of the different TSEs to support prokaryotic growth. Serial dilution vials were incubated at 95 °F (35 °C) for 28 days before they were examined for growth.

Compatibility tests were carried out for mixed waters — TSE with FB at different mix ratios — using simple, classical jar tests, considered adequate for this operation, which does not involve high-pressure or high temperature conditions. This test involved using synthetic FB and introducing TSE water to form 10%, 30%, 50%, 70% and 90% TSE solutions. The unfiltered TSE water was mixed with the FB in varying amounts and monitored for precipitation at room temperature, after which the mixed fluids were placed in an oven for 16 hours (temperature = 150 °F). Visual inspection of the mixed fluid samples was used to appraise the fluid's clarity.

All three treatment plant TSE liquid samples were subjected to GAB/SRB enumeration. Only the WWPT-1 sample was subsequently subjected to coreflooding tests since it represented the best quality, based on bacteria analysis. Tests were carried out using reservoir core plugs and different injection water at a constant temperature of 150 °F to determine the relative formation permeability after injection of the different waters. The water samples used were unfiltered TSE, while the core plugs were pre-saturated with synthetic FB.

Two of the core plugs used for the coreflood experiments were taken from the reservoir section that had a porosity of 18% to 20% and permeability of 1.4 mD to 1.7 mD. Core sizes were 2.1" to 2.6" length by 1½" diameter, Table 5. The samples were flooded with synthetic FB under pressure conditions (pore pressure of 1,000 psi and confining pressure of 2,000 psi) at an oven temperature of 155 °F, which is equal to reservoir temperature, Fig. 2.

RESULTS AND DISCUSSION

The microbial analysis confirmed that common oil field bacteria, such as SRB and GAB, colonize both the TSE and formation water; however, the lack of biogenic H_2S in the formation water indicates nutritional limitation for bacterial growth. The commingling of TSE with formation water was shown to provide suitable conditions for prokaryotic growth, given the favorable conditions. The growth of SRB biomass and the associated sulfide generation is shown in Eqn. 1, where carbon is represented by equivalent acetate. The equation assumes that other physiochemical conditions, including dissolved gases, temperature profile, pressure, pH, treatment and inhibitory compounds, trace elements and mineral composition, are within the tolerance limit of the bacteria.

$$CH_3COO^- + SO_4^{2-} \rightarrow H_2O + CO_2 + HCO^-_3 + S^{2-} \quad (1)$$

The semi-quantitative MPN technique was used to access the number of viable bacteria in the effluent samples. Results of the microbial enumeration are presented in Table 6 and indicate different numbers of both SRB and GAB in the three effluents. The results show none to moderate numbers, respectively, in the WWTP-1 and WWTP-2 samples. In contrast, medium to high numbers were detected in the WWTP-3 sample, which was attributed to inadequate anti-microbial treatment at the time of sampling. Since SRB and GAB were detected in all of the different TSE and formation water mixtures, the availability of nutrients in the commingled TSE and formation water is considered a major concern as it provides the conditions for microbial proliferation. Based on Eqn. 1 and the lack of scavenging materials, it is anticipated that around 50 mg/L of H_2S would be produced. Consequently, a study is underway to establish the most suitable technique to remove organic carbon (nutrient) from TSE prior to injection, and a stringent biocide treatment has been designed to protect topside facilities from fouling and MIC. The nutritional load in injection water is of less concern in a reservoir of high TOC and high "geological" H_2S concentrations.

The inorganic scale deposition risk[9] can be inferred from a combination of the predicted SI and MD, mg/L. Only a risk of calcium carbonate (calcite) scale was identified from the simulation, and even this was considered low since the maximum MD was less than 77 pounds per thousand barrels (ptb), where 1 ptb = 2.856 mg/L, at 60% TSE content of mixed

Experiment Type/ Scenario	Core Plug No.	Length (in)	Diameter (in)	Porosity (%)	Air Permeability, K_{air} (mD)	Rock Quality Index, RQI (microns)	Brine Permeability, K_w (mD)
Injection Performance Comparison Test-1	43	2.57	1.5	20.3	1.7	0.09	NA
Injection Performance Comparison Test-2	41	2.10	1.5	19.8	1.4	0.08	1.53

Table 5. Summary of physical/petrophysical data for core plugs used for coreflood tests

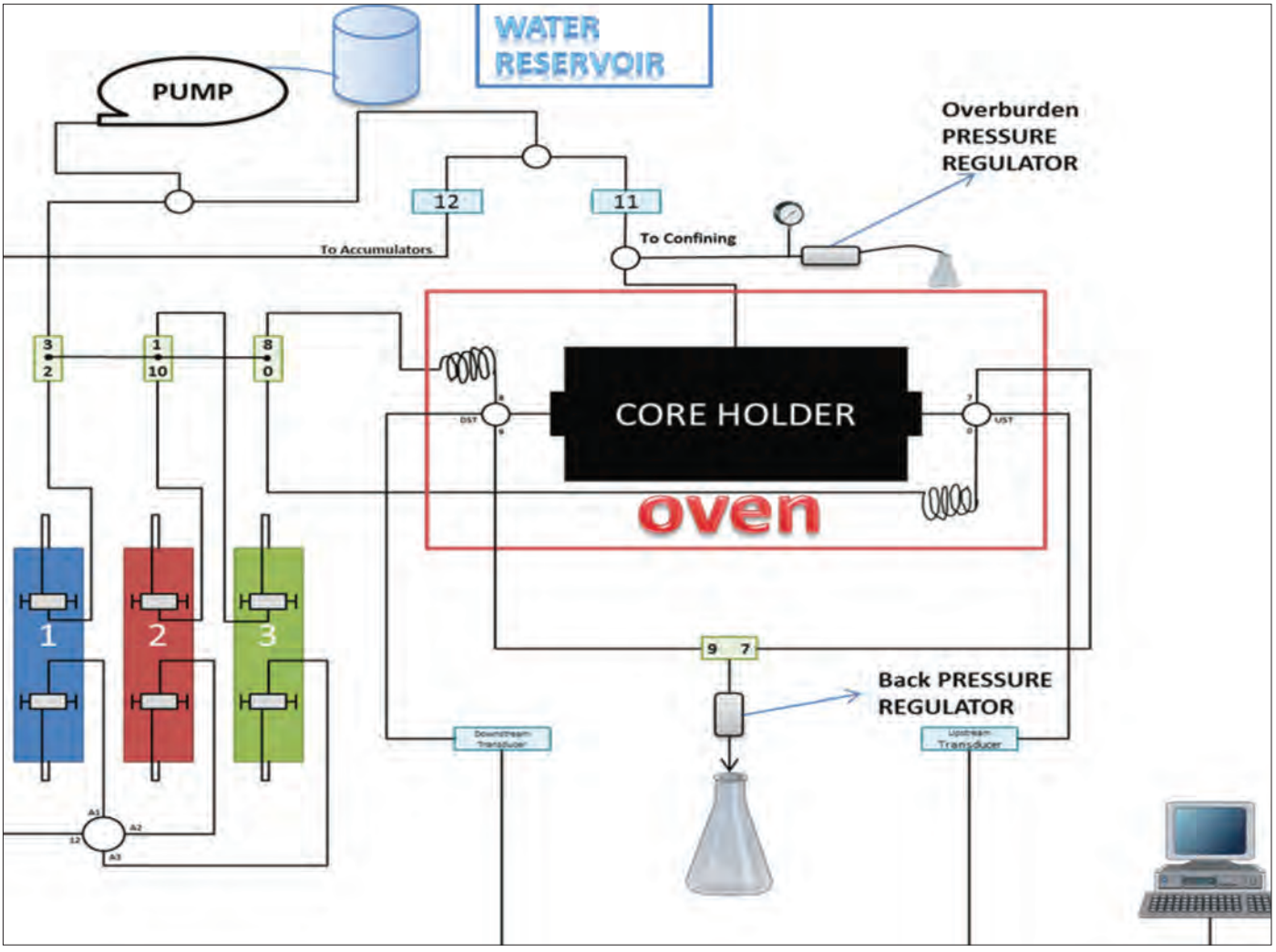

Fig. 2. Dynamic coreflood test equipment schematic.

Bacteria Content	TSE/ WWTP-1	TSE/ WWTP-2	TSE/ WWTP-3
SRB (MPN/ml)	< 0.4	0.9	9.3×10^4
GAB (MPN/ml)	< 0.4	4.3×10^2	9.3×10^6

Table 6. SRB and GAB enumeration in three TSE samples using the MPN technique

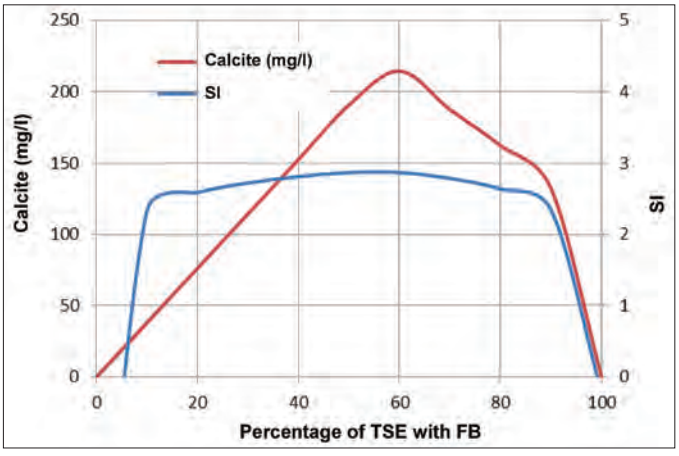

Fig. 3. Calcite SI and MD prediction (mixed TSE FB mix fluid).

brine, Fig. 3. The simulation was done for static fluids at bottom-hole conditions of 2,800 psi and 150 °F and at the expected producing wellhead conditions of 400 psi and 100 °F. The relative stability of the water or TSE-brine mix fluid may change with scale or precipitate deposition as a result of changes in pressure, temperature and pH. Figure 4 shows the fluid-fluid compatibility/scale precipitation tests at room and specific downhole test conditions (150 °F and 1,000 psi), which indicated no visible scales for different TSE/FB mixing ratios: 10/90, 30/70, 50/50, 70/30 and 90/10.

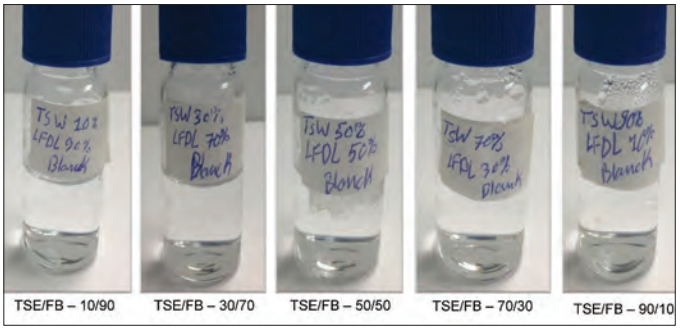

Fig. 4. Bottle test results of mixed brine compatibility/scale precipitation investigation of TSE with synthetic FB.

Experiment Type/Scenario	Stage No./Fluid Type/PV at Flow Rate					
	Stage #1	Stage #2	Stage #3	Stage #4	Stage #5	Stage #6
Injection Performance Comparison Test-1	FB 16 PV at 0.5 cc/min	TSE 30 PV at 0.5 cc/min	Produced Water 17 PV at 0.5 cc/min	Seawater 18 PV at 0.5 cc/min	FB 24 PV at 0.5 cc/min	
Injection Performance Comparison Test-2	FB 18 PV at 0.5 cc/min	TSE 38 PV at 0.5 cc/min	Produced Water 22 PV at 0.5 cc/min	Seawater 22 PV at 0.5 cc/min	TSE 20 PV at 0.5 cc/min	FB 13 PV at 0.5 cc/min

Table 7. Details of coreflood tests using single mode/lateral injection

The coreflood experiments, Table 7, were carried out using different injection water in an axial mode, as shown here:

- Injection Performance Test-1 (core plug 43): FB (16 PV) → TSE (30 PV) → Field Produced Water (17 PV) → Seawater (18 PV) → FB (24 PV).
- Injection Performance Test-2 (core plug 41): FB (18 PV) → TSE (38 PV) → Field Produced Water (22 PV) → Seawater (22 PV) → TSE (20 PV) → FB (13 PV).

The coreflood tests showed the impact of different injection waters on the formation permeability for the two core plugs, Figs. 5 and 6, respectively. The first part of each coreflood experiment was conducted to determine the base permeability by using the synthetic FB as the displacement fluid prior to subsequent injection of other fluids at the same flow rate. Although the initial synthetic FB displacement for sample 43 did not reach equilibrium conditions as the differential pressure (DP) was still declining after injection of 16 pore volumes (PVs), the relative permeability of the subsequent injection waters — i.e., TSE, produced water (from developed offset reservoirs) and seawater — was estimated at the same bottom-hole conditions of temperature and pressure. Analysis of the differential pressure trends with the PV at the constant injection rate of 0.5 cc/min indicated that TSE had the lowest potential for causing damage in the reservoir. The highest DP was observed during produced water injection, thereby indicating the poorest injectivity performance.

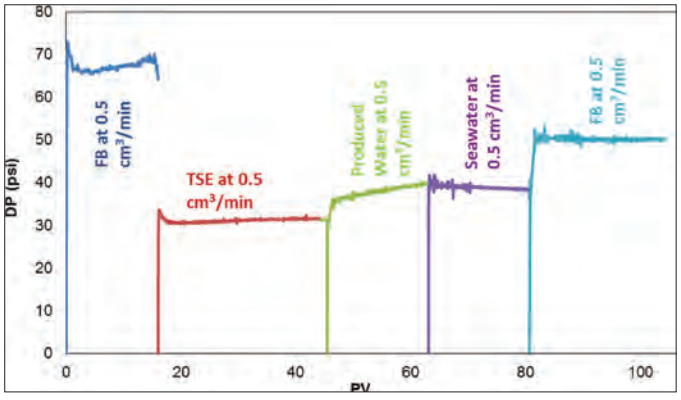

Fig. 5. Coreflood test/comparative injection performance — differential pressure vs. PV (core sample #1).

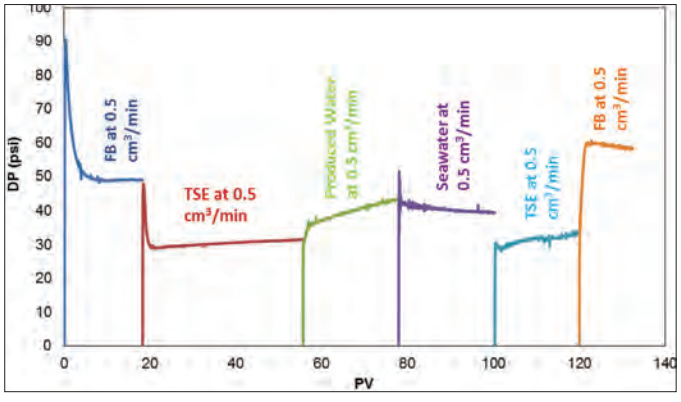

Fig. 6. Coreflood test/comparative injection performance — differential pressure vs. PV (core sample #2).

CONCLUSIONS

1. Common oil field bacteria, SRB and GAB, were detected in the three different TSE samples collected from considered wastewater treatment plants.
2. Commingled TSE and formation water represents a high risk of bacteria proliferation; however, a study is underway to remove the organic compounds of TSE prior to injection, while a stringent biocide treatment has been devised to protect topside facilities from fouling.
3. The injection of TOC-free TSE supported by a stringent biocide treatment and comprehensive monitoring scheme is expected to curtail microbial growth and associated H_2S generation.
4. The inductively coupled plasma generated chemical ion concentrations indicated that TSE is relatively "sweet" compared to other water samples — it has the least calcium, sodium, chloride, sulfate content and TDS. Only calcium carbonate (calcite) scale risk was observed, and this was appraised to be low relative to the scale risk of other injection water sources in the field — max SI ~3, and MD < 100 ptb. In addition, the heavy metals content was observed to be below the critical threshold for hazardous materials.
5. The content of heavy metals, i.e., arsenic, cadmium, chromium, copper, lead, mercury and zinc, with densities

General Physical Properties	Heavy Chemicals/Hazardous Components
TSE should be colorless and odorless	Most hazardous heavy metals content (mercury, arsenic, cadmium and chromium) < 1 mg/L.
Total suspended solids < 0.2 mg/L	Other heavy metals content (lead, zinc, aluminum and iron) < 10 mg/L.
*Solids particle size (D_p) > 2 microns	Non-acidic gas content with pH ~7.0.
Total suspended oil/oil-in-water < 1 ppm	
Inorganic Scale-Related Chemical Ions	**Microbial/Biochemical-Related Components**
Bicarbonate content – as low as possible	BOD < 10 mg/L.
Sulfate content < 500 mg/L	Ammonia content < 10 mg/L.
Phosphate content < 10 mg/L	SRB < 10 count/mL and total bacteria content < 10^4 count/mL (in customarily treated TSE from WWPT-1 and WWPT-2).
*Solids specification based on average pore throat size.	

Table 8. Critical injection TSE parameters specified for formation damage prevention

above 4 g/cc was found to be below the critical threshold for hazardous materials.

6. For water injection in the low permeability carbonate reservoir, the acceptable minimum water quality can be defined by the solids' particle size (D_p) and distribution with respect to the target injection reservoir pore throat size, i.e., D_p > 1/3 pore throat diameter. This is in addition to the critical ion concentration that exacerbates corrosion, scale precipitation and formation damage risk.
7. The critical formation damage-related parameters were grouped under four major categories: General Physical Properties, Heavy Chemicals/Hazardous Components, Potential Inorganic Scale-Related Chemical Ions and Microbial/Biochemical-Related Components, Table 8.
8. Coreflood experiments were carried out to compare the injectivity performance of TSE against that of the Arabian Gulf seawater and current field produced water; results indicated that TSE was the least damaging when used for water injection in the low permeability reservoir.
9. The integration of the microbial study with the conventional formation damage-related laboratory study was highly beneficial in determining the suitability of TSE for secondary recovery injection in the carbonate reservoir.

ACKNOWLEDGMENTS

The authors would like to thank the management of Saudi Aramco for their support and permission to publish this article. We would also like to thank the laboratory technicians of the Formation Damage and Stimulation Unit (Advanced Technical Services Department) and Materials Performance Unit (Research and Development Center Department) for their support.

This article was presented at the SPE International Symposium on Oil Field Chemistry, The Woodlands, Texas, April 13-15, 2015.

NOMENCLATURE

a_w osmotic pressure
D_p average solids particle diameter

REFERENCES

1. Simmons, J.D.: "Use of Sewage Effluent as a Water Flood Medium — Mattoon Pool, Illinois," SPE paper 706-G, presented at the Fall Meeting of the Petroleum Branch of the American Institute of Mining, Metallurgical and Petroleum Engineers, Los Angeles, California, October 14-17, 1956.
2. Bresnahan, W.T.: "Water Reuse in Oil Refineries," paper 0567, presented at the NACE International Annual Conference and Exposition, Houston, Texas, 1996.
3. U.S. Environmental Protection Agency: "Primer for Municipal Wastewater Treatment Systems," Report EPA 832-R-04-001, September 2004, 30 p.
4. Canada, Environmental Protection Service: "Guidelines for Effluent Quality and Wastewater Treatment at Federal Establishments," Report EPS-1-EC-76-1, April 1976.
5. Majnouni, A.D. and Jaffer, A.E.: "Effective Monitoring of Non-Chromate Chemical Treatment Programs for Refinery Cooling Systems Using Sewage Water as Make-Up," paper 0577, presented at the NACE International Annual Conference and Exposition, Houston, Texas, 1996.
6. Mackay, E.J., Sorbie, K.S., Kavle, V.M., Sorhaug, E., Melvin, K.B., Sjursaeter, K., et al.: "Impact of In Situ Stripping on Scale Management in the Gyda Field," SPE

paper 100516, presented at the SPE International Oil Field Scale Symposium, Aberdeen, U.K., May 31 - June 1, 2006.

7. Elkewidy, T.I.: "Integrated Evaluation of Formation Damage/Remediation Potential of Low Permeability Reservoirs," SPE paper 163310, presented at the SPE Kuwait International Petroleum Conference and Exhibition, Kuwait City, Kuwait, December 10-12, 2012.
8. Bennion, D.B., Thomas, F.B. and Bennion, D.W.: "Effective Laboratory Coreflood Tests to Evaluate and Minimize Formation Damage in Horizontal Wells," paper prepared for presentation at the 3rd International Conference on Horizontal Well Technology, Houston, Texas, November 12-14, 1991.
9. Hinrichsen, C.J.: "Preventing Scale Deposition in Oil Production Facilities: An Industry Review," paper NACE 061, presented at the NACE Corrosion Conference and Exhibition, San Diego, California, March 22-27, 1998.
10. Dubber, D. and Gray, N.F.: "Replacement of Chemical Oxygen Demand (COD) with Total Organic Carbon (TOC) for Monitoring Wastewater Treatment Performance to Minimize Disposal of Toxic Analytical Waste," *Journal of Environmental Science and Health*, Part A, Vol. 45, No. 12, October 2010, pp. 1595-1600.

BIOGRAPHIES

Peter I. Osode is a Petroleum Engineer Specialist with the Formation Damage and Stimulation Unit of Saudi Aramco's Exploration and Petroleum Engineering Center – Advanced Research Center (EXPEC ARC).

He has over 30 years of diverse upstream industry experience spanning well site petroleum engineering operations, production technology (well and reservoir management, production optimization and production chemistry), and drilling and completion fluids management. Peter started his career with Baroid/Halliburton as a Technical Fluid Sales Engineer before moving to Shell Petroleum Development Company in Nigeria and Shell International's affiliate — Petroleum Development Oman (PDO) — in Oman. He has participated in a number of Shell Global E&P Well Performance Improvement projects and was the subject matter expert on drilling fluids performance assessment prior to joining Saudi Aramco in 2009.

Peter is an active member of the Society of Petroleum Engineers (SPE) and has authored a number of published technical papers. He is currently involved in the formation damage evaluation of reservoir drilling and completion fluids, well remediation chemical treatment, scale management and flow assurance studies.

Peter received his B.S. degree with honors in Petroleum Engineering from the University of Ibadan, Ibadan, Nigeria.

Dr. Tony Y. Rizk joined Saudi Aramco's Research and Development Center (R&DC) in July 2006 and is currently a Science Specialist. Throughout his career of more than two-decades in the oil and gas industry, he has initiated and managed a number of research and deployment projects. Tony has pioneered the development of new technologies that have been successfully implemented worldwide. His research activities have been featured on BBC-1 television as a part of a program covering innovative science in the northwest area of the United Kingdom.

Tony assumed a number of roles while at the R&DC and is now focusing on technical activities to better serve the field. His work has involved microbially induced corrosion, encapsulation for downhole slow release, microbial enhanced oil recovery methodologies, nitrate corrosion, corrosion inhibitor and biocide selection, corrosion evaluation under high shear stress, hydrotesting and treated sewage effluent (TSE) for secondary recovery.

Tony has chaired a number of international, regional and local conferences and seminars including:

- The Energy Institute, Reservoir Microbiology Forum, London (2007 and 2008).
- Saudi Aramco Technical Exchange Forum, Dhahran (2010 and 2011).
- Technical Chairman of the 14th and 15th Middle East Corrosion Conference and Exhibition, Bahrain (2012 and 2014).
- Session Chairman of the Society of Petroleum Engineers (SPE) conference on MIC at Calgary, Canada (2009).

He is currently the Chairman of the National Association of Corrosion Engineers (NACE) Dhahran Saudi Arabia Section.

Tony received his M.S. degree in Quality and Reliability Engineering/Management from Birmingham University, Birmingham, U.K., and in 1992, his Ph.D. degree in Corrosion Science, from Manchester University, Manchester, U.K.

Marwa A. Al-Obied is a Petroleum Engineer working for Saudi Aramco's Exploration and Petroleum Engineering Center – Advanced Research Center (EXPEC ARC). She has been with Saudi Aramco since 2008 and specializes in well stimulation. In addition, Marwa is a regular contributor to the women's development organization in Saudi Aramco, and she is an active organizer with the Society of Petroleum Engineers – Saudi Arabia Section (SPE-SAS).

Marwa received her B.S. degree in Chemistry Science from the University of Oklahoma, Norman, OK. She also completed several courses in Petroleum Engineering while there.

Ahmed S. Alutaibi is a Senior Engineer working for Saudi Aramco's Khurais Producing Department. He has over 16 years of experience at different oil upstream functions, including process, inspection and project engineering at the Qurayyah plant, water injection pump stations in the North and South Ghawar fields and at various Khurais and Central Arabia oil plants and fields. Ahmed has worked in various scale projects throughout his career where he devoted his technical and projects execution knowledge to offer high cost avoidances and quality deliverables, especially at the largest increment in the world — the Khurais Central Processing Facility and fields projects.

In 2011, he established and led the Central Arabia plants and fields Assets Enhancement Committee that was also responsible for achieving a better way of saving precious aquifer water through maximizing an old plant production from processing high water cut producers and using that associated water for injection at a new nearby field that use groundwater for injection after having assured its compatibility.

Ahmed worked with other stakeholders in deploying — for the first time in the company — a reinforced thermoplastic pipe into hydrocarbon service at an oil flow line, providing a benchmark for a reliable, high quality, quick installation product, to help eliminate internal corrosion and increase the hydrocarbon value chain. He is now member of the Nonmetallic Piping Deployment Team for the Southern Area Oil Operations fields.

Ahmed won the Southern Area Oil Operation's VP Innovation Award twice. The first was in 2012 for conducting an experiment to connect impressed cathodic protection (CP) current fed from one source between two bare casing wells distanced more than specified in the old version of the company standard, which helped provide continuous and adequate protection to both well structures in case of theft and vandalism of a well's CP source. This experiment provided a mathematical and practical methodology that can be used at other fields to guarantee enough protection with a secure design. The results of the experiment and recommended modifications were evaluated and well endorsed and enabled revising the company standard to provide conditional flexibility in case of theft and vandalism. The second award was in 2014 for work done on treated sewage effluent (TSE) for reservoir injections. The TSE initiative was also a major qualifier that led to Ahmed's department winning the President's Award for Environmental Excellence in 2014.

In 1998, Ahmed received his B.S. degree in Mechanical Engineering from the University of Maine, Orono, ME.

Dr. Mohammed H. Al-Khaldi is a Petroleum Engineer in Saudi Aramco's Exploration and Petroleum Engineering Center – Advanced Research Center (EXPEC ARC). He has more than 15 years of experience in upstream research and technology. Since joining Saudi Aramco, he has been involved in applied research projects dealing with hydraulic/acid fracturing, VES technology, formation damage mitigation, corrosion control, drilling fluids and conformance control. Currently, he is leading a group of 15 engineers and 10 technicians.

Mohammed's experience includes the investigation of microbial corrosion by evaluating sulfate-reducing bacteria, development of mechanical methods to remove iron sulfide scale, and corrosion inhibition during acidizing of deep gas wells. Additionally, he has designed and optimized water shut-off techniques using gels and viscoelastic surfactants. Mohammed developed a new acid treatment for the acid-sensitive crude oils of new oil field developments. He has identified and provided field solutions to formation damage occuring during the drilling and completion of tight, unconventional gas reservoirs.

Mohammed has written more than 60 technical papers, has contributed to journals and many technial reports, and holds seven patents. He is an active member of the Society of Petroleum Engineers (SPE) and has chaired SPE workshops and conferences. In addition, Mohammed has been invited to give presentations at various universities and research organizations all over the globe. He is recognized as a lead researcher worldwide in the field of formation damage and well stimulation. Mohammed received the Vice President's Recognition Award for significant contributions toward the safe and successful completion of the first 100 fracture treatments of gas wells and the 2011 GCC SPE Award for best young professional technical paper.

He received his B.S. degree in Chemical Engineering from King Fahd University of Petroleum and Minerals (KFUPM), Dhahran, Saudi Arabia, and his M.S. and Ph.D. degrees in Petroleum Engineering from the University of Adelaide, Adelaide SA, Australia.

Setting a New Milestone in Carbonate Matrix Stimulation with Coiled Tubing

Authors: Nasser M. Al-Hajri, Abdullah A. Al-Ghamdi, Fehead M. Al-Subaie, Salih R. Al-Mujaljil, Zakareya R. Al-BenSaad, Abhiroop Srivastava, Danish Ahmed, Mohammed Aiman Kneina, Nestor Molero and Souhaibe Barkat

ABSTRACT

Horizontal carbonate reservoir stimulation has attracted considerable attention in the past decade as one of the major areas for development in matrix stimulation engineering. Modern technologies have enabled interventions in extended reach and even mega-reach wells. In the Middle East especially, carbonate field development strategies have used mega-reach wells as the main technique in achieving the highest possible reservoir contact. In such a case, coiled tubing (CT) intervention becomes a necessity.

With carbonate acidizing — since more than 50% of the matrix is soluble in acid — the objective is to bypass the formation damage and increase productivity by creating new highly conductive channels called wormholes. The success of a treatment is a function of fluid penetration, acid reactivity, injection rate and diversion. To increase the success of the treatments, improvements have been made recently in injection rate and diversion using the latest CT intervention technologies. The introduction of CT provides significant advantages in stimulation execution, yet also presents some challenges. Real-time downhole measurements transmitted with fiber optic telemetry are used frequently to improve chemical diversion and fluid placement; however, when this technology is deployed, pumping rates are significantly limited to a maximum of 2.0 barrels (bbl)/min.

Extensive engineering work was invested in finding a solution to this challenge. The main objective was to obtain optimum diversion using downhole "point" and distributed measurements without sacrificing high injection rates. So, modifications to the existing downhole measurement system were introduced that enable pumping rates beyond 5.0 bbl/min. The key focus of the redesign was the repackaging of the downhole tools, as well as improvements in the telemetry link to surface. The result has been an expansion of the operating envelope of the technology.

Yard testing has been completed, and results have been encouraging. The solution has been piloted in the field, and a field case study showed remarkable injectivity improvement.

INTRODUCTION

Most of the reservoirs in Saudi Arabia are carbonates with gas wells, oil producing wells and water injection wells. Injectivity in water injection wells that are drilled in carbonate reservoirs is mostly affected by injection carryover — materials/particles in the injected water that can impair permeability. With permeability reduced, well pressure builds up and injectivity drops. A matrix stimulation treatment, preferably with coiled tubing (CT), is then needed to overcome the formation damage and restore permeability and injectivity. Field-A in Saudi Arabia is produced using water injection as a means of pressure maintenance. Water injection improves sweep efficiency and restricts the pressure decline. Water injection takes place at the reservoir peripheries; sometimes the water injectors are in the same layer as the oil producers, but when aquifer mobility is very low and cannot act as an effective water drive, they may be in a water layer below the oil layer.

Field-A reservoirs are carbonates that are mostly completed as open holes. The reservoir has added complexity due to the presence of fractures, fissures and fault networks. As the only purpose of water injectors is to support oil producers, water injection into these wells must be homogeneous and at a high rate with low injection pressures. Because of the nature of carbonates when water is injected, the water preferentially takes the path of least resistance, which is provided by fissures, fractures and faults. Therefore, to achieve injection into a rock matrix, an intervention of matrix acidizing is needed. Fluid placement in appropriate zones is very crucial to the success of the treatment.

FIELD AND RESERVOIR DESCRIPTION

Reservoir-A consists entirely of mud supported limestones that lack megascopic pore spaces. Porosity is in the form of micropore spaces (< = 10 µm in size). Evidence for this microporosity includes the high porosities, 5% to 32%, within these fine-grained rocks shown in porosity logs and core plug analyses; the absence of any visible porosity — even in thin sections — to account for the high pore volumes; and 2,000x scanning electron microscope images that show a crystal framework texture composed of microrhombic calcite crystals with 2 µm to 5 µm pore spaces between them. The microporosity is thought to reflect the retention of primary intercrystalline spaces within the precursor lime mud sediment, with little introduction of allochthonous calcite to occlude the pore spaces. Flow meters indicate that the reservoir is capable of producing/

injecting large volumes of oil/water, but that stratigraphic predictability of the flow is lacking, and that thin (2 ft to 10 ft), low porosity (< 15%) intervals can contribute over 60% of the entire flow. These reservoir attributes, coupled with the low "matrix" permeabilities — 0.1 millidarcy (mD) to 10 mD — of the reservoir, indicate the presence of an apparent permeability that is controlling fluid flow. Core studies revealed that this apparent permeability is in the form of high angle fractures. The fractures are ≤1 mm wide, contain hydrocarbon residue and calcite cement, and in many cases are in close association with high amplitude stylolites. This suggests a genetic link between stylolitization and fracturing; borehole imaging log data are providing valuable insight into fracture location, abundance, orientation and size in noncored wells. Reservoir-A is separated from another reservoir, which has highly favorable rock properties, by over 450 ft of fine-grained and impermeable carbonates; however, there is evidence that these two reservoirs are in pressure fluid communication via a network of fractures. This reservoir communication, together with the reservoir heterogeneity of Reservoir-A in the form of micropores and associated fractures, presented a challenge for reservoir geology and reservoir engineering as a development plan involving horizontal producers was formulated; the need was to mitigate reservoir communication and to efficiently and effectively extract the reserves within this reservoir[1].

JOB OBJECTIVES AND CHALLENGES

The well in this study is a 6⅛" open hole water injector drilled in 2001, Fig. 1. The well had been shut-in since its completion. It was decided to stimulate the well after initial injection results showed a rate of 6,000 barrels per day (B/D) at 1,786 psi wellhead pressure (WHP). The goal of the stimulation was to increase the injection rate, and the following job objectives were identified:

- Determine tight or damaged zones for proper placement of stimulation fluid[2].
- Determine high permeability thief zones for proper placement of diverting fluid[2].
- Determine bottom-hole temperatures (BHTs) to verify working temperatures of stimulation fluids[2].
- Determine bottom-hole pressures (BHPs) during stimulation so that stimulation treatment is carried out below fracturing pressure[2].
- Perform pre-stimulation and post-stimulation well test analysis to identify reservoir parameters.

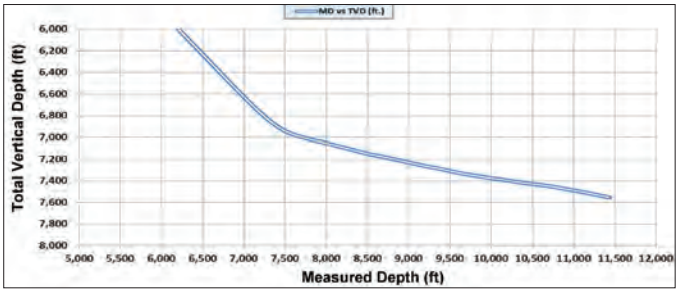

Fig. 1. Open hole horizontal water injector.

PROPOSED SOLUTON AND PRE-JOB PLANNING

Considering the challenges of the operation, the use of CT with fiber optics was deemed essential since this technology enables real-time downhole measurement. It consists of optic fiber, inside the CT, connected to the bottom-hole assembly (BHA), where this fiber acts as a source of telemetry from the downhole tools to the surface in real time. When the CT is stationary at total depth (TD), the fiber can also be used to make distributed temperature measurements all the way down the well.

A distributed temperature survey (DTS) has been conventionally used to monitor the performance of water injectors by employing the warm-back technique. The well is shut-in for a period of time and the temperature response is recorded while the well warms back toward the geothermal gradient. Under injection conditions, the cold water injected into the well cools the surrounding rock, including the nonpermeable intervals above the reservoir; it is the warming of these intervals that is measured. Normally, the only information that can be obtained during injection is the lowest extent of fluid injection; in unusual cases, if the flow rate is low enough, the injection profile can be determined by using the geothermal gradient and inflow profile into the reservoir. In most cases, though, injection is stopped, and the surrounding rock warms back to the geothermal gradient over time as a function of the formation's thermal properties. If a permeable interval has been injected with cold water, the rock cools in a much greater radius around the wellbore than the rock in intervals that were not injected with cold water, such as those behind the casing. Therefore, the injected intervals warm back up at a much slower rate than those that were not injected with cold water. The magnitude of this effect is a function of the injection rate, interval permeability, time and the thermal properties of the fluid and rock.

The downhole tools[3] at the end of the CT also provide real-time measurements of bottom-hole parameters. These tools are:

- The BHT sensor.
- The BHP gauge (to measure the inside and outside pressure of the CT).
- The casing collar locator for depth correlation.
- The use of gamma rays for depth correlation and lateral identification.
- Tension and compression tools for bottom-hole CT tension and compression forces.

Conventional downhole tools that are used to conduct a DTS and to obtain real-time bottom-hole parameter measurements are sized to 2⅛", and flow rates when using these tools are limited to only 2.0 bbl/min. This low rate and some limitations

with respect to fiber parameters, results in the following during matrix stimulation:

- Long pumping time, leading to a long job execution time.
- An inability to obtain deeper penetration of stimulation fluids, which restricts the depth of wormholes.
- A tendency for the low-tensile strength Inconel fiber carrier, which carries fibers inside for the DTS and is used for telemetry purposes, to break at high pump rates.
- The adverse effect on the Inconel fiber carrier of certain fluids, especially when sticky or highly viscous fluids are pumped.

Because the above limitations lead to low execution efficiency, a new tool was developed specifically for CT interventions with real-time bottom-hole parameter measurements during stimulation that included the following upgrades:

- The new 3¼" BHA consists of (1) BHT sensor, (2) BHP gauge (to measure the inside and outside pressure of the CT), and (3) gamma ray for depth correlation and for lateral identification.
- The tool is rated up to 8.0 bbl/min. This high rate enables deeper penetration of fluids and leads to the creation of deeper wormholes.
- The tensile strength for the Inconel fiber carrier to be used with this tool is double that of the fiber for the 2⅛" tool, which permits not only high pump rates, but also the pumping of very viscous fluids that could not be pumped when conventional CT tools were deployed for measuring real-time bottom-hole parameters.
- The high rate permitted by the new tool can also help in faster descaling and clean out jobs.

Given the availability of this high flow rate tool for CT intervention with real-time bottom-hole parameter measurements, it was decided that the stimulation pumping schedule would be optimized by using DTS, and to decrease the time of the job, a pressure gauge would be used to conduct pre-stimulation and post-stimulation well tests using the concept of injection and falloff analysis[4].

Injection and falloff testing, Fig. 2, is pressure transient testing during the injection of a fluid into a well. It is analogous to drawdown testing for both constant and variable rates. Shutting in an injection well results in a pressure falloff that is similar to pressure buildup in a production well. The distinction between injection/falloff and conventional drawdown/buildup testing is that the flow characteristics of the injected fluid are different from those of the original reservoir fluids, so that multiphase reservoir flow must be considered when interpreting these tests[5].

The following operational job steps were defined and executed to meet the job objectives:

- Confirm wellbore accessibility to TD.

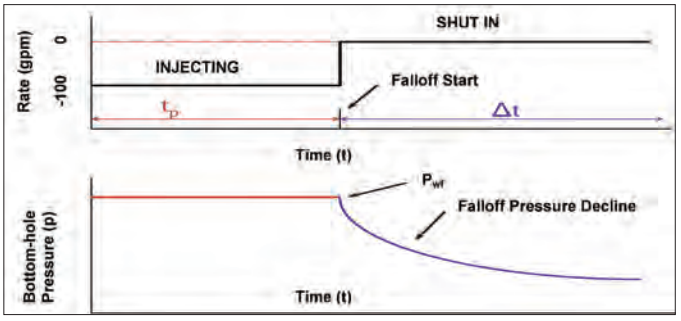

Fig. 2. Injection and falloff well test[4].

- Perform DTS when CT is at TD. Record baseline DTS.
- Perform pressure transient analysis (PTA) while CT is at casing shoe. Monitor bullheaded water.
- Reciprocate CT along open hole interval while pumping preflush. Reach TD to perform DTS. Conduct preflush warm-back and record response. Optimize pumping schedule based on preflush warm-back response.
- Pump stimulation treatment of acid, diverter and emulsifying agent. Run CT in hole to TD and perform DTS. Reciprocate CT along the open hole interval while pumping post-flush. Conduct post-flush warm-back.
- Perform PTA while CT is at casing shoe. Monitor bullheaded water.
- Pull CT out of hole.

JOB EXECUTION

The job was executed as per the job steps previously mentioned. This section describes the different parts of the job: pre-stimulation evaluation, stimulation execution and post-stimulation treatment evaluation.

Pre-stimulation Evaluation

As the well was an injector, it was agreed to have the well on injection for some time before running the CT in hole. This provided an idea of the pre-stimulation maximum injection rate. It was also agreed to shut-in the well for some time so that once the CT was run in hole (RIH) and the DTS was conducted, the well would show the extent that fluid at the maximum injection rate had reached in the open hole section. This would also show the high permeability thief zones and the low permeability tight/damaged zones. Figure 3 shows the CT downhole parameters during the first DTS, the baseline measurement. Table 1 explains Figure 3.

Figure 4 shows the results from the baseline DTS that was conducted. Baseline data were acquired for nearly 3 hours. The dark green trace shows the last trace recorded during the baseline acquisition. It clearly shows tight/damaged intervals near the heel and toe section, whereas from 9,200 ft to 10,795 ft, it shows high permeable thief zones; the highlighted section

shows the complete open hole interval. The baseline DTS provides the long-term injection temperature of the well.

The CT was brought to the casing shoe after the baseline DTS recording to conduct the injection/falloff pressure transient testing.

The preflush was then pumped via the CT while reciprocating the CT in the open hole section, as shown in Fig. 5. Table 2 explains Fig. 5.

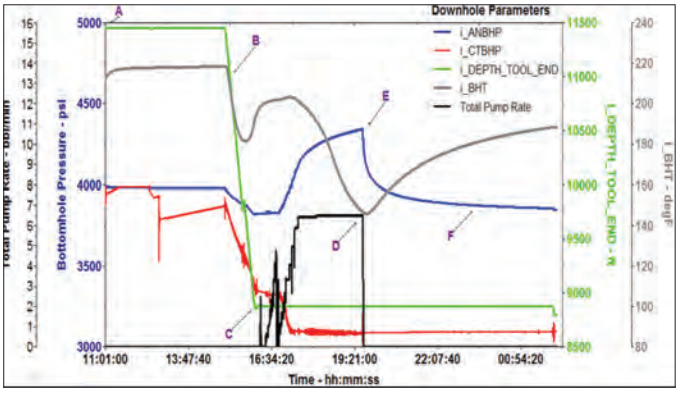

Fig. 3. Pre-stimulation DTS (baseline) and PTA execution, with CT downhole parameters.

Parameter	Event
A	CT at TD. Started baseline DTS.
B	End DTS. Pull out of hole (POOH) to casing shoe.
C	Stop POOH to inject through annulus.
D	Dropped pump rate to 0 bbl/min at 980 bbl pumped.
E	Measure pressure response with pump rate increase up to 6.42 bbl/min in gradual steps at WHP of approx. 1,400 psi.
F	Performed PTA for 6 hours.

Table 1. Pre-stimulation DTS (baseline) and PTA execution

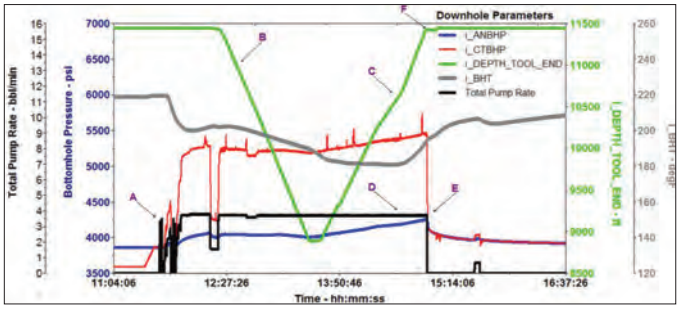

Fig. 5. Preflush DTS (warm-back) execution and with CT downhole parameters.

Parameter	Event
A	CT at TD. Started pumping preflush using jetting tool.
B	POOH from CT to casing shoe while pumping.
C	RIH from casing shoe to TD while pumping.
D	Maintain pump rate maintained at 3.75 bbl/min (maximum circulation pressure 5,000 psi).
E	Finished pumping preflush.
F	Start conducting warm-back DTS for 3 hours.

Table 2. Preflush DTS (warm-back) execution

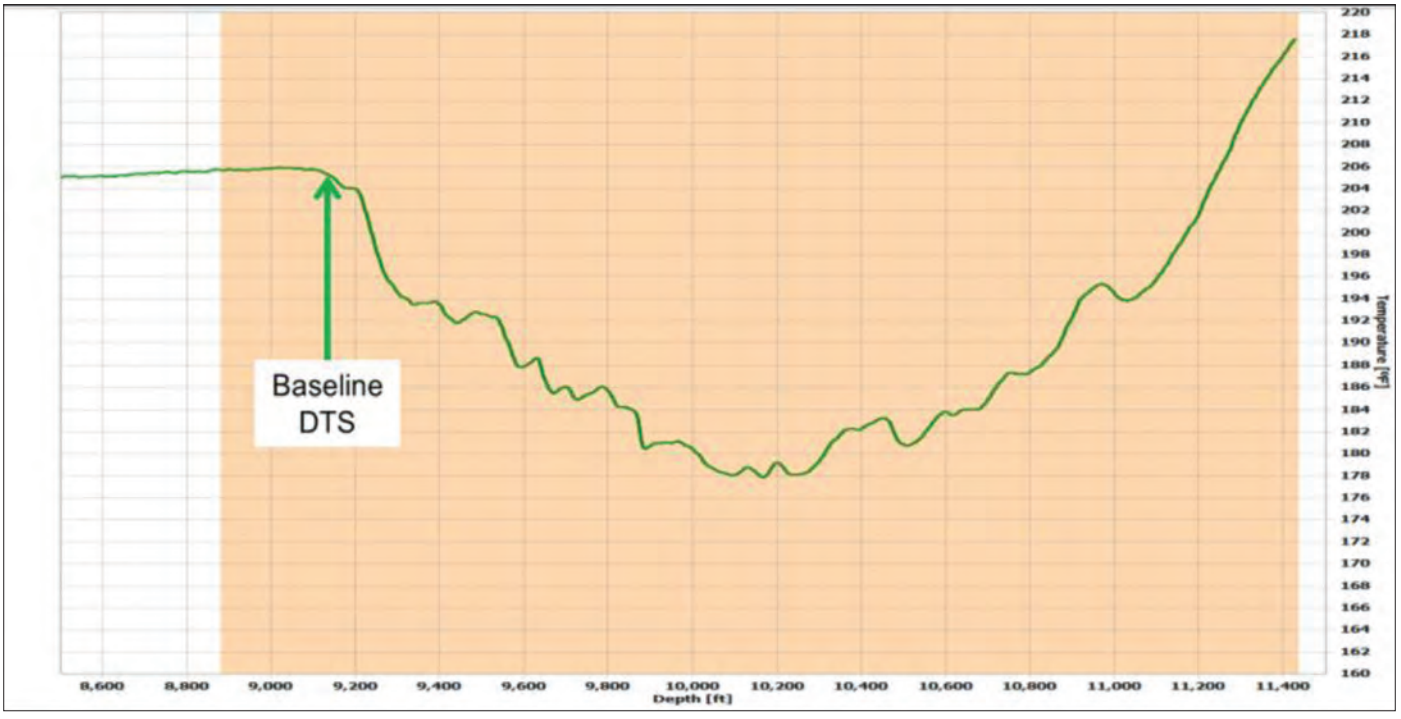

Fig. 4. DTS baseline.

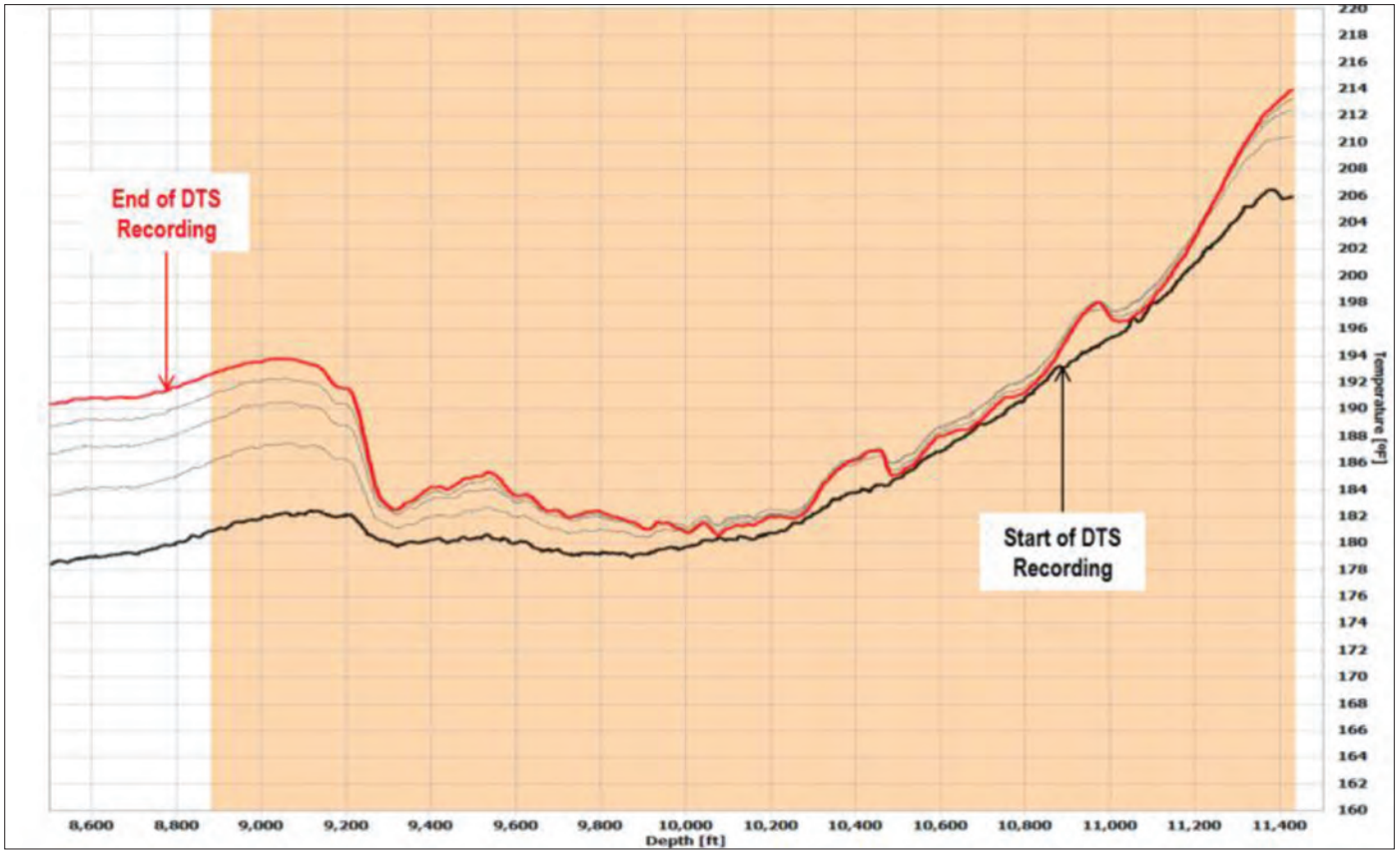

Fig. 6. Preflush DTS warm-back.

The CT was then RIH to TD to record the preflush warm-back DTS, Fig. 6. High permeability thief zones and tight/damaged zones were identified, and the stimulation treatment was optimized accordingly. Tight/damaged zones were identified at 9,040 ft to 9,240 ft, 9,400 ft to 10,005 ft, 10,295 ft to 10,490 ft, 10,870 ft to 11,010 ft, and 11,140 ft to 11,431 ft.

Stimulation Treatment Execution

Figure 7 shows the optimized stimulation treatment that was pumped as per a modified schedule, with downhole CT parameters. The stimulation treatment consisted of hydrochloric acid, a diverter and a retarded acid for deeper wormhole penetration. The pumping rate was maintained between 3.3 bbl/min and 3.75 bbl/min, limited by a circulation pressure of 5,000 psi, as per the program. The retarded acid was generally pumped at a lower rate of 3.3 bbl/min, and the diverter was pumped at a higher rate of 3.75 bbl/min. The downhole pressures, Fig. 7, indicated a constant pressure differential (i_CTBHP – i_ANBHP) of about 1,100 psi on the jetting tool throughout the stimulation sequence, indicating very good jetting through nozzles. Table 3 provides an explanation of Fig. 7.

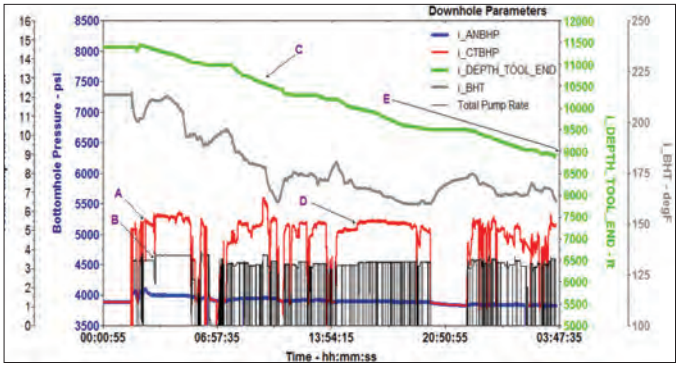

Fig. 7. Stimulation treatment with CT downhole parameters.

Post-Job Evaluation

After the stimulation treatment, a post-flush was pumped with CT while reciprocating the CT in the open hole section. The CT then was RIH to TD to record the warm-back DTS. When

Parameter	Event
A	Start pumping stimulation treatment.
B	Maintain pump rate maintained between 3.3 bbl/min and 3.75 bbl/min (<5,000 psi circulation pressure).
C	POOH from TD to casing shoe while pumping treatment stages.
D	Treatment fluid consists of acid, retarded acid, spacer, and diverter.
E	Finished pumping treatment. RIH again to TD while pumping post-flush.

Table 3. Stimulation treatment execution

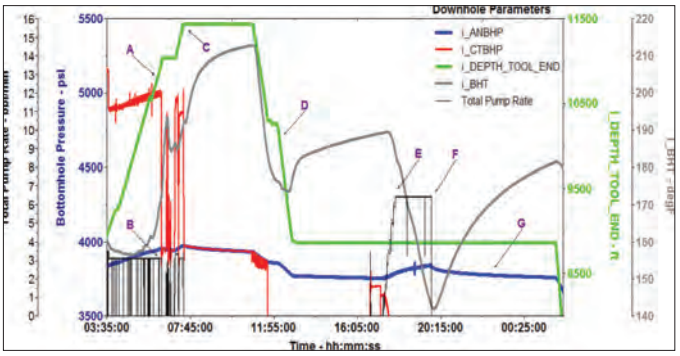

Fig. 8. Post-stimulation evaluation: post-flush DTS warm-back and PTA execution with CT downhole parameters.

Parameter	Event
A	RIH from casing shoe to TD while pumping post-flush.
B	Pumping displacement.
C	With post-flush out of CT (at TD), start warm-back DTS for 3 hours.
D	POOH CT just above casing shoe.
E	Line up to annulus and increase pump rate in steps to 6.42 bbl/min at WHP of approximately 900 psi.
F	Finished post-stimulation injection. Stop pumps.
G	Performed PTA for 6 hours.

Table 4. Post-stimulation evaluation

the DTS warm-back recording was finished, the CT was POOH to the casing shoe, and water was injected from the annulus of the CT while recording the downhole parameters for the injection/falloff PTA. Figure 8 shows the CT downhole parameters while pumping the post-flush. Table 4 explains Fig. 8.

Figure 9 shows the DTS warm-back after the post-flush. This was used for post-stimulation treatment evaluation by comparing it with the preflush warm-back DTS. The post-stimulation warm-back analysis shows a relatively uniform profile as compared to the pre-stimulation DTS warm-back graph.

The final pumping rate achieved was 6.4 bbl/min, where it was kept steady until the end — 820 bbl overall. Significant drops in WHP — from 1,300 psi pre-stimulation to 950 psi post-stimulation at 6.4 bbl/min — and drops in downhole pressure — from 4,350 psi pre-stimulation to 3,850 psi post-stimulation at 6.4 bbl/min — were observed. The downhole pressures were monitored for 6 hours while performing the PTA. Results were compared to the results for the PTA conducted before stimulation. Figure 10 shows the log-log plot for the falloff conducted pre-stimulation (orange — pressure and its derivative) and post-stimulation (green — pressure and its derivative). The log-log plot behavior shows that skin was reduced; the zones that previously had not been contributing to injection were now contributing. Consequently, determination of effective length, skin and permeability was possible for pre- and post-stimulation. The injectivity index of the pre-stimulation injection was 20.0 B/D psi, whereas the injectivity index of the post-stimulation injection was 200.9 B/D psi.

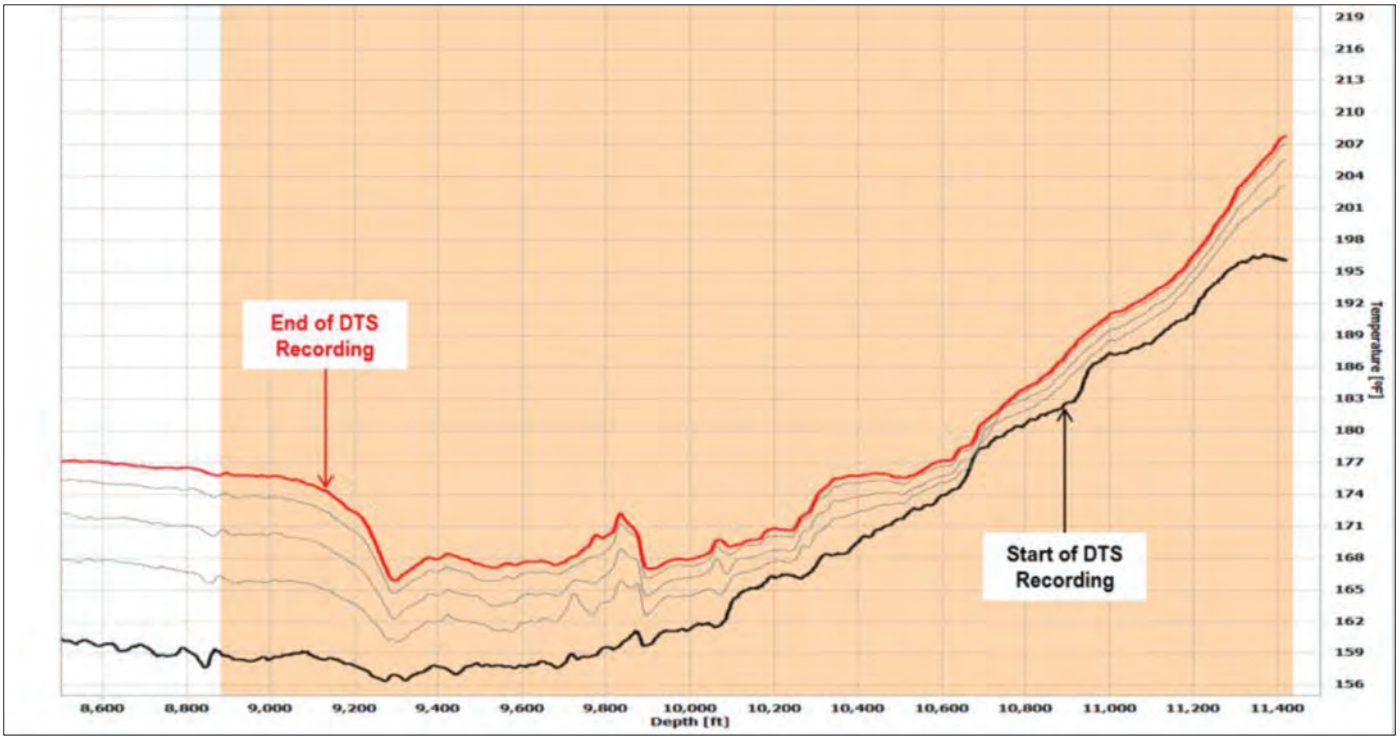

Fig. 9. Post-flush DTS warm-back.

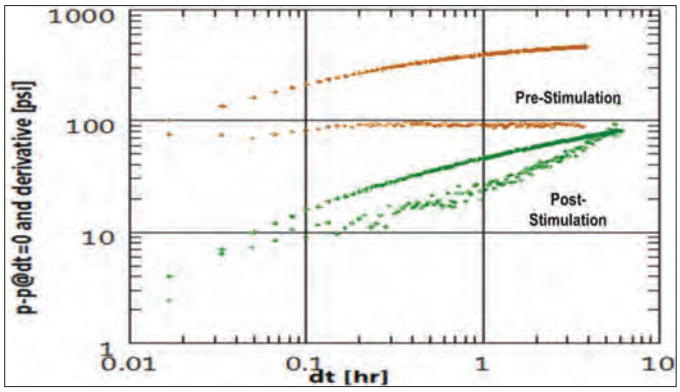

Fig. 10. Log-log plot showing pre- and post-stimulation falloff PTA results.

LESSONS LEARNED AND POST-JOB RESULTS

The first worldwide deployment of the high flow rate system via CT with real-time bottom-hole parameter measurements was very successful, with tangible improvements; the post-stimulation injection rates were 10 times the initial injection rates. High flow rate matrix stimulation achieved efficient jetting through the downhole tools. Use of DTS and PTA resulted in better evaluation of the treatment and enabled the modification of the pumping schedule, which could be customized for the well. The increased effectiveness of the on-the-fly treatment schedule and less time spent stimulating the well are additional benefits observed on this job.

Because of the limitation on circulation pressure of 5,000 psi in this job, the tool configuration did not allow for a pump rate greater than 3.7 bbl/min when pumping the preflush and post-flush from the CT. Also, while conducting the pre-stimulation and post-stimulation injection via the annulus for the PTA, WHP was 1,400 psi and 900 psi, respectively, at 6.42 bbl/min. After stimulation, the well was put on injection of 14,000 B/D at 1,010 psi WHP.

ACKNOWLEDGMENTS

The authors would like to thank the management of Saudi Aramco and Schlumberger for their support and permission to publish this article. The authors would also like to thank Mahtab Singh Soin, Tamer Elsherif and Ramy Ahmed for their intense contribution to the completion of this article.

This article was presented at the SPE Middle East Oil and Gas Show and Conference, Manama, Bahrain, March 8-11, 2015.

REFERENCES

1. Grover Jr., G.A.: "Abqaiq Hanifa Reservoir: Geologic Attributes Controlling Hydrocarbon Production and Water Injection," SPE paper 25607, presented at the SPE Middle East Oil Show, Bahrain, April 3-6, 1993.
2. Al-Gamber, S.D., Mehmood, S., Ahmed, D., Burov, A., Brown, G., Barkat, S., et al.: "Tangible Values for Running Distributed Temperature Survey as Part of Stimulating Multilateral Injection Well," SPE paper 167490, presented at the SPE Middle East Intelligent Energy Conference and Exhibition, Manama, Bahrain, October 28-30, 2013.
3. Olarte, J.D., Haldar, S., Said, R., Ahmed, M., Burov, A., Stuker, J., et al.: "New Approach of Water Shutoff Techniques in Open Holes and World First Applications of Using Fiber Optic Services with Tension Compression Sub," SPE paper 149116, presented at the SPE/DGS Saudi Arabia Section Technical Symposium and Exhibition, al-Khobar, Saudi Arabia, May 15-18, 2011.
4. Johnson, K. and Lopez, S.: "Nuts and Bolts of Falloff Testing," U.S. Environmental Protection Agency Report, March 5, 2003, 80 p.
5. Banerjee, R., Thompson, L.G. and Reynolds, A.C.: "Injection/Falloff Testing in Heterogeneous Reservoirs," SPE paper 38721, presented at the SPE Annual Technical Conference and Exhibition, San Antonio, Texas, October 5-8, 1997.

BIOGRAPHIES

Nasser M. Al-Hajri joined Saudi Aramco in 2013 as a Production Engineer working in the Southern Area Production Engineering Department. He is currently working in the North Ghawar Production Engineering Division, where he is involved with many aspects of the production/injection operations in three major fields. Nasser's interests include well stimulation, systems hydraulic simulation and well performance modeling.

In 2013, he received his B.S. degree in Petroleum Engineering from King Fahd University of Petroleum and Minerals (KFUPM), Dhahran, Saudi Arabia.

Abdullah A. Al-Ghamdi joined Saudi Aramco in 2008 as a Production Engineer working in the Southern Area Production Engineering Department. He has worked in several areas within the company, including Oil/Water Production Engineering, Well Completion and Services, the Southern Area Laboratory Division and the Sea Water Injection Department. Abdullah is currently on assignment with Halliburton as part of the service company training program.

He is a member of the Society of Petroleum Engineers (SPE).

Abdullah received his B.S. degree in Petroleum Engineering from King Fahd University of Petroleum and Minerals (KFUPM), Dhahran, Saudi Arabia.

Fehead M. Al-Subaie joined Saudi Aramco in 2003. He is a Production Engineering Supervisor working in the Southern Area Production Engineering Department, where he is involved in gas and oil production engineering, reservoir engineering, well completion and stimulation activities. Fehead is mainly interested in the field of production engineering, production optimization and new well completion applications.

In 2002, he received his B.S. degree in Petroleum Engineering from King Saud University, Riyadh, Saudi Arabia.

Salih R. Al-Mujaljil joined Saudi Aramco in January 1981 as a Field Services Operator (Field Engineer). Since that time, he has had several development assignments with Drilling & Workover, Reservoir Management and the Production & Facilities Development Department. Salih is now a Senior Production Engineer in the North Ghawar Water Injection Unit.

In 1986, he received his B.S. degree in Petroleum Engineering from the University of Southern California, Los Angeles, CA.

Zakareya R. Al-BenSaad is a Production Engineering General Supervisor. His work assignments include oil production engineering, plant engineering and well services. Zakareya has been active on many teams and his achievements have been well recognized. He has also coauthored several published Society of Petroleum Engineers (SPE) papers.

In 1998, Zakareya received his B.S. degree in Petroleum Engineering from the University of Tulsa, Tulsa, OK.

Abhiroop Srivastava is a CoilTOOLS Engineer-in-Charge, who has worked extensively with coiled tubing (CT) downhole technologies since he began in Well Intervention at Schlumberger Saudi Arabia in 2010. Abhiroop's experience involves working with varied CT applications under different conditions across the breadth of the Saudi Arabia/Bahrain market. He has extensive experience in matrix stimulation and the optimization of treatments using fiber optic enabled CT services. Abhiroop has also worked with downhole applications of real-time CT sensing on shifting inflow control devices, abrasive perforations, logging and extended reach jobs.

In 2009, he received his B.E. degree in Electrical Engineering from Delhi College of Engineering, New Delhi, India.

Danish Ahmed is a Senior Intervention Production Engineer currently working with Schlumberger Well Intervention – Coiled Tubing Services, supporting the ACTive Services Platform. His experience includes working as a Field Engineer with Well Production Services based in 'Udhailiyah, Saudi Arabia, where he supported proppant/acid fracturing and matrix acidizing jobs, followed by working as a Production Technologist with Petro Technical Services (formerly Data and Consulting Services) in Dhahran, Saudi Arabia. Danish began working for Saudi Schlumberger in 2007.

In 2007, he received his M.S. degree in Petroleum Engineering from Heriot-Watt Institute of Petroleum Engineering, Edinburgh, Scotland.

Mohammed Aiman Kneina is the Account Manager for Oil South. He began working with Well Intervention – Coiled Tubing Services (CTS) in Schlumberger Algeria in 1999. His CTS experience involves working in 'Udhailiyah, Saudi Arabia, supporting coiled tubing and matrix stimulation jobs.

In 1998, he received his B.E. degree in Instrumentation from the Algerian Petroleum Institute of Engineering, Boumerdes, Algeria.

Nestor Molero is a Sales & Technology Manager for Schlumberger Well Intervention in Mexico and Central America. He is a Technical Engineer with more than 15 years of experience in the design, execution and evaluation of coiled tubing (CT) workover interventions in onshore and offshore environments.

From March 2013 until September 2014, Nestor was Technical Manager for Schlumberger Well Intervention in Saudi Arabia, leading the Schlumberger CT Technical Team and supporting Saudi Aramco on the technical aspects of CT interventions in oil, gas and power water injector wells. He assisted in matrix stimulation, descaling, perforating, clean outs, milling, fishing, zonal isolation, etc. Prior to this assignment, he held technical and sales positions in Egypt and Mexico, where he was responsible for the introduction of new technologies involving CT and matrix stimulation. Nestor started his career in Venezuela in 1999 as a Field Engineer for Schlumberger Well Services, and he completed his field assignment in Colombia and Ecuador.

He has authored several Society of Petroleum Engineers (SPE) papers and articles that have appeared in various industry magazines.

Nestor received his B.S. degree in Mechanical Engineering from Universidad del Zulia, Maracaibo, Venezuela.

Souhaibe Barkat is a Coiled Tubing (CT) Account Manager who began his career in 2005 working for NASA Johnson Space Center in Houston, TX, doing electrical hardware design. In 2006, he joined Agilent Technologies in Colorado Springs, CO, as a Hardware Design Engineer, then moved to Product Management in 2007, managing the logic analyzer product worldwide.

Souhaibe joined Schlumberger CT in ʻUdhailiyah, Saudi Arabia, in December 2009. There he gained field experience before moving to CoilTOOLS in March 2012. After managing the Downhole Tools and Fiber Optic Enabled CT Services in Saudi Arabia, Souhaibe took on a new role in November 2013 as the CT Services Account Manager for the Drilling and Workover Department.

In 2007, he received his B.E. degree in Computer Engineering from the University of Colorado at Boulder, Boulder, CO, and in 2009, he received his M.S. degree in Electrical Engineering from the University of Colorado, Colorado Springs, CO.

Numerical Analysis of Heat Transfer in Circular Ducts Subjected to Magnetohydrodynamic Forces

Authors: Dr. Maher M. Shariff, Dr. Regis D. Vilagines and Dr. Khalid N. Alammar

ABSTRACT

This article is focused on the main results from a computational modeling effort to study the effects of magnetohydrodynamics (MHD) on fluid and heat flow characteristics in pipes, using a zero-equation turbulence model. MHD forces are an inherent part of some processes, such as nuclear reactors. MHD can also be used externally to reduce or increase the heat transfer in other applications, including the stirring of molten metal, turbulence control in induction furnaces, the damping of buoyancy-driven flow during solidification and the shaping of steel ingots. This article describes how the magnetic field effect is applied to a conductive fluid, which results in what is known as the Lorentz force, and how it alters both hydrodynamic and thermal boundary layers.

This work involved simulating fully developed, Reynolds averaged, turbulent MHD pipe flows with wall heating. Uncertainty was approximated through grid independence and model validation. The effects of the Reynolds, Hartmann and Prandtl numbers on heat transfer characteristics were investigated. With an increasing Hartmann number, heat transfer was found to increase toward the side layer. Increasing the Prandtl number was shown to enhance heat transfer. Increasing the Reynolds number decreased the effect of the Hartmann number. Heat exchanger enhancement by MHD can potentially find practical applications, since MHD can increase heat transfer in pipes, although at the cost of greater pressure drop.

INTRODUCTION

The technique for controlling boundary layers by means of an electromagnetic force known as the Lorentz force is useful for controlling fluid and heat flows. The technique is relatively old, tracing its origins to the mid-1930s[1-3]. Interest in the technique has revived in recent years, and more numerical and experimental investigations have been carried out, benefiting from the rapid advancement in computational simulation. Applications include reducing the drag of blunt bodies in seawater, and enhancing liquid delivery in pipes and cooling in nuclear reactors. Recent work[4] has been done on fusion reactors and magnetohydrodynamics (MHD) flow. In studies, MHD flows in ducts are divided into three regions: The core region, the Hartmann layer and the side layer, Fig. 1.

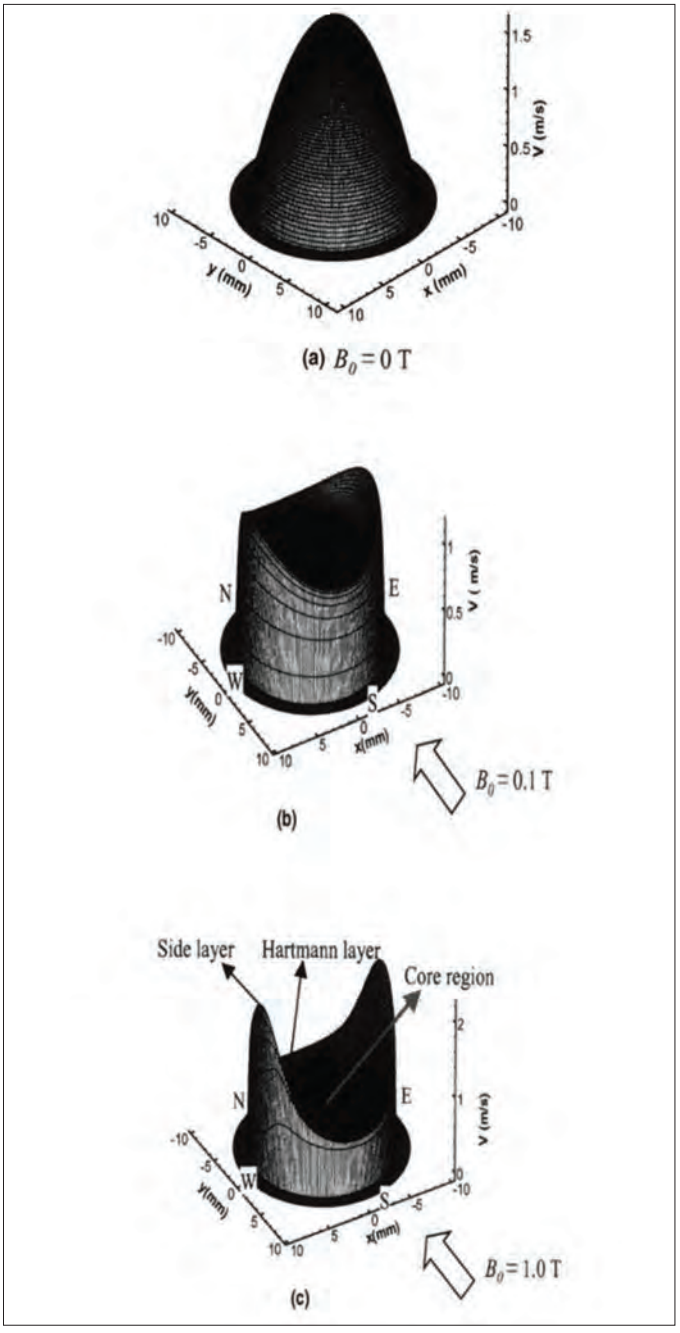

Fig. 1. Three distinct regions of MHD flow in a duct.

Viscous forces are negligible in the core region where velocity

is nearly constant. Near the solid wall, the shear stress is high due to viscous forces and the magnetic force's interaction in the Hartmann layer (normal to the applied magnetic field). The flow structure in the side layer is strongly dependent on the wall conductance and the current density distribution of the applied field.

The objective of the current work is to characterize flow and heat transfer in pipes in the presence of a transverse magnetic field, and to provide correlations as functions of Reynolds, Prandtl and Hartmann numbers. A range of Reynolds numbers from 500 to 100,000 will be investigated, as will the Prandtl numbers of 0.1 and 1.0, and the Hartmann numbers of 0, 10 and 100.

In a MHD duct flow, the flow speed in the side layers is higher than that in the other two regions, forming what is known as M-shaped velocity profiles. Due to its fundamental and practical importance, the effect of MHD on turbulence has drawn special attention. Moffat (1967)[3] was the first to show analytically that turbulent velocity fluctuations can be damped by applying a uniform magnetic field. Fraim and Heiser (1968)[5] studied the influence of a high intensity magnetic field on the turbulent flow of liquid mercury in a circular duct. The strength of the magnetic field plays a major role in turbulence generation as well as its suppression.

Experimental work[6] has shown that the magnetic force, when applied in the flow direction of an electrically conducting fluid, produces an increase in the velocity field near the wall; the thickness of the boundary layer is reduced, as well as its turbulence fluctuations. The generated electromagnetic force also increases the mean wall shear stress and reduces turbulence. The effect of applying a MHD force on turbulent salt-water in a channeled flow has been studied[7]. Their results show that the drag is reduced when a Lorentz force is applied.

The energy needed to generate the Lorentz force is much higher than the energy saved due to the reduced drag. Yamamoto et al. (2008)[8] studied the flow and heat characteristics of fluids having a low magnetic Reynolds number and Prandtl number. Their work utilized direct numerical simulation and the k-ε model simulation of MHD flow. They found that the similarity law between the velocity and the temperature profiles was not satisfied with an increasing of the Hartmann number, especially near the critical Hartmann condition needed to maintain turbulent flow. At higher Reynolds number conditions, MHD models coupled with the k-ε model were able to reproduce the MHD pressure loss trend with an increasing Hartmann number.

THEORY AND METHODOLOGY

Hannes Alfvén was the first to introduce the term "Magneto-hydrodynamics." He described astrophysical phenomena as belonging to an independent scientific discipline. The official birth of incompressible fluid MHDs came in 1936-1937 when Julius Hartmann and Freimut Lazarus performed theoretical and experimental studies of MHD flows in ducts. The most appropriate name for the different phenomena would be "MagnetoFluidMechanics," but the original name of "Magnetohydrodynamics" is still generally used. MHD deals with the dynamics of electrically conducting fluids and their interactions with magnetic fields. Table 1 shows various electrically conducting fluids.

The velocity field, v, and the magnetic field, B, are coupled. Any movement of a conducting material in a magnetic field generates electric currents, J, which in turn induce a magnetic field. Each unit volume of liquid having J and B experiences an MHD force, ~J × B, known as the "Lorentz force," Fig. 2.

MHD is divided into two distinct areas of interest: The MHD accelerators, which accelerate fluids through the Lorentz force, J × B, Fig. 3; and the MHD generators, which convert the kinetic energy of a fluid and its enthalpy into electricity. The study in this article is focused on the MHD accelerators.

The mathematical model consisted of the following Reynolds averaged Navier-Stokes and electric potential equations:

Continuity:

$$\nabla \vec{u} = 0 \qquad (1)$$

Liquid	σ, {1/Ω•m}
Weak electrolytes	10^{-4} to 10^{-2}
Strong electrolytes Water + 25% NaCl (20 °C) Pure H_2SO_4 (20 °C)	10^{1} to 10^{2} 21.6 73.6
Molten salts (FLiNaBe, FLiBe at 500 °C)	~150
Liquid metals Mercury (20 °C)	10^{6} to 10^{7} 1.0×10^{6}

Table 1. Electrical conductivities of some fluids that have the potential to interact with a magnetic field

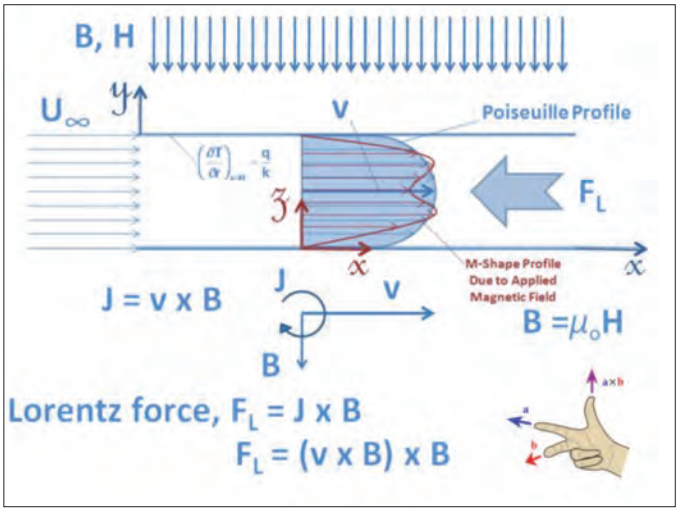

Fig. 2. Vector representation of MHD flows in a duct.

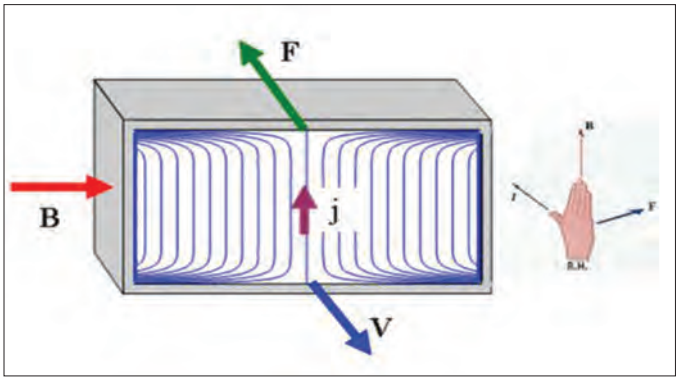

Fig. 3. MHD accelerators application.

Momentum:

$$\rho \vec{u} \cdot \nabla \vec{u} = \rho g - \nabla p + \vec{J} \times \vec{B} + \mu \nabla^2 \vec{u} \quad (2)$$

Conservation of Charge:

$$\nabla \cdot \vec{J} = 0 \quad (3)$$

Ohm's Law:

$$\vec{J} = \sigma(-\nabla \varphi + \vec{u} \times \vec{B}) \quad (4)$$

Energy:

$$\vec{u} \cdot \nabla T = \alpha \nabla^2 T \quad (5)$$

Boundary Conditions

- No-slip condition, given velocity inlet, and a prescribed pressure gradient: $u_z = 0 \;\; at \;\; r = R$
- Electrically insulated wall: $\frac{\partial \varphi}{\partial r} = 0 \;\; at \;\; r = R$
- Thermally, constant heat flux at wall: $\left[\frac{\partial T}{\partial r}\right]_{r=R} = \frac{q}{k}$

Assumptions

1. The viscous dissipation and Joule heating are neglected in the energy equation.
2. The interaction of the induced magnetic field with the flow is negligible compared with the interaction of the applied magnetic field with the flow.
3. The flows are fully developed both hydrodynamically and thermally, and in a 2D cylindrical coordinate system.
4. The density, viscosity, specific heat and thermal conductivity of the liquid and the electrical conductivity are constant.

A commercial computational fluid dynamics (CFD) code was used in this study. The structured grid was built in a Gambit preprocessing environment. The mesh comprised 20,000, 30,000 and 40,000 hybrid cells. Figure 4 shows the physical geometry of the pipe. Figure 5 shows computational simulations of mesh quality and varied wall thicknesses. The numerical modeling was carried out using the Semi-Implicit Method for Pressure Linked Equations (SIMPLE) algorithm. SIMPLE is a widely used numerical procedure to solve the Navier-Stokes

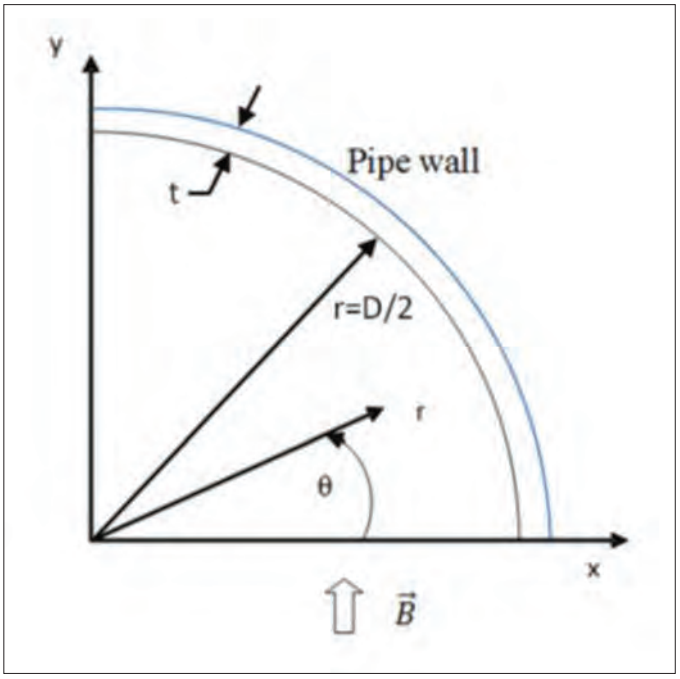

Fig. 4. Cross section of the pipe (first quadrant) with the constant field vector, $\vec{B}$.

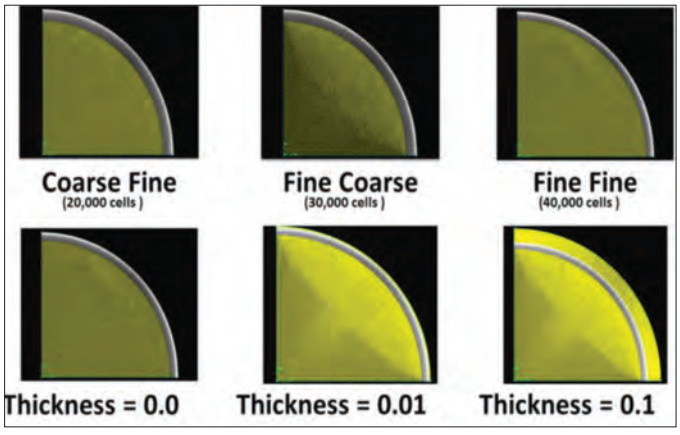

Fig. 5. Computational grid sizes with varied wall thicknesses.

equations[9] and second order schemes. The linearized equations were solved by employing the Gauss-Seidel technique with an algebraic multi-grid scheme[10].

There are two sources of uncertainty in CFD, modeling uncertainty and numerical uncertainty[11]. Modeling uncertainty can be approximated through theoretical or experimental validation, while numerical uncertainty can be approximated through grid independence. The velocity distributions in Figs. 6 and 7 show grid independence and model validation for the cases without and with a magnetic field, respectively. The numerical prediction with 40,000 cells is within ±5%. Therefore, we assumed the modeling uncertainty to be ±5%.

Grid independence and model validation were based on the solution of Gold (1962)[1]. Velocity distribution, pressure drop, inductive electric current density distribution and heat transfer characteristics were produced to clarify the mechanisms of asymmetric heat transfer in liquid MHD flow. The side layers, where the velocity is increased, are formed in the liquid film

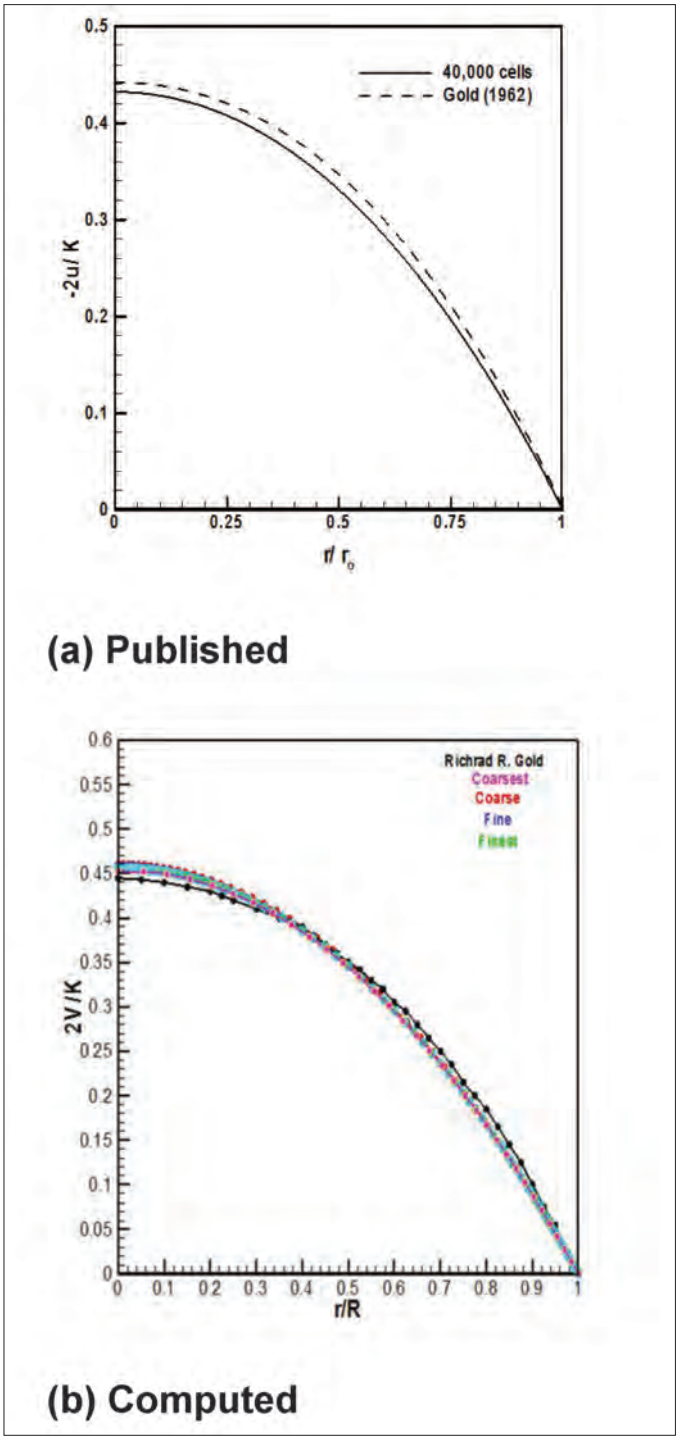

Fig. 6. Velocity distribution in the transverse direction without a magnetic field: (a) published, and (b) computed.

near the side walls. The side layers become thinner in the direction perpendicular to the magnetic field with an increase in the applied field strength.

The dimensionless parameters used are defined as follows:

- Reynolds number: The ratio of the inertial to the viscous forces in the flow.

$$Re = \rho UD/\mu \tag{6}$$

- Prandtl number: The ratio of momentum diffusivity to thermal diffusivity.

$$Pr = \frac{\nu}{\alpha} \tag{7}$$

- Hartmann number: The ratio of the electromagnetic force to the viscous force.

$$Ha = BL\sqrt{\frac{\sigma}{\mu}} \tag{8}$$

- Nusselt number: The ratio of convective to conductive heat transfer.

$$Nu = \frac{hD}{k} \tag{9}$$

Correlations were developed as functions of wall thickness and Reynolds, Prandtl and Hartmann numbers for a total of 72 cases. The test matrix is shown in Table 2.

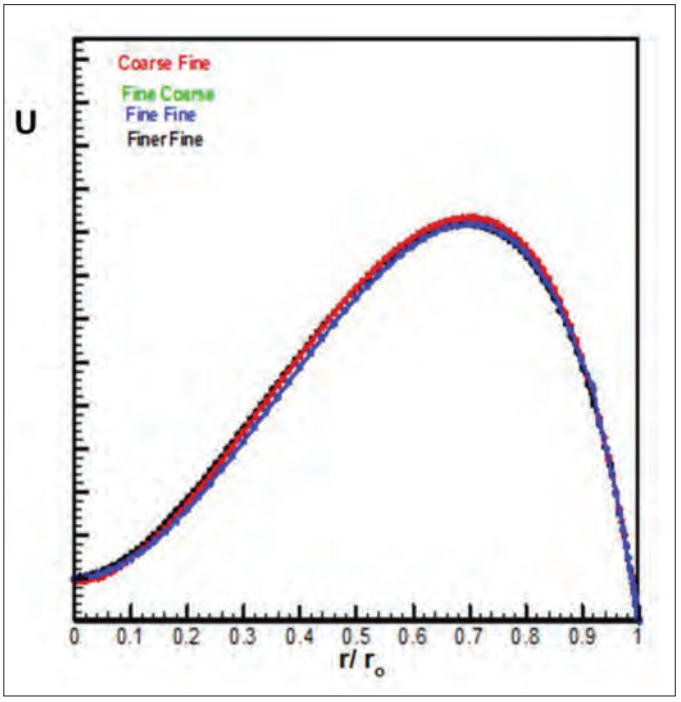

Fig. 7. Velocity distribution in the transverse direction with magnetic field; Prandtl number = 0.1, Hartmann number = 63, and Reynolds number = 200.

RESULTS AND DISCUSSION

Laminar Flow

Figure 8 shows the laminar flow simulation results with zero wall thickness at a Reynolds number of 500, at a Prandtl number

Wall Thickness (t/D)	Reynolds Number	Prandtl Number	Hartmann Number
0.00	500	0.1	0
0.01	5,000	1.0	10
0.10	10,000		100
	100,000		

Table 2. Matrix for the numerical simulations performed

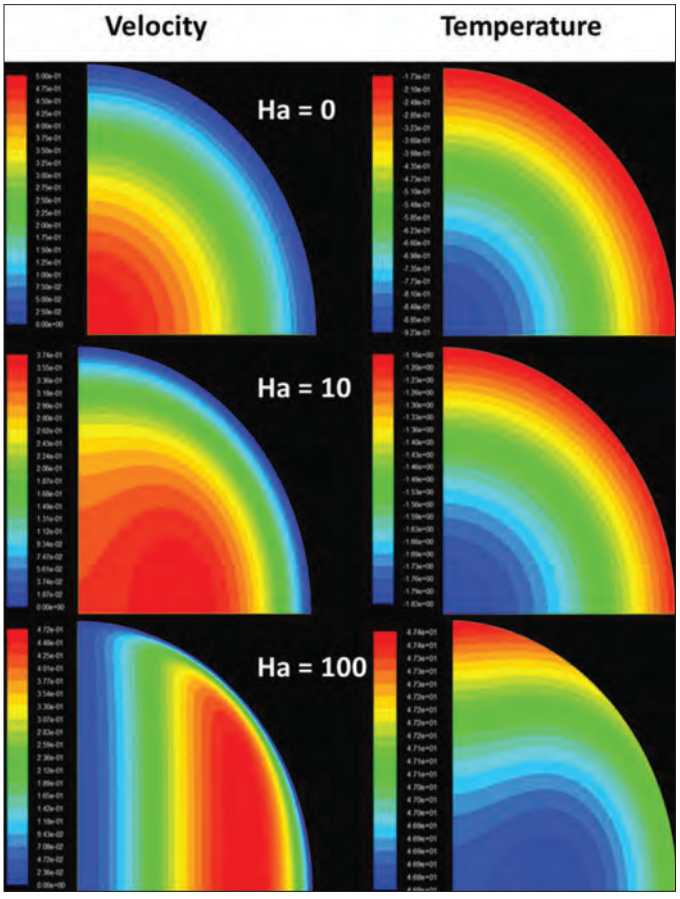

Fig. 8. The "Laminar Case."

of 1 and at three values of the Hartmann number, 0, 10 and 100.

Figure 9 shows the predicted heat transfer as enhanced at a higher Hartmann number and lower wall thickness.

Figure 10 shows that the computed friction factor is reduced in the pipe's centerline and at a lower wall thickness.

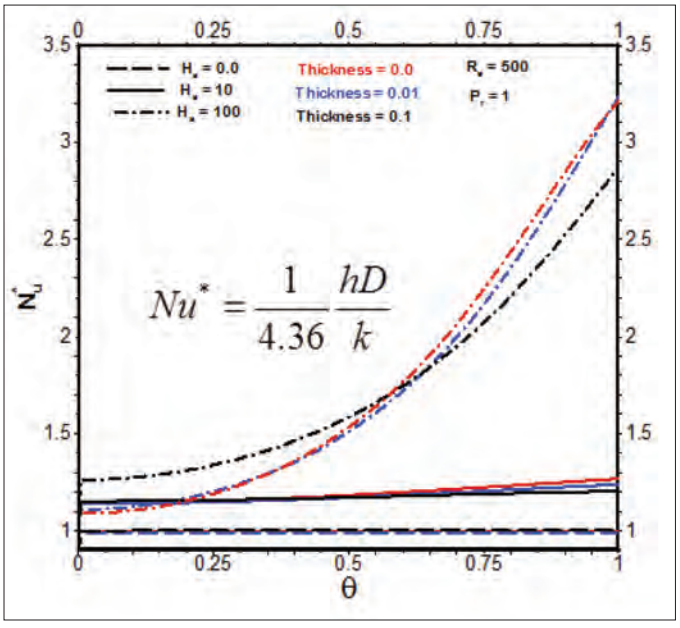

Fig. 9. Normalized Nu *along the wall of the pipe.*

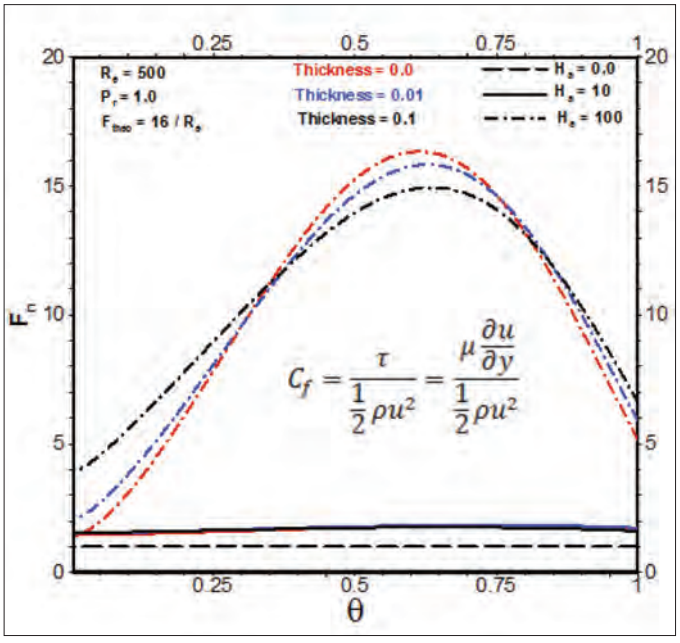

Fig. 10. Normalized friction factor along the wall of the pipe.

Turbulent Flow

Assuming that the magnetic force has no effect on turbulence, the turbulent flow can be determined based on the pressure drop given by the Moody's chart. The procedure used for calculating the turbulent flow field is as follows.

- Determine the friction factor from the Moody's chart for smooth pipe at a specified Reynolds number, *Re*.
- Determine the pressure drop from the correlation.
- Adjust the shear stress to satisfy continuity.

$$\frac{dP}{dx} = \frac{1}{2D} f\rho u^2 \tag{10}$$

By replacing the molecular viscosity in the momentum equation with the effective viscosity, μ_{eff}, we define the eddy viscosity ratio (EVR) as a given value. Then the momentum equation becomes:

$$\rho\, \vec{u}\, \nabla\, \vec{u} = \rho\vec{g} - \nabla p + \vec{J} \times \vec{B} + \mu_{eff}\, \nabla^2 \vec{u} \tag{11}$$

Using the turbulent $Pr_t = 0.87$, we evaluate the turbulent thermal conductivity, k_t, as:

$$k_{eff} = k_l + k_t \tag{12}$$

$$k_t = \frac{\mu_t C_p}{Pr_t} \tag{13}$$

$$\varepsilon = \frac{\mu_t}{\mu} \tag{14}$$

$$k_t = \frac{\varepsilon\mu}{0.87} \tag{15}$$

So, the thermal boundary condition becomes:

$$\left(\frac{\partial T}{\partial r}\right)_{r=R} = \frac{q}{k_{eff}} \quad (16)$$

Figure 11 shows a contour comparison of velocity, electric potential and temperature for both the laminar flow case at a Reynolds number of 500 and the turbulent flow case at a Reynolds number of 100,000. The Prandtl number was set at 1, and wall thickness was zero. The electric potential resembles the force working against the fluid, slowing it down in the red colored region of the contour plot.

Heat Transfer

Figure 12 shows the turbulent flow results for the Nusselt number at Reynolds number = 5,000, EVR = 2.05 and k_t = 0.2356. Maximum heat transfer enhancement occurs at Hartmann number = 100 and zero wall thickness. Table 3 shows the computed values of the simulation's parameters.

Figure 13 shows the turbulent flow results for the Nusselt number at Reynolds number = 10,000, EVR = 3.84 and k_t = 0.22. Maximum heat transfer enhancement occurs at Hartmann number = 100 and zero wall thickness. Table 4 shows the computed values of the simulation parameters.

Figure 14 shows the turbulent flow results for the Nusselt number at Reynolds number = 100,000, EVR = 26.8 and k_t = 0.154. Maximum heat transfer enhancement occurs at Hartmann number = 100 and zero wall thickness. Table 5 shows the computed values of the simulation parameters.

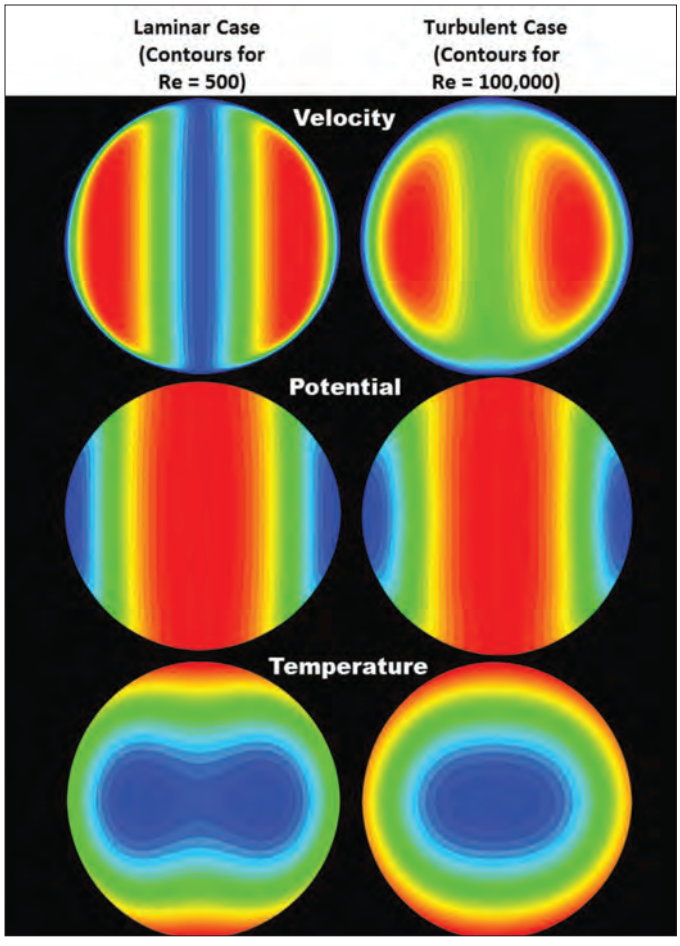

Fig. 11. The effect of magnetic field on fluid and heat flows.

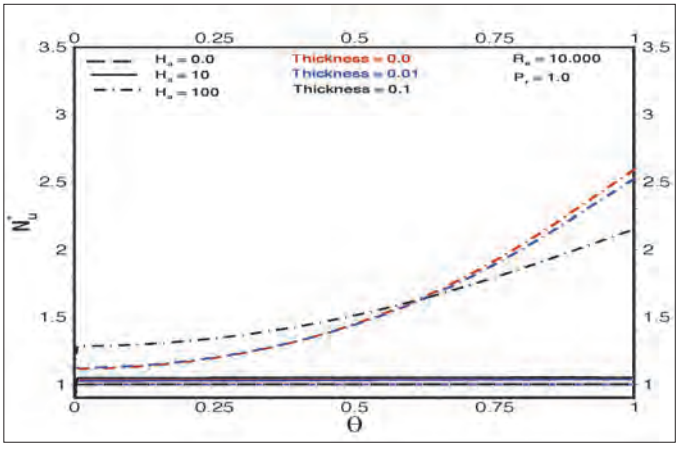

Fig. 12. Nusselt number variations along the pipe circumference; Reynolds number = 5,000, Prandtl number = 1.

Case	Ha [B]	ΔP {Pa/m}	{m/s}
1	0 [0 T]	0.61	0.250008
2	10 [0.16 T]	1.27	0.249
3	100 [0.5 T]	12.3	0.248

Table 3. Simulation run's parameters for the Nusselt number variation curves of Fig. 12; Reynolds number = 5,000, Prandtl number = 1

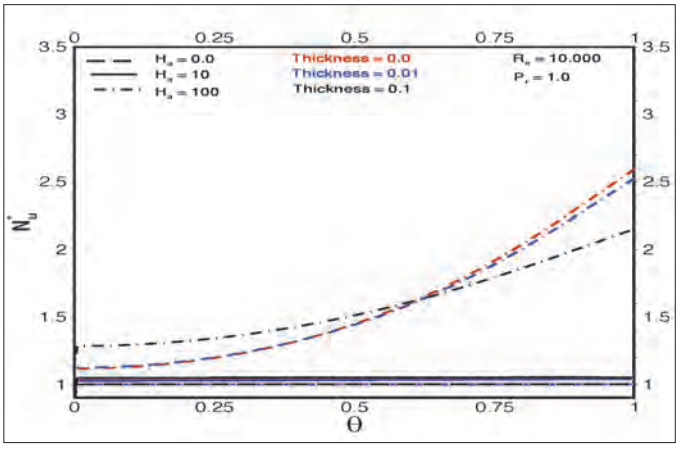

Fig. 13. Nusselt number variations along the pipe circumference; Reynolds number = 10,000, Prandtl number = 1.

Case	Ha [B]	ΔP {Pa/m}	{m/s}
1	0 [0 T]	0.484	0.250008
2	10 [0.16 T]	0.83	0.249
3	100 [0.5 T]	8.16	0.248

Table 4. Simulation run's parameters for the Nusselt number variation curves of Fig. 13, Reynolds number = 10,000, Prandtl number = 1

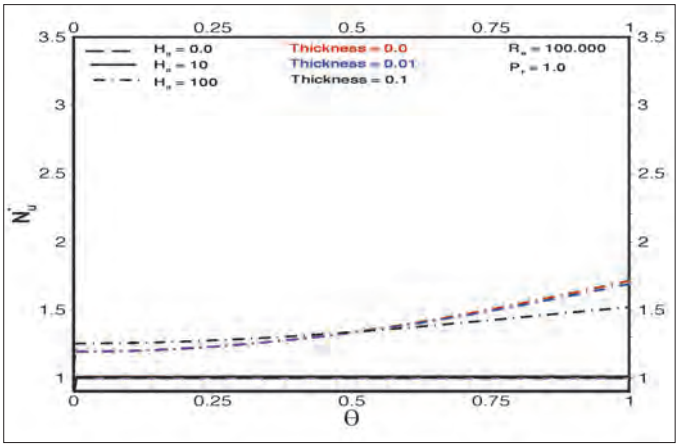

Fig. 14. Nusselt number variations along the pipe circumference; Reynolds number = 100,000, Prandtl number = 1.

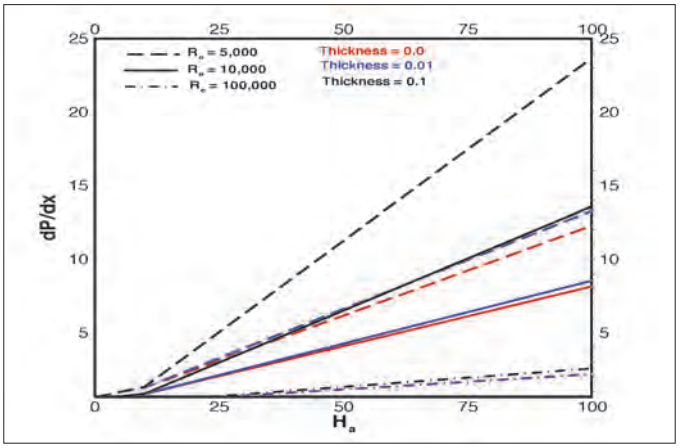

Fig. 15. Pressure drop vs. Hartmann number at varied Reynolds numbers and wall thickness.

Case	Ha [B]	ΔP {Pa/m}	{m/s}
1	0 [0 T]	0.484	0.250008
2	10 [0.16 T]	0.83	0.249
3	100 [0.5 T]	8.16	0.248

Table 5. Simulation run's parameters for the Nusselt number variation curves of Fig. 14; Reynolds number = 100,000, Prandtl number = 1

Pressure Drop

The pressure drop was calculated from Eqn. 10 and Eqn. 17, where the friction factor follows the Moody diagram for smooth pipe; it is adjustable based on roughness.

$$\frac{1}{\sqrt{f}} = -1.8\, Log\left[\frac{6.9}{Re} + \left(\frac{e/D}{3.7}\right)^{1.11}\right] \qquad (17)$$

Figure 15 shows that at low Reynolds numbers and high pipe wall thickness, a higher pressure drop occurs. Table 6 shows the computed values of the pressure drop.

CONCLUSIONS

The flow of conductive liquid in a circular pipe subjected to a transverse magnetic field was computed using a commercial CFD code. Under the assumption that the turbulence was not being affected by the magnetic field, it was found that the heat transfer at the pipe wall can be enhanced significantly due to the effect of the Lorentz force.

The heat transfer enhancement was found higher in laminar flow conditions. In turbulent conditions, the computations found that the side layers of flow were squeezed in a direction perpendicular to the applied magnetic field — a stream-wise direction.

Although heat transfer enhancement could be achieved, the simulation showed that this enhancement comes at the cost of increasing the pressure drop by an order of magnitude or higher.

ACKNOWLEDGMENTS

The authors would like to thank the management of Saudi Aramco for their support and permission to publish this article. The contributions of Shaker S. Abdullah and Zakariya M. Kaneesamkandi from KSU are highly appreciated.

	Thickness (t/D) = 0.0			Thickness (t/D) = 0.01			Thickness (t/D) = 0.1		
Re / Ha	5,000	10,000	100,000	5,000	10,000	100,000	5,000	10,000	100,000
0	0.61	0.484	0.278	0.61	0.484	0.278	0.61	0.484	0.278
10	1.27	0.83	0.313	1.275	0.83	0.313	1.32	0.85	0.316
100	12.3	8.16	2.175	13.3	8.55	2.19	23.7	13.6	2.57

Table 6. Calculated numerical values of pressure drop {Pa/m} vs. Hartmann number

NOMENCLATURE

B, $\vec{B}$	magnetic field (T)
C	specific heat (kJ/kg·K)
D, R	pipe diameter (m)
e	absolute roughness (mm)
F	force (N)
f	friction factor
g	Earth gravitational acceleration (m/s^2)
H, $\vec{H}$	magnetic field strength (A/m)
h	convective heat transfer coefficient (W/m^2·K)
j, J, $\vec{J}$	electric current density (A/m^2)
k	thermal conductivity (W/m·K)
L	characteristic length scale (m)
p	pressure (Pa)
r	polar coordinate axis (m)
q	heat transfer rate (W)
T	temperature (K)
t	thickness of pipe wall (m)
v,$\vec{U}$,U	velocity (m/s)
x	Cartesian coordinate axis, x-axis (m)
y	Cartesian coordinate axis, y-axis (m)
α	thermal diffusivity (m^2/s)
ε	ratio of turbulent to laminar viscosity
φ	electric potential (volt)
Θ	polar coordinate angle (rad)
μ	dynamic viscosity (kg/m·s)
μ_o	magnetic permeability (N/A^2)
ν	kinematic viscosity (m^2/s)
ρ	density (kg/m^3)
σ	electric conductivity (1/$\Omega \cdot$ m)
τ	shear stress (N/m^2)

SUBSCRIPTS

eff	*effective*
l	*laminar*
L	*Lorentz*
p	*constant pressure*
t	*turbulent*
∞	*free stream*

REFERENCES

1. Gold, R.R.: "Magnetohydrodynamic Pipe Flow, Part 1," *Journal of Fluid Mechanics*, Vol. 13, No. 4, August 1962, pp. 505-512.
2. Shercliff, J.A.: "Magnetohydrodynamic Pipe Flow, Part 2, High Hartmann Number," *Journal of Fluid Mechanics*, Vol. 13, No. 4, August 1962, pp. 513-518.
3. Moffat, H.K.: "On the Suppression of Turbulence by a Uniform Magnetic Field," *Journal of Fluid Mechanics*, Vol. 28, No. 3, May 1967, pp. 571-592.
4. Morley, N.B., Smolentsev, S., Barleon, L., Kirillov, I.R. and Takahashi, M.: "Liquid Magnetohydrodynamics — Recent Progress and Future Directions for Fusion," *Fusion Engineering and Design*, Vols. 51-52, November 2000, pp. 701-713.
5. Fraim, F.W. and Heiser, W.H.: "The Effect of a Strong Longitudinal Magnetic Field on the Flow of Mercury in a Circular Tube," *Journal of Fluid Mechanics*, Vol. 33, No. 2, August 1968, pp. 397-413.
6. Henoch, C. and Stace, J.: "Experimental Investigation of a Salt Water Turbulent Boundary Layer Modified by an Applied Streamwise Magnetohydrodynamic Body Force," *Physics of Fluids*, Vol. 7, No. 6, June 1995, pp. 1371-1383.
7. Berger, T.W., Kim, J., Lee, C. and Lim, J.: "Turbulent Boundary Layer Control Utilizing the Lorentz Force," *Physics of Fluids*, Vol. 12, No. 3, March 2000, pp. 631-649.
8. Yamamoto, Y., Kunugi, T., Satake, S. and Smolentsev, S.: "DNS and k-ε Model Simulation of MHD Turbulent Channel Flows with Heat Transfer," *Fusion Engineering and Design*, Vol. 83, Nos. 7-9, 2008, pp. 1309-1312.
9. Patankar, S.V. and Spalding, D.B.: "A Calculation Procedure for Heat, Mass and Momentum Transfer in Three-Dimensional Parabolic Flows," *International Journal of Heat and Mass Transfer*, Vol. 15, No. 10, October 1972, pp. 1787-1806.
10. Sharov, D. and Nakahashi, K.: "Hybrid Prismatic/Tetrahedral Grid Generation for Viscous Flow Applications," *AIAA Journal*, Vol. 36, No. 2, February 1998, pp. 157-162.
11. Stern, F., Wilson, R.V., Coleman, H.W. and Paterson, E.G.: "Verification and Validation of CFD Simulations," Iowa Institute of Hydraulic Research (IIHR) Report 407, College of Engineering, University of Iowa, Iowa City, Iowa, September 1999.

BIOGRAPHIES

Dr. Maher M. Shariff is a Senior Scientist at Saudi Aramco's Oil and Gas Treatment Division of the Research and Development Center. He joined Saudi Aramco in February 2003. Maher's research interests lie in the areas of drilling and completion fluids, gas-oil-water separation, magnetohydrodynamic pipe flows with heat transfer and advanced reactor design. He is credited with more than 20 regional and international publications and presentations and a U.S. patent (US 8,337,603).

In September 2001, Maher joined SABIC Research and Technology Center in Jubail, Saudi Arabia, and was employed there in the Materials and Corrosion Section as a Senior Mechanical Engineer until February 2003. Prior to joining SABIC, he worked for the Cessna Aircraft Company in Wichita, KS, for one year as an Analytical Design Engineer in the Environmental Control Systems Unit. In August 2012, Maher joined Tulsa University Fluid Flow Projects for one year as a visiting scholar at The McDougall School of Petroleum Engineering, University of Tulsa, OK.

He has been a member of the American Society of Mechanical Engineers (ASME) since 1989, as well as numerous other professional societies, including the Society of Petroleum Engineers (SPE) and the American Chemical Society (ACS). Maher has also served as editor-in-chief and vice chair of the ASME – Eastern Saudi Arabia Section. He is a certified Mechanical Engineering Consultant with the Saudi Council of Engineers. Maher is also a member of several honor societies, including Sigma Xi (scientific research), Tau Beta Pi (engineering) and Phi Kappa Phi (academic).

He received his B.S. degree in Mechanical Engineering from Bradley University, Peoria, IL; his M.S. degree in Mechanical Engineering from Washington University, St. Louis, MO; and another M.E. degree from Vanderbilt University, Nashville, TN. Maher received his Ph.D. in Mechanical Engineering with highest honors from Wichita State University, Wichita, KS. His dissertation work at Wichita State University, in association with the National Institute for Aviation Research, was in the area of computational fluid dynamics.

Dr. Regis D. Vilagines joined Saudi Aramco in 2006. He is leading the Oil Treatment Team in the Oil and Gas Treatment Division at the Research & Development Center (R&DC). Regis previously worked with IFP in France, where he was a Project Manager in Multiphase Production and Flow Assurance as well as R&D Group Leader in the Drilling and Production Division. He was also involved in teaching courses in turbomachinery and fluid dynamics at the University of Lyon.

Regis is a Graduate Mechanical Engineer. He holds a Post-Graduate Diploma from the Von Karman Institute for Fluid Dynamics, Rhode-St.-Genèse, Belgium, and a Ph.D. degree from the University of Nantes, Nantes, France. Regis holds the degree of Ability to Lead Scientific Research in Fluid Dynamics from the University of Lyon, Lyon, France.

Dr. Khalid N. Alammar is an Associate Professor in the Mechanical Engineering Department of King Saud University, Riyadh. He has published numerous articles in various refereed journals and proceedings in his field of expertise. Khalid's interests include turbulence modeling and computational fluid dynamics, applied to fluid flow and heat transfer.

Khalid is also an FAA certified commercial pilot with multiengine instrument ratings.

He received his B.S., M.S. and Ph.D. degrees in Aerospace Engineering, specializing in Thermo-fluids, from the University of Oklahoma, Norman, OK.

Formation Tester and NMR Heavy Oil Characterization during Placement of a Horizontal Injector at a Tar/Oil Interface

Authors: Stig Lyngra, Dr. Gabor G. Hursan, Dr. Murat M. Zeybek, Richard G. Palmer, K. Ahmed Qureshi and Hazim A. Ayyad

ABSTRACT

A case history is presented for a horizontal injector well drilled at the base of a moveable oil column on top of a tar mat in a carbonate oil reservoir in the Middle East. The well was placed utilizing real-time logging-while-drilling (LWD) nuclear magnetic resonance (NMR) oil viscosity correlations and formation tester mobility data.

As this was a pilot water injector placed at an oil/tar interface with limited historic oil viscosity vs. depth data, obtaining quality calibration oil samples was considered critical. Both LWD and pipe conveyed tough logging conditions (TLC) formation tester data sets were acquired. Consequently, direct comparisons of LWD acquired and TLC acquired formation pressures and formation mobilities were possible. The comparison proved the reliability of the LWD formation mobility data. The LWD measured formation pressures, however, were supercharged compared to the TLC formation tester measured formation pressures, which were largely in line with expected formation pressures.

The oil viscosity results from the TLC formation tester in situ viscosity fluid analyzer and from the NMR viscosity correlation compared favorably with the laboratory results from the fluid samples acquired by the TLC formation tester. This indicates that accurate real-time in situ fluid property determination is possible with a modern formation tester and NMR tools.

In this reservoir, during the early phase of acquiring oil viscosity vs. depth data at the oil/tar transition zone, the main lesson learned was that the deeper section of the case study well contained higher asphaltene content, which caused the wellbore plugging that prevented reservoir access after suspending the well for tie-in. A clean out operation was unsuccessful, as plugging reoccurred. Current plans are for the well to be sidetracked again in the 3 centipoise (cP) to 20 cP oil interval at the top portion of the oil/tar transition zone.

INTRODUCTION

In Saudi Arabian oil fields with reservoir situations where heavy oil zones/tar mats exist, logging-while-drilling (LWD) formation tester mobility steering is commonly used for optimization of water injector well placement[1-4]. The mobility measurements from the LWD formation tester are stationary measurements that require halting the actual drilling operation. These point tests, typically measured at regular intervals of a few hundred feet during drilling of the reservoir section, are used as positive proof that the well has not entered into the low mobility or immobile reservoir interval of high viscosity heavy oil/tar located below the recoverable oil in the reservoir.

In heavy oil/tar mat applications, the availability of real-time LWD nuclear magnetic resonance (NMR) measurements provides relatively strong evidence of heavy oil/tar. As described elsewhere[5, 6], tar can be detected using the missing porosity tar indicator and excess bound fluid concept. Moreover, a fairly robust NMR oil viscosity correlation has been developed[7] that allows for estimation of the oil viscosity on the basis of the real-time LWD NMR data. In Saudi Aramco well placement operations, the LWD NMR data is routinely processed twice a day for oil viscosity determination. If the missing porosity and/or excess bound fluid tar detectors indicate heavier oil at the drill bit, the drilling operation is stopped. The formation tester then acquires mobility measurements, and the oil viscosity correlation algorithm is run for validation. If the measurements confirm high viscosity/low mobility, a decision is made to drill stratigraphically upward to return the drill bit to the lower viscosity in situ oil.

In this reservoir, only limited historic oil viscosity vs. depth data at the actual oil/tar interface was available. As the well described in this article was a pilot water injector placed at the interface, obtaining calibration oil samples was considered critical. The NMR viscosity correlation[7] had been developed on the basis of samples from a different Saudi Arabian oil field with a similar tar mat problem. Therefore, it was necessary to verify that the NMR oil viscosity correlation provided reasonable results in this particular reservoir. Fluid samples were acquired using the pipe conveyed tough logging conditions (TLC) formation tester and tested in the laboratory to allow comparison of the actual laboratory oil viscosity and density results with the fluid analyzer viscosity and density measurements from the TLC formation tester, as well as with the oil viscosity calculated from the NMR viscosity correlation.

Since LWD formation tester data was already being acquired for mobility steering purposes and a TLC formation tester run was necessary to obtain the calibration fluid samples,

a unique opportunity presented itself to acquire LWD and TLC formation pressure and formation mobility measurements at the same depths and to compare the two data sets for validation purposes.

Because Saudi Arabian water injector well placement case histories utilizing formation testers and NMR data have previously been published[6, 8, 9] — and the intent in this article is not to share the same operational information as in the previous articles — the actual well placement of this pilot water injector well is only briefly described as required for context. The focus of this publication is to present the in situ oil characterization obtained from both formation tester evaluation and NMR data, including validation with oil sample laboratory results.

FIELD DESCRIPTION AND THE HEAVY RESERVOIR DEVELOPMENT HISTORY

The well described in this article was drilled in a giant mature oil field in the Kingdom of Saudi Arabia. The field was discovered in the early 1940s and has mainly been produced from two large fractured carbonate oil reservoirs[10, 11]. The field contains various other hydrocarbon-bearing reservoirs. Many of these hydrocarbon reservoirs are associated with a high-relief dome structure[10]. Saudi Aramco is currently pursuing further delineation, including pilot production and injection programs, for several of these secondary reservoirs with the intent to cost-effectively produce all hydrocarbons through the existing infrastructure[12]. As the field is mature and the infrastructure is ageing, optimum value can only be achieved by not delaying the investment in the secondary reservoir development wells too far into the future[12].

One of the dome structure reservoirs, the "Heavy" reservoir, is an ample heavy oil accumulation located above the two main producing horizons[12]. This heavy oil accumulation was discovered in 1941 and has been produced since 1947[13]. Due to the ease of operations in extracting oil from the main producing horizons — and other highly prolific Saudi Arabian giant oil fields — the Heavy reservoir is at this point virtually undepleted[12]. An extensive data acquisition program that has taken place over the past few years made it clear that the mobile heavy oil is under laid by 300 ft of tar, which totally separates the oil column from the aquifer[13]. In 2010, the first pilot injector well was placed at the oil/tar interface. This pilot water injector is the case history well presented in this publication.

OIL CLASSIFICATION AND PHYSICAL OIL PROPERTIES

Crude Oil Classification

The terminologies "heavy oil," "tar," "bitumen" and "asphalt" are not consistently applied in the oil industry. Different definitions exist, but many apply these terms almost interchangeably. A U.S. Geologic Survey (USGS) Fact Sheet[14] suggests one approach to defining the petroleum types, Fig. 1.

A study group formed by the World Petroleum Congress (WPC) in 1980, with representatives from the five WPC member countries (Canada, the Netherlands, the United Kingdom, the United States and Venezuela), reviewed the oil and gas classification and nomenclature systems used by various countries and recommended the universal adoption of the classification presented in Table 1[15]. The Society of Petroleum Engineers (SPE) has adopted the WPC definitions as appropriate for reserves and resource management purposes[16].

Physical Properties and Conditions Affecting In Situ Oil Viscosity

The in situ oil viscosity is dependent upon the gas-free (dead) oil viscosity and the amount of dissolved gas in the oil, i.e., the solution gas-oil ratio (GOR), measured in standard cubic feet per standard barrel (scf/sbbl). Two classic charts, Fig. 2 and Fig. 3, demonstrate the effects that the oil API gravity, reservoir temperature and GOR have on in situ oil viscosity.

The correlation from Beal (1946)[17], Fig. 2, is used to find the gas-free crude viscosity at reservoir temperature as a function of API gravity. The chart shown in the figure is reproduced from Standing's (1974)[18] student chart book. Professor Standing based his chart on the version in the Petroleum Production Handbook (1962)[19] rather than Beal's more complicated original. Beal's correlation was based on 953 crude oil samples taken from 747 different oil fields, including approximately 500 U.S. fields.

The dead oil viscosity, as determined from Fig. 2, is then adjusted for the amount of solution gas the crude contains in the reservoir by means of the correlation from Chew and Connally (1959)[20], Fig. 3, which determines the in situ oil viscosity at saturation conditions. Figure 3 is also reproduced from Standing (1974)[18]. Chew and Connally's correlation was based on 456 crude samples, mainly from U.S. reservoirs, but the sample

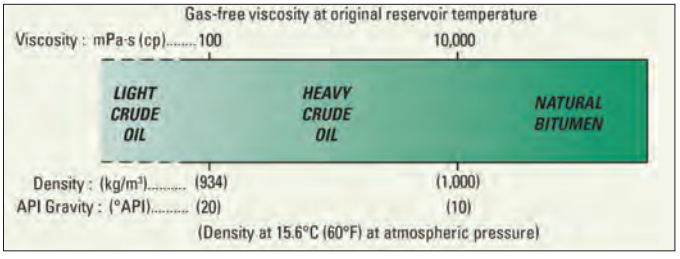

Fig. 1. Definition of petroleum types[14].

Crude Classification	Minimum API (degrees)	Maximum API (degrees)
Light Oil	31.1°	N/A
Medium Oil	22.3°	31.1°
Heavy Oil	10°	22.3°
Extra Heavy Oil	N/A	10°

Table 1. WPC crude classification[15]

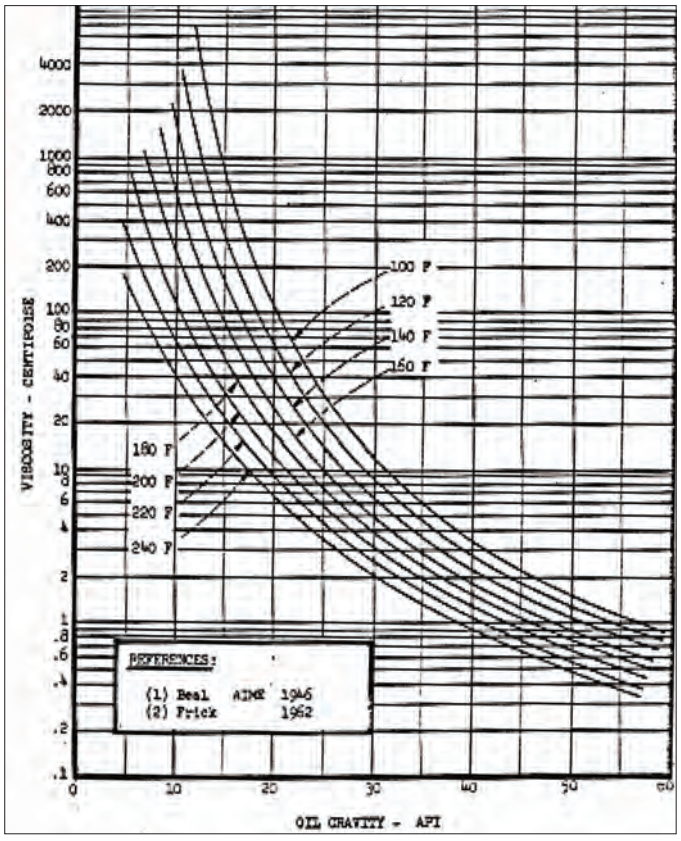

Fig. 2. Beal's gas-free (dead) oil viscosity correlation[17-19].

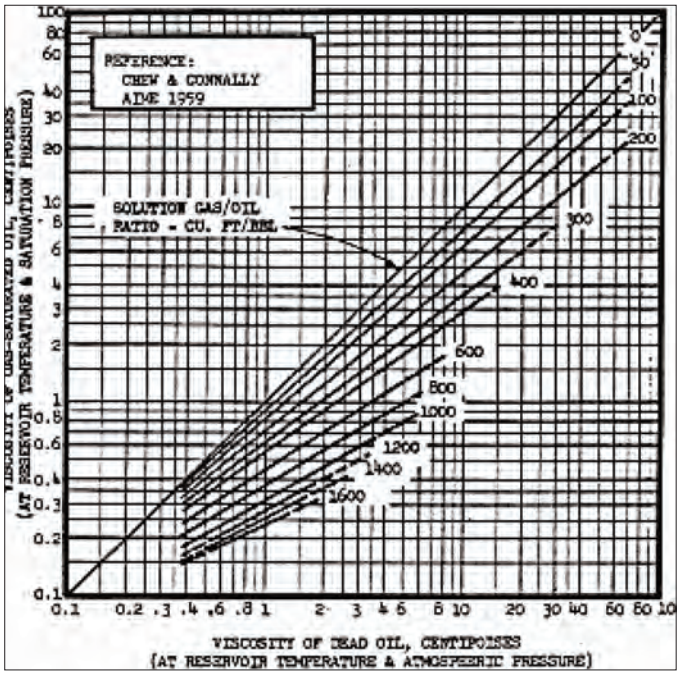

Fig. 3. Chew and Connally's gas saturated (live) crude viscosity correlation[18, 20].

set also included ~20 Canadian and South American samples.

If the reservoir pressure is greater than the saturation (bubble point) pressure, a further adjustment (increase) of the oil viscosity is required to account for the degree of undersaturation at reservoir conditions.

Heavy Reservoir: Crude Classification and In Situ Oil Viscosity

Table 2 presents the actual fluid data for the Heavy reservoir, or the mobile oil column located above the tar mat. Based on the USGS crude definitions[14], this oil is classified as light oil. The WPC classification[15] defines this crude as medium oil.

Based on the data reported in Table 2, using the API gravity and reservoir temperature as input for Beal's correlation in Fig. 2, the estimated dead oil viscosity is ~3 centipoise (cP). Using this estimated dead oil viscosity and the reported solution GOR, the estimated in situ oil viscosity at saturation pressure determined from Chew and Connally's correlation in Fig. 3 is ~2 cP.

Figure 4 presents the actual laboratory oil viscosity results for the Heavy reservoir at reservoir temperature as a function of pressure above crude saturation pressure, i.e., undersaturation pressure. The presented curve is a linear regression curve based on data from four fluid samples.

Using Beal's correlation combined with Chew and Connally's correlation for approximating the in situ oil viscosity appears to work reasonably well for the lighter Heavy reservoir crude located above the tar mat. As has been pointed out[21], however, these correlations do not consider the chemical nature of the hydrocarbons that make up the crude part of the reservoir oil. The actual chemistry is important in predicting liquid hydrocarbon viscosity behavior, particularly when the fraction of heavier components starts to increase dramatically at the oil/tar interface.

Fluid Parameter	Data	Unit
API Gravity	27.4	°API
Field Solution GOR	145	scf/bbl
Flash Solution GOR	205	scf/bbl
Reservoir Temperature	215	°F

Table 2. Heavy reservoir fluid properties

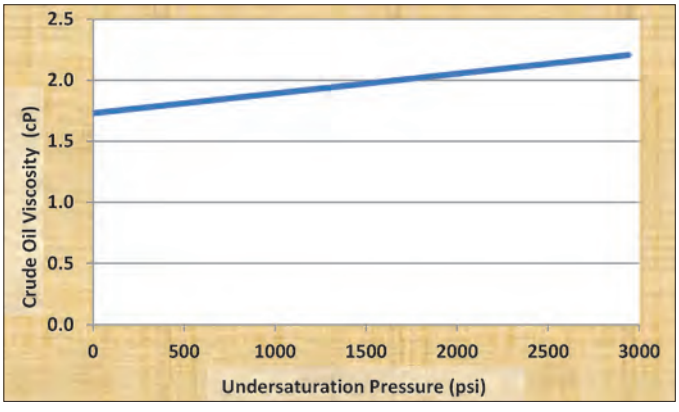

Fig. 4. Heavy reservoir crude viscosity at reservoir temperature as a function of the degree of undersaturation.

Below the Oil/Tar Interface: State-of-the-Art Heavy Oil/Asphaltene Science

In recent years, the understanding of the asphaltene's molecular properties, especially the distribution of asphaltene molecular weight, has considerably improved. The increased asphaltene understanding is a result of research and field studies conducted by Schlumberger's Oliver Mullins et al.[22-29], Andrew Pomerantz et al.[30, 31] and Julian Zuo et al.[32, 33] together with Saudi Aramco's Doug Seifert et al.[34, 35] and co-researchers from service/operating companies, universities[36, 37] and research affiliations.

A key concept in this research is that the asphaltene's aggregate structures, first found in laboratory solvents, are also found in crude oils. A simple representation of the molecular and colloidal structures of asphaltenes in crude oils and laboratory solvents was first published as *the modified Yen model*[22], named after the founder of modern asphaltene science, the Chinese professor Teh Fu Yen. This published model was later renamed *the Yen-Mullins model*[38]. The predominant molecular and colloidal structures of asphaltenes, as presented in the *Yen-Mullins model*[22], are shown in Fig. 5, which indicates that at low concentrations, as in condensates, asphaltenes are dispersed as a true molecular solution (left); for black oils, asphaltenes are dispersed as nanoaggregates of molecules (center); and for heavy oils, asphaltenes are dispersed as clusters of nanoaggregates (right).

Figure 6 displays the percent of asphaltene in an oil/tar transition zone for a giant Saudi Arabian Jurassic oil field. The oil samples used for deriving the previously mentioned NMR viscosity correlation[7] were obtained from this oil field. As presented in Fig. 6, the oil/tar transition zone from the mobile oil zone (asphaltene ~3%) to the immobile tar mat (asphaltene > 35%) in this oil field is approximately 275 ft true vertical depth (TVD).

A new asphaltene equation of state (EoS), the Flory-Huggins-Zuo (FHZ) EoS, has been developed as part of this research[32, 33]. With the particle size known, the effect of gravity can be determined. As described by Archimedes buoyancy, the asphaltene particles are negatively buoyant in the smaller particle crude oil. In the FHZ EoS, the gravity term — given by Archimedes buoyancy in the Boltzmann distribution — is combined with a chemical solubility term and an entropy term to fully describe the asphaltene behavior.

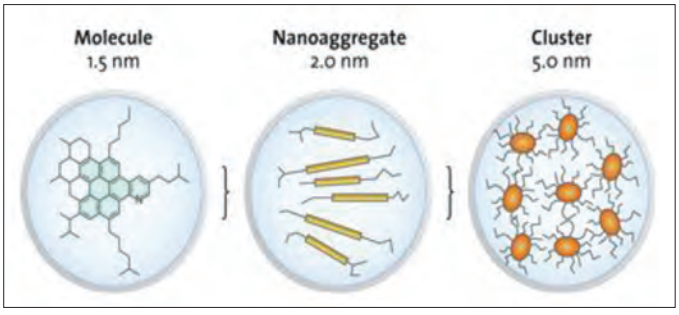

Fig. 5. The Yen-Mullins asphaltenes model[22].

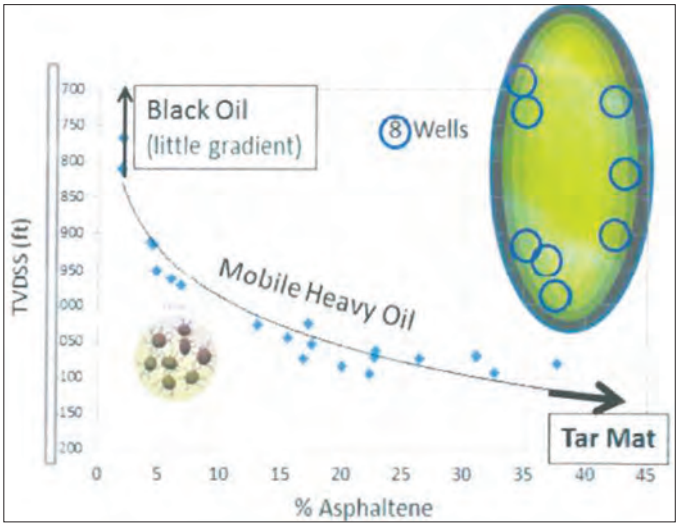

Fig. 6. Aspalthene percentage as a function of depth in a Saudi Arabian oil field[27, 28, 34, 35].

Application of Heavy Reservoir Case Study Well Fluid Samples

The purpose of acquiring the fluid samples from the case study well was to gain understanding of the asphaltene percent vs. depth at the oil/tar interface and the resulting oil viscosity relationship. This new knowledge of the crude's chemical nature will improve pre-drilling trajectory planning for future horizontal water injector wells and allow fine-tuning of the NMR viscosity correlation[7] to data from this field. After the correlation has been tuned with further crude samples, the NMR crude viscosities measured from all wells will be used with NMR data in this reservoir for a spatial oil property characterization. The tuned NMR viscosity correlation will also enhance the real-time mobility steering when placing new water injector wells. If required, once the actual asphaltene percentage vs. depth for this field is known, an FHZ EoS can be calibrated to further enhance the spatial understanding of the oil/tar transition zone.

HEAVY RESERVOIR: HEAVY OIL AND TAR INDICATORS

Triple Combo and NMR Data Tar Indicators

Conventional log interpretation to detect viscosity variations is limited to qualitative observations, such as noting washouts in caliper logs, diminished invasion and/or unusual vertical distributions of water and oil. These circumstantial relationships do not provide operationally reliable viscosity estimations. The problem is illustrated in the side-by-side comparison of two evaluation wells, Well-1 and Well-2, drilled in the same reservoir as the case history pilot water injector, Fig. 7. The top interval in the Heavy reservoir for Well-1 was 425 ft above the target entry for the pilot water injector well, while Well-2 penetrated the structure 155 ft deeper than the case history well. Despite the 680 ft difference in structural elevation between

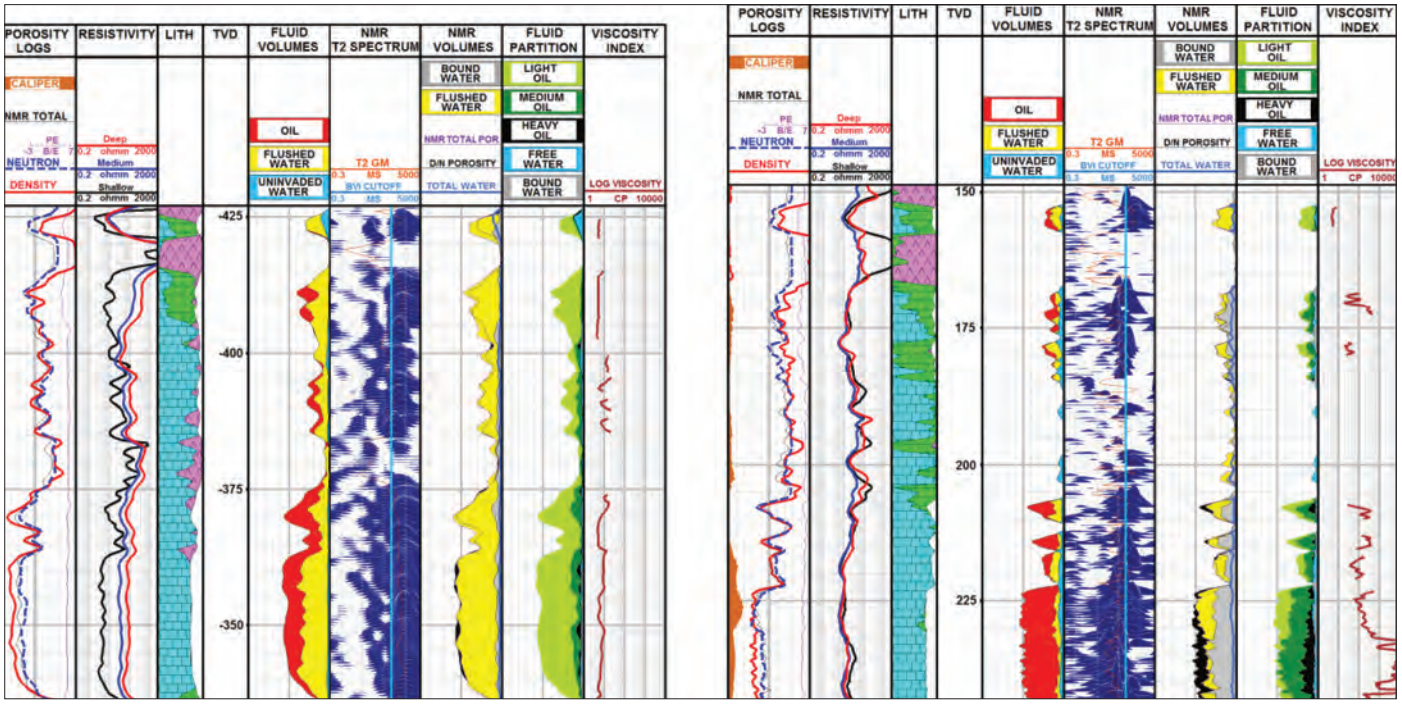

Fig. 7. Well-1 (left) and Well-2 (right) porosity and NMR logs.

the two wells, the conventional logs and the calculated total and water-filled porosity are remarkably similar, as seen in Tracks 1, 2 and 5 of Fig. 7. Well-2 may indicate heavy oil with less water-based mud (WBM) invasion and more borehole irregularities in the caliper logs than Well-1, but these effects could also result from differences in drilling conditions and formation permeability instead of fluid property variations.

Since the advent of NMR logging, the strong and unique connection between oil viscosity and NMR relaxation times has been the underpinning of a number of powerful downhole viscosity evaluation techniques[5, 7, 39-46]. For this case study, the volumetric decomposition approach[7] was utilized. This method has been implemented for operational use in other Saudi Arabian fields with similar reservoir conditions. The algorithm uses conventional total and water-filled porosity, and NMR total and bound fluid porosities as inputs, and calculates three oil volumes differentiated by their NMR properties. The heaviest part, shown in black in Track 8, relaxes too fast to be measured by NMR tools. The second intermediate component appears as bound fluid in the NMR spectrum, whereas the light constituent contributes to the NMR free fluid signature. These intermediate and light components are shown in Track 8 as medium and light green, respectively. The relative contributions of medium and heavy components have been calibrated with laboratory viscosity measurements of oil samples taken by downhole formation testers[7].

The NMR-based volumetric calculations and viscosity tracks reveal a striking difference between Well-1 and Well-2. Well-1 indicates mostly light oils in the entire reservoir, whereas Well-2 presents significant volumes of medium and heavy components with a downward-trending decrease of light components to where the significant missing NMR porosity indicates very heavy oils toward the bottom of the reservoir. Well-1 and Well-2 practically demonstrate the oil viscosity endpoints for the Heavy reservoir. Other wells are expected to display oil viscosities somewhere in between these two extremities.

Heavy Oil Formation Tester Response

Prior to drilling the case study well, wireline or LWD formation testers were run in a total of nine wells. Figure 8 presents the formation pressure results. The reported formation pressures are shown relative to the saturation pressure of the Heavy reservoir crude, and the TVD scale is the same as in Fig. 7, i.e., relative to the entry point of the case study well. The Well-1 pressure profile is shown as green squares. The measured data points form a clear oil gradient consistent with the oil sample results reported in Table 2. The Well-2 pressure

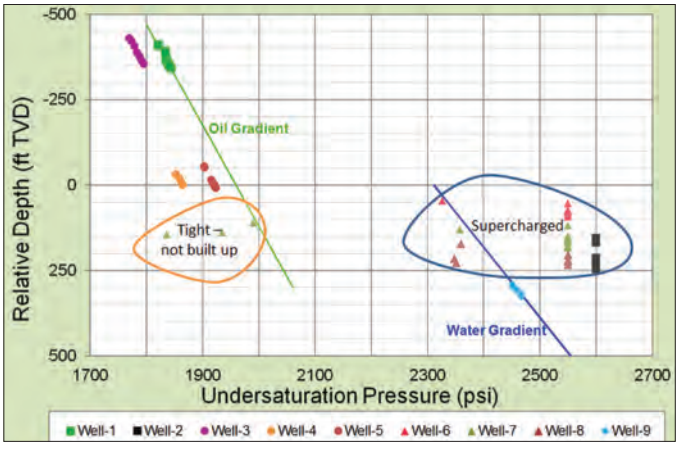

Fig. 8. Heavy reservoir formation pressure results for nine wells.

results, displayed as black squares, were all supercharged.

Wells 3 to 5 display distinct oil gradients similar to that observed with the Well-1 measurements. The wells do not plot on the same gradient due to slight location dependent reservoir pressure differences, caused by production pressure depletion effects. All these wells are clearly drilled in the mobile oil column of the Heavy reservoir.

Wells 6 to 8 all demonstrate the same supercharged effect as observed for Well-2. Some Well-7 pressure points were also reported as tight or not built up. The pressures were reported as supercharged if the measured pressure was within 100 psi of the static mud pressure or measured higher than the original reservoir pressure prior to the 1947 production startup. The pressure points flagged as supercharged have been set to the same pressure for illustration purposes rather than using the actual measured pressure, which is only indicative of the static mud pressure at the time of the measurements. The NMR data for these three wells all show the typical missing porosity and excess bound fluid tar indicators. In essence, the supercharged effect reported by the formation tester can be considered another heavy oil/tar indicator.

The formation tester pressure data for Well-9 form a water gradient consistent with the regional aquifer's water salinity. There has been no historic water injection into the Heavy reservoir. Subsequent to Well-9, two additional aquifer wells, one well drilled 40 km (25 miles) away, confirmed that the data of Well-9 was in line with the original aquifer pressure.

The data presented in Fig. 8 reveals that the Heavy reservoir oil column and aquifer are separated by 300 ft TVD of heavy oil/tar[13], which also acts as a pressure barrier. The oil reservoir is ~350 psi to 400 psi depleted due to production, while the aquifer is at its original pressure.

THE CASE STUDY HEAVY RESERVOIR PILOT WATER INJECTOR WELL

Well Placement and Formation Tester Results

As previously shown in Fig. 8, prior to drilling the pilot water injector well, the bottom pressure point from Well-5 defined the lowest known limit of the mobile oil column as slightly below the zero reference depth. The top supercharged pressure point from Well-6 was located ~50 ft below the reference depth. Figure 9 shows these pressure results on an enlarged depth scale. This 50 ft depth band was defined as the target interval for the case study injector.

During placement of the pilot water injector, Well-10, LWD formation tester data was acquired. These results are presented in Fig. 9 with the yellow "X" symbols. Some of these pressure points were supercharged, while other measurements did not meet the supercharged criteria. It is not possible to draw any gradients from these scattered pressure points.

Because obtaining calibration oil samples was considered critical to the understanding of this complex fluid system, a

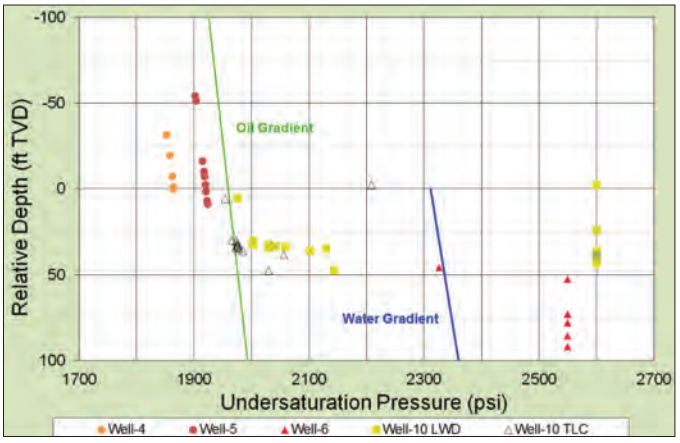

Fig. 9. Well-10 case study injector formation tester results.

TLC formation tester data set was also acquired. The Well-10 TLC pressure data are shown as black-outlined white triangles in Fig. 9. While the LWD measured formation pressures were largely supercharged, the TLC formation tester measured formation pressures were principally in line with expected formation pressure. The TLC data is more scattered than the observed pressures for the oil column wells — Well-1 and Wells 3 to 5 — but an apparent extension of the Well-1 gradient line is evident. The deviation from the gradient line with depth is expected, a result of the increased percent of asphaltenes as a function of depth.

Acquiring the two data sets made a comparison of LWD and TLC acquired formation pressures possible. The pressure results vs. depth are shown in Fig. 9. The selected depths for the TLC run were purposely picked to be the same as those for the LWD run to facilitate a direct comparison. Figure 10 is a comparison plot of the measured pressures. The plot demonstrates that the pressures measured during the LWD run were consistently higher than those measured during the TLC run. The LWD pressure results are considered largely invalid due to a slight supercharging; the exception is the two pressure points plotted close to the unit slope comparison line. Regarding the two LWD pressure points that fully meet the supercharge criteria, it should be noted that they were measured in low mobility

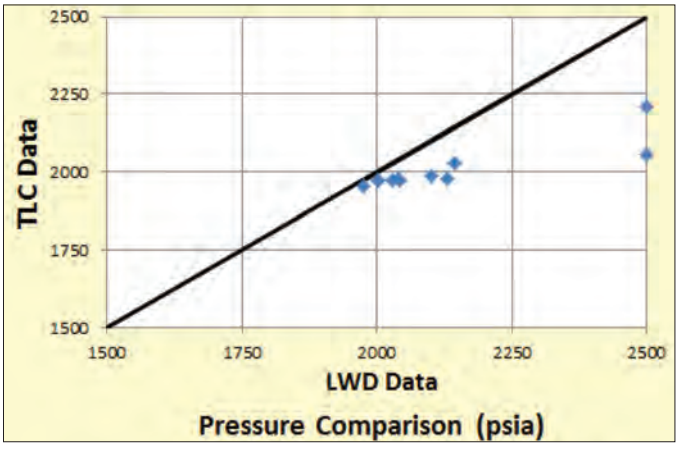

Fig. 10. LWD/TLC formation tester pressure comparison.

rock with some supercharging being apparent, as was also true for the comparable measured TLC pressures. Some of the supercharged LWD pressure points presented in Fig. 9 were skipped during the TLC run; therefore they are not included on the comparison plot in Fig. 10.

Figure 11 presents a comparison of the LWD and TLC formation mobility measurements. This plot demonstrates a much better agreement than is the case for the measured pressure comparison previously presented in Fig. 10. These results are not intuitive given that even a small depth difference in a carbonate can lead to a substantial difference in formation mobility due to reservoir heterogeneity, while the formation pressure is not expected to change much. These results indicate reliable LWD formation mobility measurements, including cases where the measured pressure is clearly supercharged.

Logs and NMR Results

The impetus for conducting an in situ oil viscosity analysis in this well is twofold. The first objective is to enhance the understanding of reservoir fluids along the well path. The well intersects the boundary between the normal and the supercharged pressure measurements previously taken using the formation tester in the field. The NMR viscosity index log could provide additional support for the reasoning that the normal and supercharged pressures are largely driven by oil property variations. Second, the laboratory viscosity analysis of the TLC fluid samples in this well could determine whether the published correlation between the compositional logs and viscosity[7] is sufficiently accurate for the Heavy reservoir application.

Figure 12 presents the conventional and NMR log results, acquired while drilling, on a TVD scale. The well is subdivided into lobes A, B, C, D, E and F, as denoted in Track 5. Note that although the TVD section is short, the logged interval is ~2,700 ft. A log viscosity analysis is performed only where: (a) the conventional and NMR logs are of good quality, i.e., free of spikes and washouts, and (b) the oil-filled porosity is at least 5% porosity units.

Lobes A and B are clearly dominated by light oils, as evidenced by the long T2 signatures. Lobe C was not processed and interpreted for viscosity due to the presence of washouts, as indicated by the caliper log in Track 1, and the large spike at ~10 milliseconds (ms) in the T2 spectrum. Lobe D shows elevated bound fluids compared to lobe B. This translates to an increase of an order of magnitude in the viscosity index. A systematic downward increase in viscosity can be observed within the lobe. Surprisingly, the top of lobe E shows a slight decrease in viscosity compared to the bottom of lobe D. Further confirmation is needed to prove whether this is a real phenomenon or a processing artifact due to the low porosity. Lobe F is clearly the heaviest component of this log section. The appearance of missing porosity is similar to that observed in Well-2. Overall, the NMR analysis in Well-10 demonstrates a remarkable heterogeneity in oil viscosity, ranging from a few cP to thousands of cP.

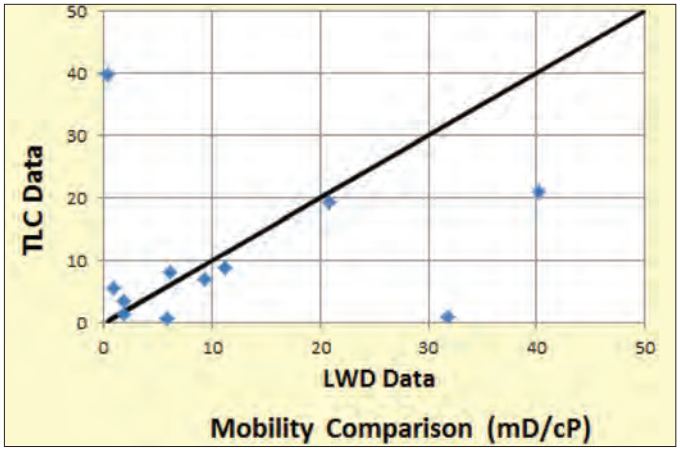

Fig. 11. LWD/TLC formation tester mobility comparison.

Oil Sample Results

Table 3 presents the laboratory results from the three oil samples acquired during the Well-10 TLC formation tester run. The average pressure-volume-temperature (PVT) parameters from the oil column above are included for comparison purposes. One sample was taken from lobe B and two samples were acquired from the top of lobe D. The measured depth difference between sample 2 and sample 3 was approximately 400 ft. The three actual sample points are marked as black squares in Fig. 12, Track 9 (sample viscosity).

The three crude samples were taken over an interval of less than 30 ft TVD. The WPC classification places the top sample as still being medium crude oil (25.2° API), just slightly heavier than the crude in the oil column above, but the two lower samples are classified as heavy oil, 20.4° API and 18.0° API, respectively. The reported flash GOR and methane (C1) content remain surprisingly constant with only a slight light end reduction trend with increasing depth.

Figure 13 displays the asphaltene weight percent (wt%) plotted vs. depth. It is clear from these plots that the increase of aspalthenes is quite dramatic over a short vertical depth interval. When asphaltene content exceeds 35 wt%, it is expected that an impermeable tar mat has been formed. A heavy oil FHZ EoS has been applied for these data and suggests a large asphaltene gradient due to gravitational equilibrium, with cluster-type asphaltene in large particles (6.5 nm).

In the Saudi Arabian field example, Fig. 6, the distance from 10% asphaltene content to the projected oil/tar contact is ~100 ft. In Fig. 13, it is apparent that this distance is significantly shorter at < 50 ft. In Fig. 6, the asphaltene content starts to increase sharply with depth from ~15% asphaltene and up. This may also be the case in the case study field. It is possible that the two lower samples were acquired close to an even more distinct actual oil/tar contact interface. More crude samples are required to fully understand the asphaltene gradient in the vicinity of the oil/tar interface in the Heavy reservoir.

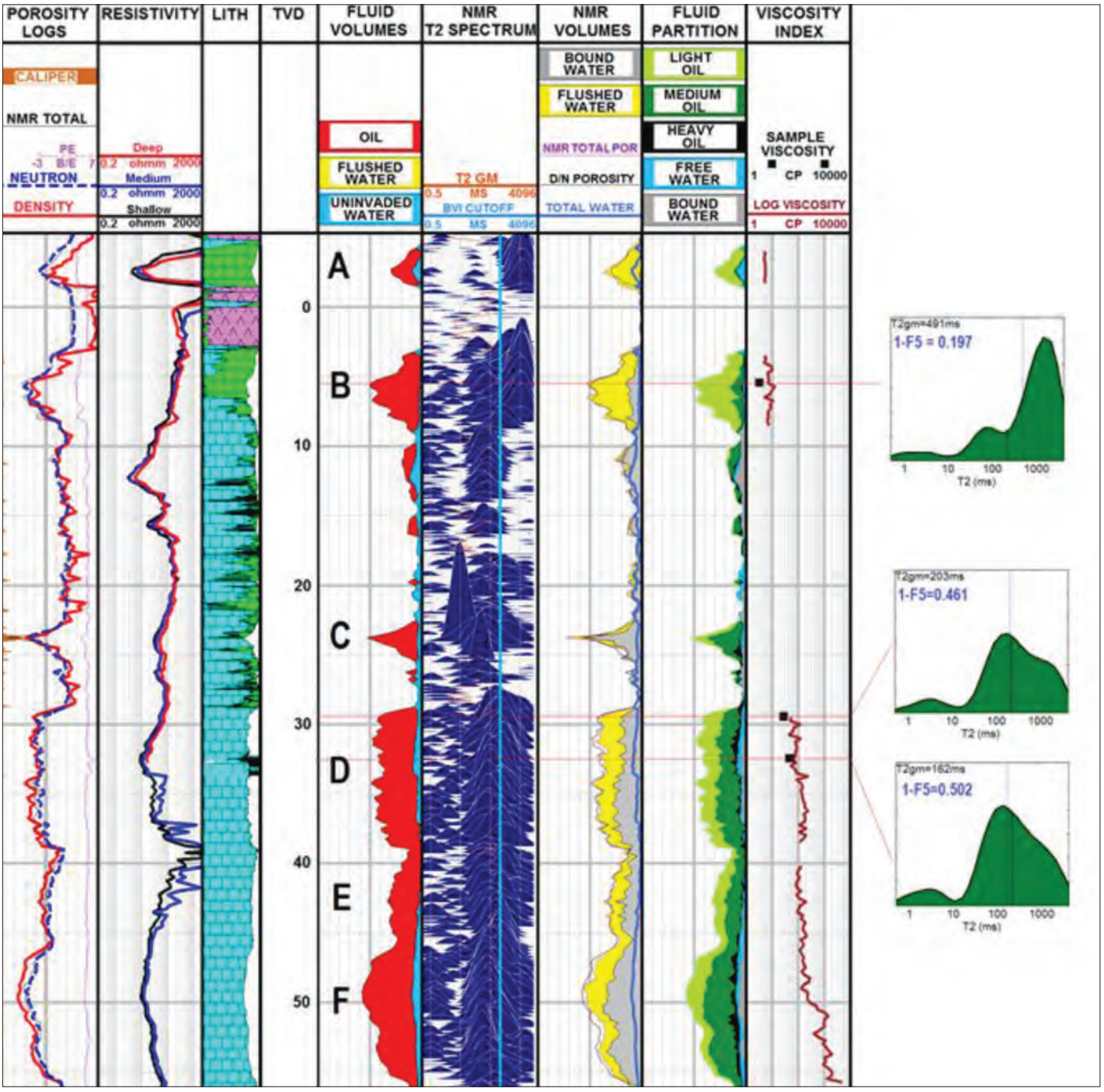

Fig. 12. Well-10 triple combo and NMR log interpretation.

The oil viscosity vs. depth data from Well-10 are presented in Fig. 14. Despite the content of the lighter hydrocarbons remaining relatively constant, the effect of the increase in asphaltene percentage creates a very sharp increase in the crude viscosity.

Using the data from Table 3 as input for the two classic crude viscosity correlations, Figs. 2 and 3, makes it clear that Standing (1977)[21] is correct in his statement that these correlations do not consider the chemical nature of the hydrocarbons that make up the crude part of the reservoir oil. For the lower sample point, the Beal correlation combined with the Chew and Connally correlation estimates the in situ oil viscosity to be 6 cP to 8 cP, while the laboratory measurement of the physical sample was 45 cP. The reason for this is essentially that the correlations do not take into account the viscosity effect of nanoaggregate cluster particles.

Comparison of Measured Crude Sample Data with NMR Oil Viscosity Correlation and Formation Tester Sampling Data

In Table 4, the in situ oil viscosity and liquid density results from the TLC formation tester fluid analyzer and the NMR viscosity correlation are compared with the laboratory results from the acquired formation tester fluid samples.

Fluid Parameter	Oil Column	Sample #1	Sample #2	Sample #3	Unit
Sample Reference Depth	<0	7	30	34	ft TVD
API Gravity	27.4	25.2	20.4	18.0	°API
Dead Oil Density	891	903	931	947	kg/m³
Crude Classification USGS	Light	Light	Light	Heavy	
Crude Classification WPC	Medium	Medium	Heavy	Heavy	
Flash GOR	205	190	183	172	scf/bbl
C1	6.4	6.4	6.1	5.7	mole %
C7+	58	61	64	66	mole %
C10+	43	46	51	53	mole %
In Situ Liquid Density	818	832	855	N/A	kg/m³
Asphaltenes	N/A	11	23	24	wt%
In Situ Oil Viscosity	~2	3.2	19	45	cP
Reservoir Temperature	215	215	215	215	°F

Table 3. Well-10 oil samples laboratory results

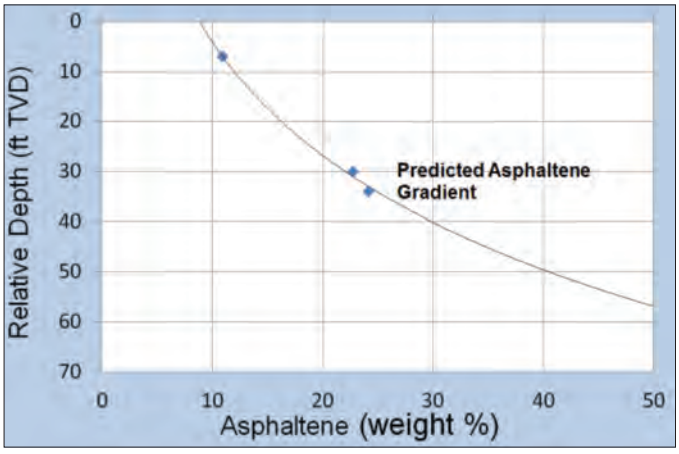

Fig. 13. Asphaltene wt% vs. depth.

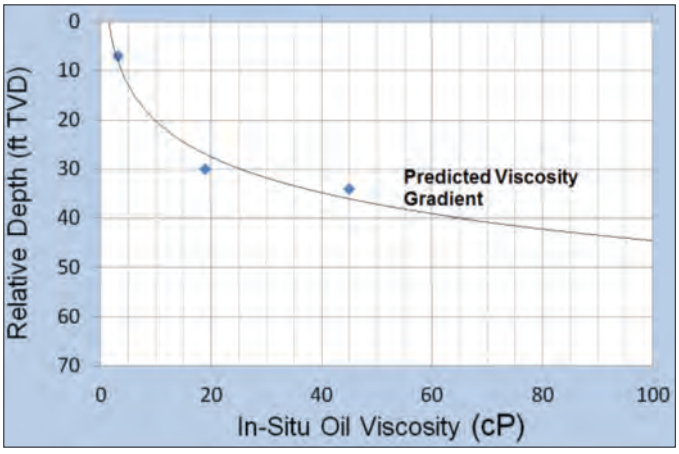

Fig. 14. In situ oil viscosity vs. depth.

Fluid Parameter	Sample #1	Sample #2	Sample #3	Unit
Sample Reference Depth	7	30	34	ft TVD
Sample In Situ Oil Viscosity	3.2	19	45	cP
NMR Correlation In Situ Oil Viscosity	7.7	38	53	cP
Formation Tester In Situ Fluid Viscosity	~6	24	50	cP
Sample In Situ Liquid Density	832	855	N/A	kg/m³
Formation Tester In Situ Liquid Density	850	860	890	kg/m³

Table 4. Well-10 oil samples oil viscosity and liquid density results compared with NMR and formation tester results

Figure 15 presents the NMR oil viscosity correlation plot based on the VT-08 algorithm in Akkurt et al. (2010)[7] compared with the sample data. For the log to sample calibration, the NMR and conventional volumetric logs have been averaged to the approximate size of the drawdown volume for the straddle packer system around each sample depth. The graphs next to the log plot in Fig. 12 show the averaged T2 spectrum for each sample depth, with its geometric mean and calibration factor (1-F5) calculated by the VT-08 optimization algorithm[7]. Differences between these NMR spectra at the sample locations indicate shorter decays in the heavier crude. Sample 3 shows very good agreement with the prediction. Sample 2 deviates by a factor of 2, whereas the VT-08 algorithm overestimates sample 1 oil viscosity by a factor of ~2.5. Although NMR

logs are of great help in heavy oil detection, it is recommended to improve the existing oil viscosity correlation, VT-08, with calibration to lighter oil samples, < 10 cP, and to extend its validity by including sample results from very heavy oils.

Sampling of heavy oil in a WBM environment is challenging due to the large viscosity contrasts between drilling fluids and the formation fluid[47]. The high viscosity of the hydrocarbon phase usually results in high-pressure drawdown. During WBM formation tester pump out, the high-pressure drawdown is often compounded by the formation of emulsions due to the agitation of heavy oil and drilling fluids. For optimum real-time decisions during sampling, high resolution optical fluid sensors should be utilized to diagnose the formation of emulsions and determine oil fraction during cleanup flow. In addition to the basic parameters of flow rate and flowing pressure, a large number of supporting parameters are measured during sampling operations using the modern technology formation tester to ensure that representative clean samples are acquired.

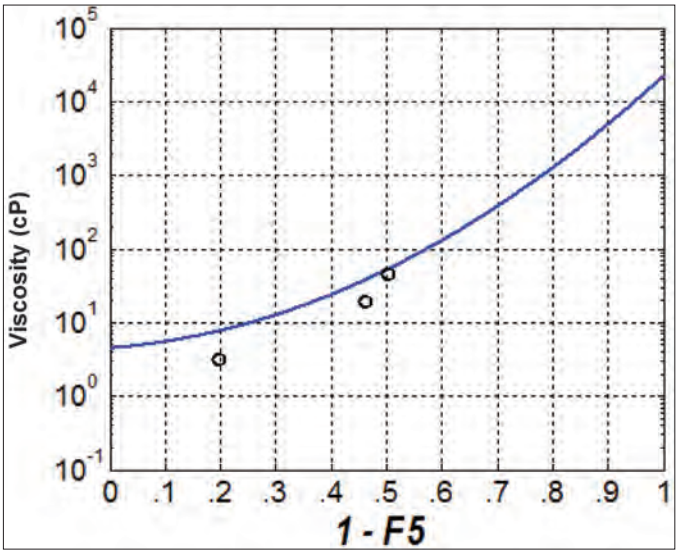

Fig. 15. NMR oil viscosity correlation plot.

Figure 16 presents a sampling plot generated while acquiring Sample 3. The flowing pressure and flow rate are represented with the green and pink lines, respectively. The cyan marking signifies the in situ fluid viscosity. As Fig. 16 shows, the measured viscosity was stable at ~50 cP for some time prior to sampling, which compares favorably with the laboratory sample result of 45 cP. As shown in Table 4, a generally good agreement can be observed for the in situ fluid viscosities and liquid densities obtained by the formation tester sensors during sampling, particularly for the two heavier samples. No laboratory liquid density was measured for Sample 3 due to insufficient sample volume, which in itself illustrates the difficulties often experienced in heavy oil sampling operations.

Lessons Learned from the Case Study Pilot Water Injector Well

The case study well was drilled at a high angle slant across the ~50 ft TVD section identified, from previous NMR and formation tester data, as the location of the oil/tar interface. The focus of this well was to maximize the data acquisition to gain as much understanding as possible about this interface for use in future development optimization. The intent was to run a flow meter after the well was put on injection to determine the highest crude viscosity that would accept injection water.

The main lesson learned was that the oil/tar transition zone

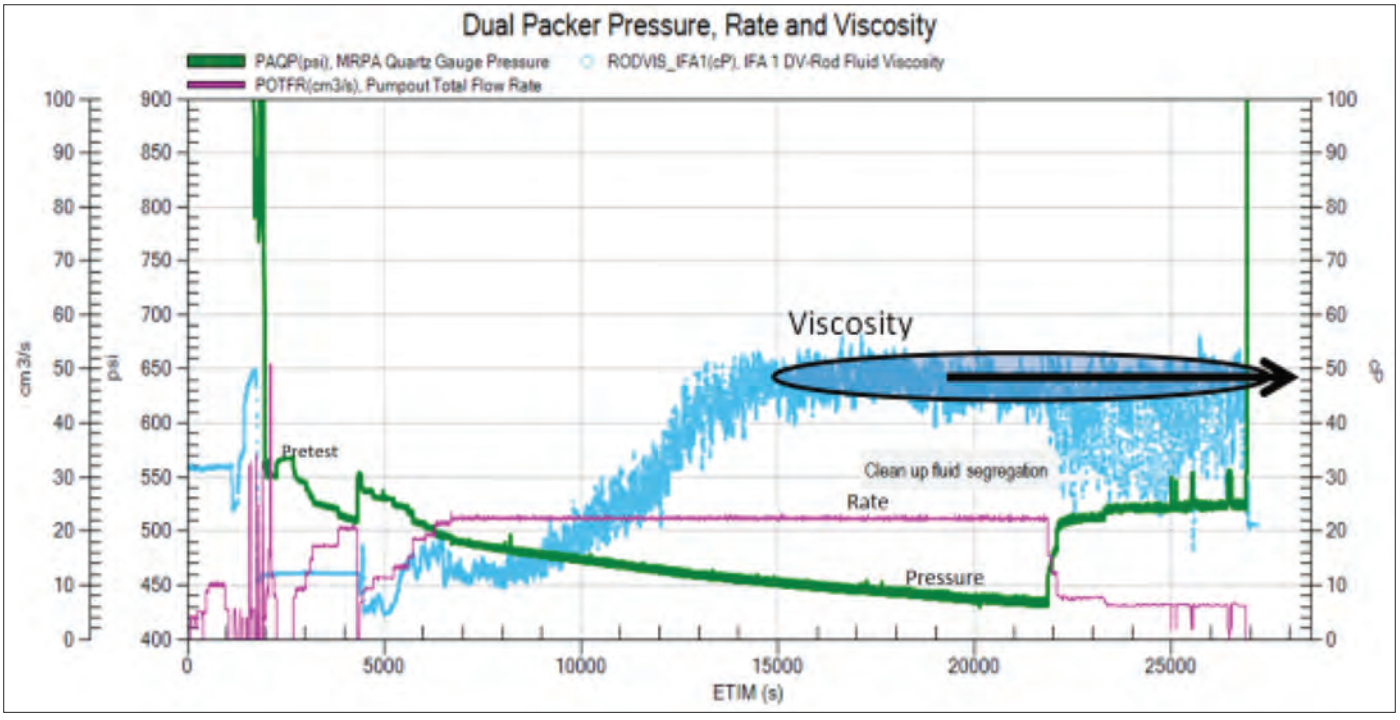

Fig. 16. Formation tester sampling data plot for Well-10 Sample 3.

is a lot shorter than observed in other Saudi Arabian reservoirs with tar mat occurrence. The post-well analyses of the data acquired suggest a large asphaltene gradient due to gravitational equilibrium, with cluster-type asphaltene with large particles (6.5 nm) occurring in the bottom ~25 ft TVD of the well. These large particle asphaltenes subsequently caused the wellbore plugging that prevented access to the reservoir section after suspending the well for tie-in. A clean out operation was unsuccessful as the plugging reoccurred. Current plans are for the well to be sidetracked again in 3 cP to 20 cP oil at the very top of the oil/tar transition zone. NMR and mobility steering will be more actively utilized in future injectors to ensure that the tar mat is not penetrated to safeguard the ability of the well to utilize injected water.

CONCLUSIONS

1. The oil/tar transition zone in this reservoir is a lot shorter than observed in other Saudi Arabian reservoirs with tar mat occurrence. A large asphaltene gradient due to gravitational equilibrium is suggested, with cluster-type asphaltene with large particles (6.5 nm) occurring in the bottom ~25 ft TVD of the well. These large particle asphaltenes caused the wellbore plugging that prevented access to the case study injector reservoir section after suspending the well for tie-in.
2. NMR and mobility steering will be more actively utilized in future injectors to ensure that the tar mat is not penetrated to ensure that the well can be utilized as a water injector.
3. It is recommended to improve the existing NMR oil viscosity correlation with calibration to lighter oil samples, < 10 cP, and to extend its validity by including sample results from very heavy oils.
4. The formation tester in situ liquid density and fluid viscosity measurements acquired during sampling are in realistic agreement with the reservoir crude sample's PVT laboratory measurements. This indicates that accurate real-time in situ fluid property determination is possible with modern formation tester technology.
5. The mobility data acquired by the LWD formation tester compared favorably with the TLC acquired mobility data.
6. In this heavy oil application, the LWD formation tester pressure data all appear supercharged, while the TLC formation pressures were in line with the anticipated reservoir pressure.

ACKNOWLEDGMENTS

The authors would like to thank the management of Saudi Aramco and Schlumberger for their support and permission to publish this article. Some of the case study well data used as the basis for this article were presented as nonpublic domain posters at ADIPEC 2013[48] and the 2nd SPE/EAGE Joint Workshop: Tar Mats and Heavy Oil[49].

This article is an edited version of the paper presented at the 19th SPE Middle East Oil and Gas Show and Conference, Manama, Bahrain, March 8-11, 2015[50].

REFERENCES

1. Neumann, P.M., Al-Salem, K.M., Tobert, G.P., Seifert, D.J., Al-Dossary, S.M., Al-Khaldi, N.A., et al.: "Formation Pressure While Drilling Utilized for Geosteering," SPE paper 110940, presented at the SPE Saudi Arabia Section Technical Symposium, Dhahran, Saudi Arabia, May 7-8, 2007.
2. Neumann, P.M., Abdul Aziz, A.K.B. and Agrawal, V.: "Mobility Steering Helps Place Injectors," *Offshore Magazine*, Vol. 69, No. 8, August 2009, pp. 80-82.
3. Seifert, D.J., Neumann, P.M., Al-Nasser, M.N., Al-Dossari, S.M. and Hibler, A.P.: "Optimizing Horizontal Well Placement Using Formation Pressure While Drilling Measurements," paper RRRR, presented at the 49th Annual SPWLA Logging Symposium, Edinburgh, Scotland, U.K., May 25-28, 2008.
4. Kelly, F.N., Ab Rahim, Z., Neumann, P.M., Logan, S.A. and Agrawal, V.: "Formation Pressure While Drilling Measurements for Reservoir Management Applications — Case Studies from Saudi Arabia," IPTC paper 13134, presented at the International Petroleum Technology Conference, Doha, Qatar, December 7-9, 2009.
5. Akkurt, R., Seifert, D.J., Al-Harbi, A., Al-Beaiji, T.M., Kruspe, T., Thern, H., et al.: "Real-Time Detection of Tar in Carbonates Using LWD Triple Combo, NMR and Formation Tester in Highly Deviated Wells," SPWLA paper 2008-XXX, presented at the 49th Annual Logging Symposium, Austin, Texas, May 25-28, 2008.
6. Ibrahim, A.M., Seifert, D.J., Neumann, P.M. and Musharfi, N.M.: "Successful Well Placement with Real-Time Petrophysical Data Optimization: Saudi Aramco Experience," SPWLA paper 2011-X, presented at the 52nd Annual Logging Symposium, Colorado Springs, Colorado, May 14-18, 2011.
7. Akkurt, R., Seifert, D.J., Eyvazzadeh, R. and Al-Beaiji, T.M.: "From Molecular Weight and NMR Relaxation to Viscosity: An Innovative Approach for Heavy Oil Viscosity Estimation for Real-Time Applications," *Petrophysics*, Vol. 51, No. 2, April 2010, pp. 89-101.
8. Al-Shehri, D.A., Kanfar, M., Al-Ansari, Y.S. and Abu Faizal, S.: "Utilizing NMR and Formation Pressure Testing While Drilling to Place Water Injectors Optimally in a Field in Saudi Arabia," SPE paper 141783, presented at the SPE Middle East Oil and Gas Show and Conference, Manama, Bahrain, September 25-28, 2011.

9. Saint, C., Glowig, T., Swain, A.S.S., Al-Khaldi, N.A., Al-Otaibi, M.H., Al Ghareeb, A.A., et al.: "Hydrocarbon Mobility Steering for Optimum Placement of a Power Water Injector above Tar Mats — A Case Study from a Light Oil Carbonate Reservoir in the Middle East," SPE paper 164282, presented at the SPE Middle East Oil and Gas Show and Conference, Manama, Bahrain, March 10-13, 2013.
10. Al-Towailib, A.I., Lyngra, S. and Al-Otaibi, U.F.: "Advanced Completion Technologies Result in Successful Extraction of Attic Oil Reserves in a Mature Giant Carbonate Field," WPC paper 19-2451, presented at the 19th World Petroleum Congress, Madrid, Spain, June 29 - July 3, 2008.
11. Widjaja, D.R., Lyngra, S., Al-Ajmi, F.A., Al-Otaibi, U.F. and Alhuthali, A.H.: "Vertical Cased Producers Outperform Horizontal Wells in a Complex Naturally Fractured Low Permeability Reservoir," SPE paper 164414, presented at the SPE Middle East Oil and Gas Show and Conference, Manama, Bahrain, March 10-13, 2013.
12. Al-Suwadi, S.H., Lyngra, S., Roberts, I., Al-Hussain, J., Pasaribu, I., Laota, A.S., et al.: "Successful Application of a Novel Mobility Geosteering Technique in a Stratified Low Permeability Carbonate Reservoir," SPE paper 168077, presented at the SPE Saudi Arabia Section Annual Technical Symposium and Exhibition, al-Khobar, Saudi Arabia, May 19-22, 2013.
13. Lyngra, S.: "Field Case 2 Saudi Arabia: The 300 ft Tar Mat Challenge," abstract presented at the Session 5: Case Studies/Lessons Learned Session of the SPE/EAGE Joint Workshop: Tar Mats and Heavy Oil, Dubai, UAE, June 1-4, 2014.
14. Schenk, C.J., Pollastro, R.M. and Hill, R.J.: "Natural Bitumen Resources of the United States," Natural Assessment of Oil and Gas Fact Sheet 2006-3133, U.S. Geological Survey (USGS), U.S. Department of Interior, November 2006.
15. Martinez, A.R., Ion, D.C., DeSorcy, G.J., Dekker, H. and Smith, S.: "Classification and Nomenclature Systems for Petroleum and Petroleum Reserves," WPC paper 22430, presented at the 12th World Petroleum Congress, Houston, Texas, April 26 - May 1, 1987.
16. Cronquist, C.: *Estimation and Classification of Reserves of Crude Oil, Natural Gas, and Condensate*. Society of Petroleum Engineers, SPE Book Series, Chapter 1, 2001, 416 p.
17. Beal, C.: "The Viscosity of Air, Water, Natural Gas, Crude Oil and Its Associated Gases at Oil Field Temperatures and Pressures," SPE paper 946094, *Transactions of the AIME*, Vol. 165, No. 1, December 1946, pp. 94-115.
18. Standing, M.B.: *Petroleum Engineering Data Book*, 1st edition, chart book compiled by Prof. Standing for the Division of Petroleum Engineering and Applied Geophysics students, The Norwegian Institute of Technology (NTH), University of Trondheim, Norway, August 1974, 70 p.
19. Frick T.C. and Taylor, R.W.: *Petroleum Production Handbook*, McGraw-Hill, New York, 1962, 696 p.
20. Chew, J-N. and Connally Jr., C.A.: "A Viscosity Correlation for Gas-Saturated Crude Oils," *Petroleum Transactions*, AIME, Vol. 216, 1959, pp. 23-25.
21. Standing, M.B.: *Volumetric and Phase Behavior of Oil Field Hydrocarbon Systems*, 8th ed., Society of Petroleum Engineers, August 1977, 123 p.
22. Mullins, O.C.: "The Modified Yen Model," *Energy & Fuels*, Vol. 24, No. 4, January 2010, pp. 2179-2207.
23. Mullins, O.C.: "The Asphaltenes," *Annual Review of Analytical Chemistry*, Vol. 4, July 2011, pp. 393-418.
24. Mullins, O.C., Sabbah, H., Eyssautier, J., Pomerantz, A.E., Barré, L., Andrews, A.B., et al.: "Advances in Asphaltene Science and the Yen-Mullins Model," *Energy & Fuels*, Vol. 26, No. 7, April 2012, pp. 3986-4003.
25. Mullins, O.C., Seifert, D.J., Zuo, J.Y., Zeybek, M.M., Zhang, D. and Pomerantz, A.E.: "Asphaltene Gradients and Tar Mat Formation in Oil Reservoirs," WHOC paper 12-182, presented at the World Heavy Oil Conference, Aberdeen, Scotland, U.K., September 10-13, 2012.
26. Mullins, O.C., Seifert, D.J., Zuo, J.Y. and Zeybek, M.M.: "Clusters of Asphaltene Nanoaggregates Observed in Oil Field Reservoirs," *Energy & Fuel*s, Vol. 27, No. 4, November 2012, pp. 1752-1761.
27. Mullins, O.C., Zuo, J.Y., Dong, C., Elshahawi, H., Seifert, D.J. and Cribbs, M.E.: "The Dynamics of Fluids in Reservoirs," SPE paper 166083, presented at the SPE Annual Technical Conference and Exhibition, New Orleans, Louisiana, September 30 - October 2, 2013.
28. Mullins, O.C., Pomerantz, A.E., Zuo, J.Y., Andrews, A.B., Hammond, P.S., Seifert, D.J., et al.: "Asphaltene Nanoscience and Reservoir Fluid Gradients, Tar Mat Formation and the Oil-Water Interface," SPE paper 166278, presented at the SPE Annual Technical Conference and Exhibition, New Orleans, Louisiana, September 30 - October 2, 2013.
29. Mullins, O.C., Zuo, J.Y., Wang, K., Hammond, P.S., De Santo, I., Dumont, H., et al.: "The Dynamics of Reservoir Fluids and Their Substantial Systematic Variations," *Petrophysics*, Vol. 55, No. 2, April 2014, pp. 96-112.

30. Pomerantz, A.E., Seifert, D.J., Bake, K.D., Craddock, P.R., Mullins, O.C. and Kodalen, B.G.: "Sulfur Chemistry of Asphaltenes from a Highly Compositionally Graded Oil Column," *Energy & Fuels*, Vol. 27, No. 8, July 2013, pp. 4604-4608.

31. Pomerantz, A.E., Seifert, D.J., Qureshi, K.A., Zeybek, M.M. and Mullins, O.C.: "The Molecular Composition of Asphaltenes in a Highly Compositionally Graded Column," *Petrophysics*, Vol. 54, No. 5, October 2013, pp. 427-438.

32. Zuo, J.Y., Dumont, H., Mullins, O.C., Dong, C., Elshahawi, H. and Seifert, D.J.: "Integration of Downhole Fluid Analysis and the Flory-Huggins-Zuo EOS for Asphaltene Gradients and Advanced Formation Evaluation," SPE paper 166385, presented at the SPE Annual Technical Conference and Exhibition, New Orleans, Louisiana, September 30 - October 2, 2013.

33. Zuo, J.Y., Mullins, O.C., Freed, D.E., Elshahawi, H., Dong, C. and Seifert, D.J.: "Advances of the Flory-Huggins-Zuo Equation of State for Asphaltene Gradients and Formation Evaluation," *Energy & Fuels*, Vol. 27, No. 4, 2013, pp. 1722-1735.

34. Seifert, D.J., Zeybek, M.M., Dong, C., Zuo, J.Y. and Mullins, O.C.: "Black Oil, Heavy Oil and Tar in One Oil Column Understood by Simple Asphaltene Nanoscience," SPE paper 161144, presented at the Abu Dhabi International Petroleum Exhibition and Conference, Abu Dhabi, UAE, November 11-14, 2012.

35. Seifert, D.J., Qureshi, K.A., Zeybek, M.M., Pomerantz, A.E., Zuo, J.Y., and Mullins, O.C.: "Heavy Oil and Tar Mat Characterization within a Single Oil Column Utilizing Novel Asphaltene Science," SPE paper 163291, presented at the SPE Kuwait International Petroleum Conference and Exhibition, Kuwait City, Kuwait, December 10-12, 2012.

36. Wu, Q., Pomerantz, A.E., Mullins, O.C. and Zare, R.N.: "Laser-Based Mass Spectrometric Determination of Aggregation Numbers for Petroleum- and Coal-Derived Asphaltenes," *Energy & Fuels*, Vol. 28, No. 1, 2014, pp. 475-482.

37. Wu, Q., Seifert, D.J., Pomerantz, A.E., Mullins, O.C. and Zare, R.N.: "Constant Asphaltene Molecular and Nanoaggregate Mass in a Gravitationally Segregated Reservoir," *Energy & Fuels*, Vol. 28, No. 5, 2014, pp. 3010-3015.

38. Sabbah, H., Morrow, A.L., Pomerantz, A.E. and Zare, R.N.: "Evidence for Island Structures as the Dominant Architecture for Asphaltenes," *Energy & Fuels*, Vol. 25, No. 4, April 2011, pp. 1597-1604.

39. Kleinberg, R.L. and Vinegar, H.J.: "NMR Properties of Reservoir Fluids," *The Log Analyst*, Vol. 37, No. 6, November-December 1996, pp. 20-32.

40. LaTorraca, G.A., Dunn, K.J., Webber, P.R., Carison, R.M. and Stonard, S.W.: "Heavy Oil Viscosity Determination Using NMR Logs," SPWLA paper 1999-PPP, presented at the SPWLA 40th Annual Logging Symposium, Oslo, Norway, May 30 - June 3, 1999.

41. Lo, S-W., Hirasaki, G.J., House, W.V. and Kobayashi, R.: "Correlations of NMR Relaxation Times with Viscosity, Diffusivity, and Gas-Oil Ratio of Methane/Hydrocarbon," SPE paper 63217, presented at the SPE Annual Technical Conference and Exhibition, Dallas, Texas, October 1-4, 2000.

42. Zhang, Y., Hirasaki, G.J., House, W.V. and Kobayashi, R.: "Oil and Gas NMR Properties: The Light and Heavy Ends," SPWLA paper 2002-HHH, presented at the SPWLA 43rd Annual Logging Symposium, Oiso, Japan, June 2-5, 2002.

43. Bryan, J., Kantzas, A. and Bellehumeur, C.: "Oil Viscosity Predictions from Low Field NMR Measurements," *SPE Reservoir Evaluation & Engineering*, Vol. 8, No. 1, February 2005, pp. 44-52.

44. Bryan, J., Kantzas, A., Badry, R., Emmerson, J. and Hancsicsak, T.: "In Situ Viscosity of Heavy Oil: Core and Log Calibrations," *Journal of Canadian Petroleum Technology*, Vol. 46, No. 11, November 2007, pp. 47-55.

45. Seccombe, J., Bonnie, R.J.M., Smith, M. and Akkurt, R.: "Ranking Oil Viscosity in Heavy Oil Reservoirs," SPE paper 97935, presented at the SPE International Thermal Operations and Heavy Oil Symposium, Calgary, Alberta, Canada, November 1-3, 2005.

46. Yang, Z., Hirasaki, G.J., Appel, M. and Reed, D.A.: "Viscosity Evaluation for NMR Well Logging of Live Heavy Oils," SPWLA paper 2011-C, presented at the SPWLA 52nd Annual Logging Symposium, Colorado Springs, Colorado, May 14-18, 2011.

47. Akkurt, R., Seifert, D.J., Neumann, P.M., Zeybek, M.M. and Ayyad, H.A.: "In Situ Heavy Oil Fluid Density and Viscosity Determination Using Wireline Formation Testers in Carbonates Drilled with Water-Based Mud," SPE paper 134849, presented at the SPE Annual Technical Conference and Exhibition, Florence, Italy, September 19-22, 2010.

48. Zeybek, M.M., Ayyad, H.A., Qureshi, K.A., Lyngra, S. and Palmer, R.G.: "Real-Time Heavy Oil Delineation to Optimize Placement of a Horizontal Water Injector in a Carbonate Reservoir," poster presented at the Abu Dhabi International Petroleum Exhibition and Conference, Abu Dhabi, UAE, November 10-13, 2013.

49. Lyngra, S., Hursan, G.G. and Zeybek, M.M.: "Placement of a Carbonate Reservoir Horizontal Water Injector above a Tar Mat: Real-Time Heavy Oil Delineation," poster presented at the 2nd SPE/EAGE Joint Workshop: Tar Mats and Heavy Oil, Dubai, UAE, June 1-4, 2014.

50. Lyngra, S., Hursan, G.G., Palmer, R.G., Zeybek, M.M., Ayyad, H.A. and Qureshi, K.A.: "Heavy Oil Characterization: Lessons Learned during Placement of a Horizontal Injector at a Tar/Oil Interface," SPE paper 172673, presented at the 19th SPE Middle East Oil & Gas Show and Conference, Manama, Bahrain, March 8-11, 2015.

BIOGRAPHIES

Stig Lyngra works in Saudi Aramco's Southern Area Reservoir Management Department as a Senior Petroleum Engineering Consultant. Before joining Saudi Aramco in 2001, he worked for Danop in Copenhagen, Denmark, where he was Petroleum Engineering Discipline Leader. For the first 10 years of his career, Stig worked for Conoco as a Reservoir Engineer, Supervising Reservoir Engineer and Commercial Coordinator, and in different joint asset management positions in various offices in the U.S., Norway and the U.K.

He is a member of the European Association of Geoscientists and Engineers (EAGE), the Society of Petroleum Engineers (SPE) and the Saudi Council of Engineers.

In 1987, he received his M.S. degree in Petroleum Engineering from the Norwegian Institute of Technology (NTH) in Trondheim, Norway. Stig also holds a degree in Business Administration from BI Norwegian Business School, Oslom, Norway.

Dr. Gabor G. Hursan is a Petrophysicist in Saudi Aramco's Reservoir Description and Simulation Department. He is Saudi Aramco's focal point for nuclear magnetic resonance (NMR) well logging and formation evaluation. Previously, Gabor worked as a Scientist and Project Leader on NMR technology development at Baker Hughes for 10 years.

He has published several papers and patents, teaches classes in NMR logging and is a reviewer for technical publications. Gabor is a member of the Society of Petroleum Engineers (SPE) and the Society of Petrophysicists and Well Log Analysts (SPWLA).

He received his M.S. degree in Geophysical Engineering from the University of Miskolc, Miskolc, Hungary, and his Ph.D. degree in Geophysics from the University of Utah, Salt Lake City, UT.

Dr. Murat M. Zeybek is a Schlumberger Reservoir Engineering Advisor and a Global Reservoir domain expert based in Saudi Arabia. He joined Schlumberger 19 years ago. He was previously a postdoctoral research associate at the University of Southern California, Los Angeles, CA. Murat also worked for Intera West consulting firm for one year in Los Angeles.

He has published more than 50 papers on analysis/interpretation of wireline formation testers, pressure transient analysis, numerical modeling of fluid flow, fluid flow porous media, water control, production logging and reservoir monitoring.

Murat is a technical editor for the Society of Petroleum Engineers (SPE) journal *Reservoir Evaluation and Engineering*. He also served as a committee member for the SPE Annual Technical Conference and Exhibition, 1999-2001. Murat has been a discussion leader and a committee member in a number of SPE and American Association of Petroleum Geologists (AAPG) Applied Technology Workshops, including a technical committee member for the SPE Saudi Technical Symposium.

He received his B.S. degree from the Technical University of Istanbul, Istanbul, Turkey, and his M.S. and Ph.D. degrees from the University of Southern California, Los Angeles, CA, all in Petroleum Engineering.

Richard G. Palmer is currently a Petrophysical Supervisor in Saudi Aramco's Reservoir Description and Simulation Department. Since joining Saudi Aramco in 2005, he has held several technical and supervisory positions in the Southern Area. Richard's specialty is formation evaluation while drilling.

Prior to joining Saudi Aramco, he was a Technical Instructor and a Senior Field Engineer with Sperry Drilling Services. Richard has also worked with Schlumberger and has authored several publications and served on technical and organizing committees of professional societies and events.

He received his B.S. degree in Civil Engineering from the University of the West Indies, St. Augustine, Trinidad and Tobago, and his M.S. degree in Petroleum Engineering from the Imperial College of Science Technology and Medicine, University of London, London, U.K.

K. Ahmed Qureshi is a Schlumberger Testing Services, Reservoir Sampling and Analysis (RSA) Business Development Manager based in Saudi Arabia. He began his career in 2001 with Schlumberger, holding a variety of critical positions that led to his extensive knowledge in reservoir characterization for heavy oil, black oil, volatile oils and gas condensates, fluid sampling and analysis. Ahmed is now responsible for technical support in job planning, execution and interpretation in sampling and analysis operations.

He received his B.S. degree in Chemical Engineering from the Northern Alberta Institute of Technology, Edmonton, Alberta, Canada.

Ahmed is an active member of the Society of Petroleum Engineers (SPE).

Hazim A. Ayyad is a Senior Reservoir Engineer for Schlumberger. He has been working for Schlumberger since 2006 when he started working as a Wireline Field Engineer in Saudi Arabia. Then Hazim moved to the Reservoir Data Interpretation Team in Saudi Arabia before moving to Kuwait in 2010. He is currently leading the reservoir and production teams for wireline in Kuwait.

Hazim received his B.S. degree in Petroleum Engineering from King Saud University, Riyadh, Saudi Arabia.

Energy is Opportunity

ارامكو السعودية
Saudi Aramco

At Saudi Aramco, our passion is enabling opportunity. From the depths of the earth to the frontiers of the human mind, we're dedicated to fostering innovation, unleashing potential, and applying science to develop new solutions for the global energy challenge. As the world's preeminent energy and chemicals company, it is our responsibility — our privilege — to maximize the opportunity available in every hydrocarbon molecule we produce. That's how we contribute to our communities, our industry, and our world. Saudi Aramco is there, at the intersection of energy and opportunity, building a better future for all.

People. Power. Progress.

www.saudiaramco.com

SUBSCRIPTION ORDER FORM

To begin receiving the *Saudi Aramco Journal of Technology* at no charge, please complete this form.

Please print clearly.

Name _____

Title _____

Organization _____

Address _____

City _____

State/Province _____

Postal code _____

Country _____

E-mail address _____

Number of copies _____

TO ORDER

By phone/email:

Saudi Aramco Public Relations Department
JOT Distribution
+966-013-876-0498
william.bradshaw.1@aramco.com

By mail:

Saudi Aramco Public Relations Department
JOT Distribution
Box 5000
Dhahran 31311
Saudi Arabia

Current issues, select back issues and multiple copies of some issues are available upon request.

The *Saudi Aramco Journal of Technology* is published by the Saudi Aramco Public Relations Department, Saudi Arabian Oil Company, Dhahran, Saudi Arabia.

GUIDELINES FOR SUBMITTING AN ARTICLE TO THE SAUDI ARAMCO JOURNAL OF TECHNOLOGY

These guidelines are designed to simplify and help standardize submissions. They need not be followed rigorously. If you have additional questions, please feel free to contact us at Public Relations. Our address and phone numbers are listed on page 85.

Length

Varies, but an average of 2,500-3,500 words, plus illustrations/photos and captions. Maximum length should be 5,000 words. Articles in excess will be shortened.

What to send

Send text in Microsoft Word format via email or on disc, plus one hard copy. Send illustrations/photos and captions separately but concurrently, both as email or as hard copy (more information follows under file formats).

Procedure

Notification of acceptance is usually within three weeks after the submission deadline. The article will be edited for style and clarity and returned to the author for review. All articles are subject to the company's normal review. No paper can be published without a signature at the manager level or above.

Format

No single article need include all of the following parts. The type of article and subject covered will determine which parts to include.

Working title

Abstract

Usually 100-150 words to summarize the main points.

Introduction

Different from the abstract in that it "sets the stage" for the content of the article, rather than telling the reader what it is about.

Main body

May incorporate subtitles, artwork, photos, etc.

Conclusion/summary

Assessment of results or restatement of points in introduction.

Endnotes/references/bibliography

Use only when essential. Use author/date citation method in the main body. Numbered footnotes or endnotes will be converted. Include complete publication information. Standard is *The Associated Press Stylebook*, 49th ed. and *Webster's New World College Dictionary*, 5th ed.

Acknowledgments

Use to thank those who helped make the article possible.

Illustrations/tables/photos and explanatory text

Submit these separately. **Do not place in the text.** Positioning in the text may be indicated with placeholders. Initial submission may include copies of originals; however, publication will require the originals. When possible, submit both electronic versions, printouts and/or slides. Color is preferable.

File formats

Illustration files with .EPS extensions work best. Other acceptable extensions are .TIFF, .JPEG and .PICT.

Permission(s) to reprint, if appropriate

Previously published articles are acceptable but can be published only with written permission from the copyright holder.

Author(s)/contributor(s)

Please include a brief biographical statement.

Submission/Acceptance Procedures

Papers are submitted on a competitive basis and are evaluated by an editorial review board comprised of various department managers and subject matter experts. Following initial selection, authors whose papers have been accepted for publication will be notified by email.

Papers submitted for a particular issue but not accepted for that issue will be carried forward as submissions for subsequent issues, unless the author specifically requests in writing that there be no further consideration. Papers previously published or presented may be submitted.

Submit articles to:

Editor
The *Saudi Aramco Journal of Technology*
C-86, Wing D, Building 9156
Dhahran 31311, Saudi Arabia
Tel: +966-013-876-0498
E-mail: william.bradshaw.1@aramco.com.sa

Submission deadlines

Issue	Paper submission deadline	Release date
Winter 2015	September 1, 2015	December 31, 2015
Spring 2016	December 1, 2015	March 31, 2016
Summer 2016	March 1, 2016	June 30, 2016
Fall 2016	June 1, 2016	September 30, 2016

Novel Insights into IOR/EOR by Seawater and Supercritical CO_2 Miscible Flooding Using Dual Carbonate Cores at Reservoir Conditions

Xianmin Zhou, Fawaz M. Al-Otaibi, Dr. Sunil L. Kokal, AlMohannad A. Al-Hashboul, Dr. Senthilmurugan Balasubramanian and Faris A. Al-Ghamdi

ABSTRACT

Oil recovery during carbon dioxide (CO_2) injection into a thick and/or fractured reservoir will be limited as a result of viscous fingering and gravity override. Due to density differences between the injected CO_2 and resident fluids in the reservoir, the CO_2, being lighter, tends to rise to the top of the reservoir, thereby bypassing some of the remaining oil. To study the impact of reservoir heterogeneity on oil recovery by seawater and CO_2 flooding, this article investigates the use of a dual-core coreflooding apparatus to evaluate the effect of both CO_2 gravity override and permeability contrast on oil recovery performance by CO_2 injection.

An Alternative Method Based on Toluene/n-Heptane Surrogate Fuels for Rating the Anti-knock Quality of Practical Gasolines

Dr. Gautam T. Kalghatgi, Robert A. Head, Dr. Junseok Chang, Yoann Viollet, Hassan Babiker and Dr. Amer A. Amer

ABSTRACT

As spark ignition (SI) engines are designed for higher efficiency, they are more likely to encounter knock. A fuel's anti-knock quality, which is currently measured by a Research Octane Number (RON) and Motor Octane Number (MON), therefore becomes more important. The RON and MON scales are based on primary reference fuels (PRFs) — mixtures of iso-octane and n-heptane — whose auto-ignition chemistry is significantly different from that of practical fuels. As a result, RON or MON alone can truly characterize a gasoline's knock behavior only at each scale's respective test conditions. The same gasoline will match different PRFs at different operating conditions. The true anti-knock quality of a fuel therefore is given by the octane index, (OI) = RON – KS where *S*, sensitivity, is RON – MON, and *K*, the empirical constant, depends on the pressure and temperature evolution in the unburned gas during the engine cycle, which means it is different at different operating conditions. *K* is negative in modern engines.

Determining Water Volume Fraction for Oil-Water Production with Speed of Sound Measurement

Dr. Jinjiang Xiao

ABSTRACT

Good production and reservoir management practices require real-time data on oil, gas and water production rates from wells. For a well with conventional completion, a single surface measurement device may be sufficient. With the proliferation of multilateral wells to achieve extreme reservoir contact, the need for rate data is moving downhole toward the measurement of an individual lateral or even compartment-based measurement. Knowing how much water production there is and where it comes from is necessary before any remedial action can be taken. Measurements downhole present both challenges and opportunities. The challenge is that the design of the metering hardware has to withstand the harsh — high-pressure/high temperature — and space constrained environments. The advantage is that, in terms of fluids, the gas phase may not be present due to the high pressure, which can potentially simplify the system design. Currently, cost-effective, reliable and compact downhole flow measurement technologies with a full range of capability are not available.

Evaluation of Synthetic Acid for Wells Stimulation in Carbonate Formations

Dr. Mohammed N. Al-Dahlan, Marwa A. Al-Obied, Khalid M. Al-Marshad, Faisal M. Al-Sahman, Ibrahim S. Al-Yami and Abdullah M. Alhajri

ABSTRACT

Acid treatments of carbonate formations are usually carried out using mineral acid (hydrochloric (HCl) acid), organic acids (formic and acetic), mixed acids (HCl formic, HCl acetic) or retarded acids. The major challenges when using these acids are their high corrosivity, fast reaction rate and health hazards. The improvement in corrosion inhibitors (CIs) makes the use of a strong acid as high as 28 wt% HCl acid possible. The acid reaction rate can be controlled by increasing acid viscosity using a gelling agent or emulsifying acid droplets, which create an acid-in-diesel emulsion. While these developments have addressed the issues of the stimulation acid's reaction and corrosion rates, the acid's health hazard rating of three by the National Fire Protection Association (NFPA) remains a major concern. A health hazard rating of three is defined as presenting an extreme danger, where short exposure could cause serious injury.